

**DUAL NUCLEAR ROLES
OF AN ESSENTIAL SCAVENGER DECAPPING ENZYME**

By

VINCENT SHEN

A Dissertation submitted to the Graduate School-New Brunswick

Rutgers, The State University of New Jersey

and

The Graduate School of Biomedical Sciences

University of Medicine and Dentistry of New Jersey

in partial fulfillment of the requirements

for the degree of

Doctor of Philosophy

Graduate Program in Biochemistry

written under the direction of

Dr. Megerditch Kiledjian

and approved by

New Brunswick, New Jersey

October, 2010

ABSTRACT OF THE DISSERTATION

Dual Nuclear Roles of an Essential Scavenger Decapping Enzyme

by

Vincent Shen

Dissertation Director

Dr. Megerditch Kiledjian

The broad findings of the current work focus on mammalian DcpS and provide an analysis of its role in pre-mRNA splicing, transcription, and its requirement in mouse development. Mutagenesis and heterokaryon assays reveal an N-terminal nuclear localization sequence and a central nuclear export sequence that account for its nucleocytoplasmic dynamics. Cell-based reporter assays reveal two novel DcpS nuclear roles that explain its prevalent nuclear presence. A cell-based mRNA assay, which detects reporter splicing patterns, indicates DcpS knockdown leads to pre-mRNA processing deficiency in the first intron. DcpS or Cbp20 overexpression partially and completely corrects this defect, respectively. Catalytically inactive DcpS displaces the Cbp20-cap interaction by competition in a reconstituted system. These results suggest DcpS is a positive regulator of pre-mRNA splicing and is in line with the idea that DcpS knockdown predictably upregulates intracellular cap structure levels. Another cell-based translation assay, which detects reporter enzyme activity, shows DcpS chemical repression or knockdown stimulates cap-dependent translation and reduces 4EBP1 protein level. The unexpected opposite effect on translation suggests DcpS catalysis does not directly regulate protein synthesis as previously thought. DcpS chemical repression

by a competitive inhibitor leads to 4EBP1 and 4EBP2 transcriptional reductions that correlate with their steady state mRNA levels. These results point toward an additional DcpS nuclear role in transcription of specific targets. On a final note, the failure to generate DcpS homozygous progeny as early as 6 days post coitum (dpc) indicates this gene is essential for mouse embryogenesis. DcpS heterozygous intercross yields approximately two heterozygotes for each wildtype during 9.5 dpc and postnatal period. DcpS heterozygotes are normal with respect to fertility. Western blots show DcpS is ubiquitously expressed in an adult tissue panel comprised of brain, liver, kidney, and heart. The present study identifies at least two nuclear roles of DcpS in pre-mRNA first intron splicing and in transcription, and its essential role in mouse development.

ACKNOWLEDGMENT

This work was not possible without the financial sponsorship and direction of Dr. Mike Kiledjian. Helpful discussion and technical expertise were kindly provided by Drs. Paul Copeland, Sam Gunderson, Terri Kinzy, Serrafin Pinol-Roma, Sophie Bail, Xinfu Jiao, Hudan Liu, Shin-Wu Liu, Mangen Song, along with colleagues Madel Durens and You Li. Assistance was also kindly offered by Drs. Lori Covey, Gabriella D'Archangelo, David Denhardt, Gutian Xia, Ping Xie, Guoliang Qing and colleagues Rodrigo Matus-Nicodemus, Anibal Valentin, and Odessa Yabut. This work was funded partly by the New Jersey Commission on Cancer Research Pre-Doctoral Fellowship under V.S. and mainly by NIH grant GM67005 under M.K.

TABLE OF CONTENTS

ABSTRACT	ii
ACKNOWLEDGEMENT	iv
TABLE OF CONTENTS	v
LIST OF TABLES	viii
LIST OF FIGURES	ix
INTRODUCTION	
Transcription	1
Co-transcriptional Modifications	3
Non-traditional Pathways of mRNA Processing	6
Exon Junction Complex (EJC) and Nuclear Export	8
Cap-dependent Translation	10
Translation Elongation	12
Cap-independent Translation	13
General mRNA Degradation	15
Transcript-specific Degradation	17
Nucleoside Diphosphate Linked Moiety (NUDIX) Decapping Enzymes	20
Histidine Triad (HIT) Hydrolases	21
DcpS, a Catalytic Cap-binding Protein	23
Broader functions of DcpS	24
MATERIALS AND METHODS	
Plasmid Constructs	26
Cell lines, transfections, lentiviral infections, D156844 stock	27

Mapping of DcpS gene trap and mouse genotyping	28
Heterokaryon assay	29
Immunofluorescence, westerns, mouse tissue, X-gal staining embryos	29
UV cross-linking, EMSA, decapping assay	30
Splicing reporter assay	31
Dicistronic reporter assay	31
mRNA decay and nuclear run on assays	31
CHAPTER I: DcpS and pre-mRNA Processing	
Summary	33
Introduction	33
Results	35
Discussion	49
CHAPTER II: DcpS and Its Regulatory Role in Gene Expression	
Summary	57
Introduction	57
Results	58
Discussion	70
CHAPTER III: DcpS and Mouse Development	
Summary	75
Introduction	75
Results	76
Discussion	83
REFERENCES	92

LIST OF TABLES

TABLE 1. DcpS was essential in early mouse development. 80

TABLE 2. Primer sequences. 90

LIST OF FIGURES

FIGURE 1.	DcpS was a nucleocytoplasmic shuttling protein that required a leucine-rich Nuclear.	37
FIGURE 2.	Identification of the DcpS nuclear import sequences.	40
FIGURE 3.	A knockdown clonal cell line is diminished in DcpS expression and catalysis.	43
FIGURE 4.	DcpS could displace Cbp20 from cap structure.	45
FIGURE 5.	DcpS could influence splicing of the first intron in cells.	47
FIGURE 6.	Model depicting consequence on nuclear splicing in the presence or reduction of DcpS.	53
FIGURE 7.	D156844 repressed DcpS activity.	59
FIGURE 8.	DcpS repression stimulated cap-dependent translation.	61
FIGURE 9.	eIF4E did not account for translational stimulation.	63
FIGURE 10.	DcpS repression reduced 4EBP1 protein level.	65
FIGURE 11.	DcpS repression reduced 4EBP1 and 4EBP2 mRNA levels.	66
FIGURE 12.	DcpS repression stimulated 4EBP1 and 4EBP2 transcription.	68
FIGURE 13.	4EBP1 and 4EBP2 knockdown stable cell lines.	69
FIGURE 14.	A gene-trap cassette randomly inserted into the second intron of DcpS locus.	78
FIGURE 15.	DcpS was expressed in the embryonic forebrain.	81
FIGURE 16.	DcpS was express ubiquitously in various adult organs.	82
FIGURE 17.	DcpS regulated cap-dependent processes.	87

INTRODUCTION

Transcription

Eukaryotic cells use two opposing processes, nuclear transcription and cytoplasmic mRNA decay, to invoke intricate patterns of gene expression. mRNA synthesis begins in the nucleus where the nascent transcript is chaperoned by cap-recognition factors that facilitate its processing and is subjected to quality control measures prior to its export. In the cytoplasm, the mRNA template is translated into protein but eventually meets its demise at the hands of the decay machinery. The components and biochemical steps of mRNA decay have been dissected and culminate in the hydrolysis of the residual cap structure mediated by DcpS, the decapping scavenger protein. DcpS is poorly understood in terms of functions that reside beyond the context of mRNA degradation. Despite its origin from the cytoplasmic fractionation, its main nuclear residence points to an undiscovered function. DcpS cap-binding ability provides a clue into its role in cellular mechanisms that use cap-recognition. The introduction presents a broad consensus of the various fields that gradually converge on topic of the decapping scavenger protein.

Eukaryotic class II transcription is modulated by the physical association between trans-factors and cognate cis-elements of the promoter (D'Alessio et al., 2009; Ho and Crabtree, 2010). The genomic template is wound around histone octamers to form nucleosomes and is tightly compacted into a higher order structure called chromatin. Cis-elements associated with histone octamers form beads on a string called nucleosomes which present a physical barrier to the transcriptional machinery. In order to overcome

this natural repression, at least three ATP-dependent chromatin modifying families are necessary to alleviate the repressive nature about the promoter in order to recruit RNA polymerase II (RNAPII). These families are the ISWI, SWI/SNF, and SWR1 chromatin remodelers, and each group can increase the accessibility of the promoter through various activities that include nucleosome assembly and re-organization, nucleosome sliding, and nucleosome insertion, respectively (Clapier and Cairns, 2009; Ho and Crabtree, 2010). In addition to chromatin modifiers, direct trans-factors and co-activators facilitate RNAPII recruitment to the promoter (Juven-Gershon et al., 2008). Once assembled, RNAPII synthesizes mRNA and leaves behind a pre-initiation scaffold complex that is ready to prime an additional round of transcription (Dvir et al., 2001). As RNAPII progresses along the template during early transcription, its largest subunit undergoes post-translational modifications in its highly conserved region known as the C-terminal domain (CTD) heptad repeat whose consensus amino acid sequence is $YS_2PTS_5PS_7$ (O'Brien et al., 1994). Serine 5 phosphorylation by CDK7 stimulates mRNA capping and is a marker for early transcription (Serizawa, 1998). On the other hand, as RNAPII proceeds through elongation and farther from the promoter, serine 5 phosphorylation tapers down as serine 2 phosphorylation by CDK9 emerges on the CTD (Wada et al., 1998). Serine 7 phosphorylation is the newest CTD modification identified to date and also the most degenerate amino acid of the heptad repeat (Chapman et al., 2007). This modification is found during early transcription similarly to serine 5, but serine 7 is more heavily involved with snRNA synthesis (Egloff et al., 2007). The observation that serine 2 phosphorylation need not precede serine 5 dephosphorylation suggests these CTD

modifications occur independently of one another. Factor-association at the promoter and CTD modification are well-established events of transcription initiation.

Co-transcriptional Modifications

RNA processing events such as 5' capping, pre-mRNA splicing, and 3' formation occur as RNAPII progresses through the chromatin. The nascent transcript in the nucleus encounters an environment full of nucleotide hydrolases that can degrade its phosphodiester bonds. The early 5' cap formation presents an unusual triphosphate link that is resistant to most nucleases and thus protects the mRNA from degradation (Shatkin, 1976). Serine 5 phosphorylation of the CTD recruits the capping machinery, encoding the triphosphatase and guanylyltransferase activities (Ho et al., 1998; Ho and Shuman, 1999). The triphosphatase cleaves the 5' triphosphate terminus of the nascent transcript into a 5' diphosphate group. Guanylyltransferase catalyzes guanosine monophosphate addition onto the diphosphate end to produce the 5' triphosphate link (Venkatesan et al., 1980). Subsequently, the terminal guanine base undergoes methylation at the N7 position through a cap methyltransferase (Mao et al., 1996). Capping of the mRNA is by far the most understood co-transcriptional event to date.

In addition to capping, mRNA splicing is a second co-transcriptional event that occurs as a sequential recruitment of the core snRNP members consisting of U1, U2, U4:U6/U5 snRNAs (Kramer, 1996). In the first step, U1 snRNP binds to the 5' splice site to form the so-called early E complex (Ruby and Abelson, 1988), and this step is facilitated by two non-snRNP factors, nuclear cap-binding complex (CBC) and ASF/SF2 (Harper and Manley, 1991; Izaurralde et al., 1994). Nuclear CBC is comprised of a

Cbp20-Cbp80 heterodimer and associates with the 5' end upon cap formation (Izaurre et al., 1994; Rozen and Sonenberg, 1987). ASF/SF2 is an SR protein rich in serine and arginine residues and stabilizes the E complex. In the second step, U2AF represents another non-snRNP that binds to the opposite 3' splice site (Ruskin et al., 1988; Zamore et al., 1992). Next, the U2 snRNP base pairs with the branch site which sits between the 5' and 3' splice sites (Zhuang et al., 1989). Finally, the U4:U6/U5 tri-snRNP complex completes the spliceosomal assembly that undergoes a conformational shift (Behrens and Luhrmann, 1991; Fortner et al., 1994; Wolff and Bindereif, 1993). Upon this switch, the complex becomes catalytically active by bringing the 5' splice site and branch site adenosine within proximity (Chiara et al., 1996; Konarska et al., 2006). The splicing reaction excises the intron in two catalytic steps. In the first step, the branch site adenosine uses its 2' hydroxyl group to form a new 2'-5' phosphodiester bond with the proximal 5' splice site to generate a lariat containing the 3' exon and free 5' exon (Kramer, 1996). In a subsequent step, the 5' exon uses its 3' hydroxyl group to form a new 3'-5' phosphodiester bond with the 3' exon by displacing the intronic portion of the lariat. According to the exon-definition model, the 3' splice site and 5' splice site for a given exon establish a bridging communication via U2AF and U1 snRNP, respectively, to designate the exon (Robberson et al., 1990). While this model readily explains the case of internal exons, the exons residing at the terminal ends require different explanation. Experiments support the idea that CBC substitutes for U2AF's lack of function at the 5' cap in first intron splicing (Izaurre et al., 1994). Analogously, PABPN1 acts in place of U1 snRNP at the 3' terminus. The reconstitution of splicing activity with in vitro transcribed RNA and nuclear extract indicates transcription and pre-mRNA splicing can

be uncoupled and the processes occur independently (Brown et al., 1986; Furneaux et al., 1985; Hernandez and Keller, 1983; Krainer et al., 1984). However, the CTD is essential for pre-mRNA splicing, suggesting the transcriptional gene product plays a role in the processing (Meininghaus et al., 2000).

Polyadenylation is similar to the capping reaction in that its product reaction protects the mRNA from exonucleases and stimulates protein synthesis. However, in contrast to 5' capping, the mechanism behind 3' end formation requires a far more complex array of polypeptides and involves cleavage followed by polyadenylation. In the 3' end of the nascent transcript, the cleavage site sits between the polyadenylation signal and G/U-rich element (Beaudoing et al., 2000; Connelly and Manley, 1988; Perez Canadillas and Varani, 2003). Polyadenylation occurs after the nascent transcript is internally cleaved by CPSF73 and ligated to a stretch of adenosines (Mandel et al., 2006). Poly(A) polymerase (PAP) is the 5' to 3' polymerase that is responsible for poly(A) tail addition, and it diverges from the traditional polymerase in that it operates template-independently (Mandel et al., 2006). Two additional complexes, CstF and CPSF, are involved in polyadenylation but are not conserved with respect to cis-element recognition and composition, respectively. The former complex is comprised of CstF50, CstF64, and CstF77 in yeast and mammals (Legrand et al., 2007). In yeast, CstF interacts with the A/U-rich element that lies upstream of the cleavage site, whereas in mammals, CstF binds the G/U-rich element that lies oppositely downstream of the cleavage site. Evolutionary pressure has led to the divergence of yeast and mammals in the composition of the CPSF complex. In mammals, CPSF consists of five polypeptides namely 30K, 73K, 100K, 160K, and hFip1, whereas in yeast, the related CPF complex contains two

subcomplexes, each of which is formed by four factors. In mammals, CPSF binds at the polyadenylation signal sequence, AAUAAA (Li et al., 2001b). Moreover, the reconstitution of polyadenylation activity with PAP, CPSF, and pre-cleaved RNA indicates the cleavage and poly(A) addition events can be uncoupled. Similar to pre-mRNA splicing, 3' end formation can be uncoupled from RNA synthesis but is dependent on the CTD of RNAPII (Manley, 1983). Physical association of the CTD with CPSF and CstF suggests the largest subunit of RNAPII recruits the 3' processing machinery. Furthermore, the physical association between CPSF and transcription initiation factor IID at the promoter implies at least parts of the 3' end formation factors load onto the transcriptional apparatus during early transcription and transfer onto the RNAPII as it leaves promoter (Dantonel et al., 1997). The nascent transcript undergoes three universal modifications that hold true for most class II genes.

Non-traditional Pathways of mRNA Processing

The aforementioned description applies to the general population of class II genes, but deviations from the fundamental models provide a better appreciation for the canonical mechanisms underlying 5' capping, pre-mRNA splicing, and 3' end formation. Most class II transcripts acquire a 5' cap structure by capping enzyme and cap methyltransferase. snRNAs are transcribed by RNAPII and thus fall under the class II category. As a result, most of these snRNAs including U1, U2, U4, U5, U7, bear a 5' cap (Bringmann et al., 1983; Southgate and Busslinger, 1989); similarly, small RNAs such as U11 and U12 snRNAs or U3 and U8 snoRNAs encounter the same fate since their promoters are RNAPII-dependent (Shimba et al., 1992). However, one distinction in

snRNA biogenesis occurs at the post-transcriptional level. Once exported into the cytoplasm, most snRNAs undergo two methyl additions by the trimethyl guanosine synthase (Hausmann and Shuman, 2005). Both methylation reactions occur at the N2 position of the 5' terminal guanine. Therefore, trimethylation serves as an additional step to the traditional monomethyl capping phase of a subset of class II RNAs undergoing processing.

In contrast to the majority of class II transcripts which receive a stretch of adenosines, the snRNA group deviates on a second general note regarding 3' end formation. Rather than undergo cleavage and polyadenylation, the nascent snRNA substitutes the traditional poly(A) signal with a 3' box. Cleavage occurs ~10 nucleotides downstream of this 3' box and bypasses the polyadenylating event entirely, leaving the snRNAs without poly(A) tails. Another group of tailess class II transcripts are the replication-dependent histones whose 3' end terminates in a stem loop (Yuo et al., 1985). The 3' end formation of the histone mRNA is complex and involves the CPSF73 endonuclease and two components that recognize the two cis-elements, a stem loop and a purine-rich downstream element (Kolev et al., 2008). The RNA component of the U7 snRNP is ~60 nucleotides in length, making it the smallest-recorded transcript directly encoded by RNAPII. Approximately 10 nucleotides at the 5' end of the U7 act as a seed sequence and anneals to the purine-rich histone downstream element. In contrast to the RNA component, SLBP and ZFP100 are protein components that bind the conserved stem loop region (Dominski et al., 1995; Wagner and Marzluff, 2006). Together, these recognition elements serve as guides to ensure CPSF73 cleaves between the designated

demarcations. In short, snRNAs and histone mRNAs represent the rare cases of poly(A) tailless class II transcripts.

A third exception to the general guidelines of class II transcript processing lies in pre-mRNA splicing. Most class II transcripts undergo splicing through a U1- and U2-dependent pathway. However, a few pre-mRNAs utilize a different set of cis-elements and trans-acting splicing factors to excise their introns. The consensus sequence about the 5' splice site and branch site are markedly distinct and longer in these rare instances. Similarly, the 3' splice site is loosely defined in terms of sequence conservation. However, the branch site adenosine remains conserved in this non-canonical pathway. Variation in cis-elements requires a different set of cognate trans-factors. U11, U12, and U4atac:U6atac snRNPs are the functional equivalence to the canonical U1, U2, and U4:U6 snRNPs (Kolossova and Padgett, 1997; Tarn and Steitz, 1996a, b; Wu and Krainer, 1997). However, the U5 snRNP is the single component common to both major and minor splicing pathways.

Exon Junction Complex (EJC) and Nuclear Export

Certain proteins dictate the maturation state of the nascent transcript and influence its transport across the nuclear envelope. PABPN1 is one such protein that spreads itself in multitude along the poly(A) tail. A larger entity in the form of a ~300 kDa EJC is deposited about 20 nucleotides upstream of each newly formed exon-exon junction. In mammals, the EJC macromolecule consists of five proteins, namely RNPS1, SRm160, Y14:Magoh, and Aly (Lau et al., 2003). Deposition of the EJC components on a pre-mRNA undergoing splicing has been dissected temporally. Three components, RNPS1,

SRm160, and Aly pre-assemble on the nascent transcript prior to splicing, whereas the stable Y14:Magoh heterodimer completes the EJC assembly sometime during the splicing reactions (Custodio et al., 2004; Kataoka and Dreyfuss, 2004). An mRNA which is fully saturated with EJCs is indicative of a mature mRNP. In mammals, the switch from a mature mRNP to an export-competent mRNP is triggered by the Aly subunit which is a common component of the EJC and the TREX complex (Reichert et al., 2002; Strasser et al., 2002). In mammals, the TREX macromolecule consists of four components including the stable THO complex, UAP56, hTex1, and the Aly subunit (Strasser et al., 2002). The common Aly substituent mediates the communication between the mRNP and Tap, an essential export factor. The major exceptional case made in yeast lies in the fact that its genome is relatively intronless and thus does not employ EJC deposition. However, the yeast TREX complex is conserved with respect to the THO complex, Sub2p/UAP56, Tex1p/hTex1, and Yra1p/Aly subunits which are found in mammals. Similarly, yeast Yra1p/Aly function is conserved in that it mediates the interaction between the mature mRNP and Mex67p/Tap (Strasser et al., 2002). Mex67p/Tap is a functional component that equips the mRNP with the capability to interface with the nuclear pore as it crosses the bilayer membrane. Unlike certain snRNAs, snoRNAs, miRNAs, and shuttling proteins which leave the nucleus in a canonically karyopherin-dependent manner, mRNA nuclear export occurs in a karyopherin-independent fashion and thus is unaffected by the RanGTP-RanGDP gradient across the nuclear bilayer (Lange et al., 2007).

Cap-dependent Translation Initiation

Upon arrival in the cytoplasm, the mRNP conservatively sheds two nuclear proteins, CBC and PABPN1, in exchange for eIF4E and PABPC1, respectively, which mediate translation of the codons into amino acids. Translation initiation is best understood in terms of 5' cap dependence and scanning mechanism. The 5' cap serves as a recognition motif for the translation initiation complex eIF4F, composed of eIF4A, eIF4G, and eIF4E. eIF4A is an ATP-dependent helicase and is believed to function in unwinding the 5' UTR secondary structure during ribosomal scanning (Ray et al., 1985). eIF4E is the direct cap-binding subunit (Altmann et al., 1987). Lastly, eIF4G serves as a scaffold and bridges the association between eIF4A and eIF4E (Li et al., 2001a). eIF4F assembly on the 5' cap disrupts the secondary structure of the 5' UTR to permit ribosomal scanning. The eIF4F complex is subject to two modes of regulation. Cap structure, m⁷GpppG, and related derivatives such as m⁷Gpp and m⁷Gp cap derivatives act as competitive inhibitors to eIF4E cap-binding ability (Altmann et al., 1988) and can potentially negatively regulate cap-dependent translation initiation (Adams et al., 1978). On the other hand, the eIF4E-binding protein (4EBP) family consists of three members, each of which can bind eIF4E at the interface recognized by eIF4G (Haghighat et al., 1995; Pause et al., 1994; Poulin et al., 1998). In doing so, 4EBP prevents eIF4F assembly and permits the secondary structure of the 5' UTR to impede the scanning ribosome. 4EBP also responds to upstream signal molecules such as insulin, growth factors, and amino acids and operates downstream of the mTOR pathway (Choi et al., 2003). Moreover, 4EBP is a phosphoprotein wherein phosphorylation disrupts its interaction

with eIF4E. Translation initiation is sensitive to the complex assembly that recognizes its 5' cap.

Normal translation initiation proceeds with the necessary formation of the ternary complex comprised of methionine-initiator tRNA, GTP:eIF2 G protein (Ranu and London, 1979; Thach et al., 1966). The ternary complex along with at least three initiator factors namely eIF1, eIF1A, and eIF3 associates with the 40S ribosome (Pestova et al., 2001). This 43S ribosomal complex enters the 5' end to form the 48S ribosome and scans the RNA in a linear manner until it encounters a start codon in the context of a Kozak sequence, $\text{GCCGCCA}^{-3}\text{CCA}^{+1}\text{UGG}^{+4}$, where the purines at positions -3 and +4 are essential for translation initiation (Kozak, 1986). This is typically the first AUG codon encountered by the scanning ribosome. However, the consensus sequence is not rigidly conserved in yeast. Along with complexes that recognize the 5' cap and scan for the start codon, a G protein cycle contributes to this early stage of translation as well. eIF1 is a fidelity factor that checks for accurate base pairing between the mRNA start codon and initiator tRNA anti-codon in the ribosomal P site (Pestova et al., 1998). Similarly, the timing of GTP hydrolysis by eIF2 G protein is controlled by the eIF5 GAP to ensure accurate base pairing between the initiator tRNA anti-codon and the authentic start codon (Huang et al., 1997). A second round of GTP hydrolysis through eIF5B G protein occurs upon the formation of the 80S ribosome (Pestova et al., 2000). The events that follow the 5' cap-dependent step assemble the ribosome in such a way that its methionine-linked tRNA component aligns with the template start codon.

Translation Elongation

In contrast to translation initiation, translation elongation is relatively conserved between eukaryotes and prokaryotes. The 80S ribosome contains three adjacent tRNA-binding sites that are located with respect to the 5' to 3' orientation of mRNA: exit (E), peptidyl (P), and aminoacyl (A) sites (Gnirke et al., 1989). The present description of the elongation phase begins with the step where a peptidyl tRNA occupies the P site and where the A site is vacant. A ternary complex composed of GTP:eEF1A and an aminoacyl tRNA binds the vacant A site (Dreher et al., 1999). Analogous to the G proteins during translation initiation, the eEF1A G protein ensures accurate base pairing between the mRNA codon and tRNA anti-codon in the A site (Carr-Schmid et al., 1999). After GTP hydrolysis, GDP:eEF1A dissociates and leaves the aminoacyl tRNA in the A site. The EF-Tu G protein performs an equivalent function in prokaryotes (Chinali and Parmeggiani, 1980). The 60S-resident peptidyl transferase center catalyzes peptide bond formation between the peptidyl group and aminoacyl tRNA, thereby elongating the peptide in an N- to C- terminal direction by a single amino acid. Analogous to the catalytically-active bacterial 23S rRNA of the 50S ribosome, the eukaryotic counterpart presumably lies in the 28S rRNA component of the 60S ribosomal core whose catalytic potency is suspect in the activation of the aminoacyl tRNA (Ban et al., 2000; Hansen et al., 2002; Nissen et al., 2000). In a substrate-substrate charge mechanism using the 23S as the case model, the terminal amino group of the aminoacyl tRNA attacks the carboxyl group of the peptidyl-tRNA ester bond that resolves into a deacylated tRNA in the P site and newly-synthesized peptidyl tRNA in the A site (Hansen et al., 2002). The peptidyl tRNA lies in a skewed hybrid state such that its peptide portion lies in the pre-occupied P

site whereas its tRNA part remains in the A site (Moazed and Noller, 1989). GTP hydrolysis by EF2 G protein, equivalent to prokaryotic EF-G, relieves the hybrid distortion and stimulates the 80S ribosome to shift three-nucleotide positions toward the 3' end of the mRNA (Skogerson and Wakatama, 1976). This shift completes the translocation of deacylated tRNA into the E site and newly-extended peptidyl tRNA into the P site, vacating the A site for an incoming aminoacyl tRNA for another round of elongation until encountering a stop codon. eRF1 enters the A site in recognition of three stop codons, UAG, UGA, and UUA, to coordinate water addition to the peptidyl-tRNA ester bond that releases the full-length peptide (Frolova et al., 1994; Song et al., 2000). By contrast, prokaryotes employ two release factors, RF1 and RF2, in recognition of UAG and UGA, respectively, in addition to the UAA codon (Grentzmann and Kelly, 1997). Thus, the nascent mRNP is converted into an efficient protein manufacturer through a conserved cycle of aminoacyl-tRNA loading, peptide bond formation, ribosomal translocation that primes its A site for aminoacyl-tRNA reloading.

Cap-independent Translation

Cap-dependent translation is an exclusive feature of eukaryotic translation initiation but viral systems have adopted various mechanisms that bypass or assimilate the host's machinery for the benefit of their own viral program. In order for a virus to make use of its host's cap-dependent translation machinery, a 5' cap is a prerequisite that is solely conferred by triphosphatase, guanylyltransferase, and methyltransferase activities. In one instance, vaccinia virus, bamboo mosaic, tobacco, brome mosaic viruses evade this impediment and have evolved their own capping activities that disguise their

own viral transcripts as cellular mRNAs. In another scenario, the influenza virus relies on its own endonuclease to cleave off the 5' capped ends of cellular mRNA so that its own 5' to 3' polymerase salvages the fragments as short primers to synthesize its viral transcripts (Dias et al., 2009). In a third instance, the L-A and vaccinia viral decapping proteins hydrolyze cellular mRNAs to give their own viral mRNAs a competitive advantage in cap-dependent translation (Parrish et al., 2007). Still other viruses prefer non-coding cis-elements to initiate cap-independent translation. Such adaptive pressures have led some viral systems to utilize a structured cis-element called an internal ribosomal entry site (IRES) which completely or partially bypasses the cap requirement for initiation factors to initiate translation. They have been categorized into groups I through IV whose ascending order corresponds to increased dependence on cellular factors (Fraser and Doudna, 2007; Ho et al., 2000; Kieft, 2008). Group I members are independent of the cellular machinery and include the Cricket paralysis virus, *Plautia stali* intestine virus, and Taura syndrome virus (Bushell and Sarnow, 2002). These viruses contain an IRES that is sufficient to recruit the cellular 40S ribosome on its own and operate independently of the methionine-initiator tRNA. Group II viruses consist of classical swine fever virus, hepatitis C virus, and porcine teschovirus 1, and these viral systems use an IRES that binds the 40S ribosome directly and operates independently of the scanning mechanism (Fraser and Doudna, 2007). The IRES employs a subset of cellular factors comprised of the eIF2 G protein, eIF3, and methionine-initiator tRNA (Ohlmann et al., 1996). Group III viral entities use nearly most of the cellular initiation factors such as eIF4A, eIF4G, and IRES trans-activating factors (ITAFs) in addition to those of Group II and are found in encephalomyocarditis virus, foot-and-mouth-disease

virus, and theiler's murine encephalomyelitis virus (Kolupaeva et al., 1998). Group IV is most reliant on the cellular machineries and requires a supplemental source of extract along with ITAFs to recruit the ribosome and include poliovirus and rhinovirus (Kieft, 2008). Viral gene expression systems have evolved various means to compete against, bypass, or adopt the host's machineries at the translation level.

General mRNA Degradation

The general mRNA decay pathways are conserved in yeast and humans with respect to a common set of factors. The core components consist of deadenylases, exonucleases, and decapping enzymes. In eukaryotes, the initial step involves the removal of the poly(A) tail by the yeast and mammalian deadenylase components Ccr4p/Pop2p and Ccr4/Caf1 (Chen et al., 2002; Moser et al., 1997). The predominant 3' mRNA decay pathway relies on the exosome to degrade the mRNA from the 3' end until it reaches a few oligonucleotide lengths away from the 5' cap, which in turn serves as substrate for the scavenger decapping protein named Dcs1 or DcpS in yeast and mammals, respectively (Liu et al., 2002). In the 5' mRNA decay pathway, the subsequent step is followed by the decapping protein Dcp2 which hydrolyzes the 5' cap (Wang et al., 2002). This exposes the 5' end to exonuclease degradation by Xrn1 (Amberg et al., 1992; Larimer et al., 1992). Xrn1 has a nuclear counterpart by the name of Rat1 exonuclease and appears to be responsible for snoRNA and rRNA processing (Petfalski et al., 1998). In summary, yeast and mammals use two major mRNA degradation pathways that are highly conserved in terms of factor involvement.

The exosome is the major eukaryotic 3' exonuclease that is conserved in yeast and humans. Yeast and human exosomes overlap in at least ten common subunits, namely Rrp40, Csl4, Rrp4, Rrp45, Rrp41, Rrp42, Mtr3, Rrp43, Rrp46, and Rrp6 (Liu et al., 2006; Mitchell et al., 1997; Shen and Kiledjian, 2006). The subset comprised of Rrp45, Rrp41, Rrp42, Mtr3, Rrp43, and Rrp46 form the core six-member ring and is associated with the ternary complex composed of Rrp40, Csl4, and Rrp4. In yeast, the catalytic activities reside exclusively with the loosely tethered components of the exosome, Rrp6p and an 11th member, Rrp44p (Bonneau et al., 2009; Phillips and Butler, 2003). Surprisingly, Rrp44p exhibits an additional endonuclease activity within its PIN domain (Schneider et al., 2009), which is distinct from its exonucleolytic RNase R domain (Barbas et al., 2008). In humans, Rrp6 is the exclusive catalytic subunit, whereas the interaction between Rrp44 and the exosome remains to be demonstrated (Liu et al., 2006). Another noteworthy observation indicates the exosome has a prokaryotic origin. The archaeal exosome is structurally and functionally similar to that of eukaryotes. The archaeal core six-member ring is comprised of an alternating arrangement of the Rrp41 and Rrp42 subunits and is associated with a ternary complex of either Csl4 or Rrp4 (Lorentzen et al., 2005). In contrast to eukaryotic exosome which promotes water addition to break phosphodiester bonds, the archaeal exosome relies on its Rrp41 and Rrp42 subunits to catalyze inorganic phosphate addition as a means to disrupt the phosphodiester bonds of mRNA (Lorentzen et al., 2005). In general, the exosomes are conserved in regards to the core ring structure but evolutionarily divergent in terms of the subunit(s) that bears the catalytic activity and the type of enzymatic activity.

Transcript-specific Degradation

In some instances, mRNA degradation occurs in a sequence-specific manner through cognate protein-mRNA recognition. AU-rich element (ARE)-mediated degradation relies on specific protein-RNA interactions to exert temporal influence over metabolic proteins, transcription factors, cell cycle regulators, hormones, cytokines, growth factors at the transcript level. TTP is the best studied ARE-binding protein and accelerates the decay of TNF-alpha and GM-CSF mRNAs (Lai et al., 1999; Lai et al., 2000). Its CCCH zinc finger motif is necessary and sufficient to bind to class II ARE cis-elements having the consensus, AUUUA, which cluster in the 3' UTR of the target mRNA (Carballo et al., 1998). BRF1 and BRF2 are paralogs of TTP that have a similar zinc finger motif that directs ARE-binding and transcript degradation (Franks and Lykke-Andersen, 2007). More specifically, ARE-mediated degradation induces rapid transcript decay by stimulating poly(A) tail removal (Lai et al., 1999). Another ARE-binding protein is KSRP and negatively regulates iNOS and IL8 transcripts through a KH domain rather than a zinc finger motif (Gherzi et al., 2004; Linker et al., 2005; Winzen et al., 2007). In contrast to ARE-binding proteins that elicit gene repression, HuR is a unique ARE-binding protein that promotes stabilization of mRNAs such as TNF-alpha, XIAP, and IL4 transcripts (Atasoy et al., 2003; Zhang et al., 2009). Still, there are at least two instances of ARE-independent mechanisms that drive transcript-specific degradation. Dcp2 is a representation of such a category and promotes Rrp41 mRNA degradation via recognition of a 60 nucleotide region in its 5' UTR (Li et al., 2008). In a fourth and final example of protein-RNA interaction triggering transcript decay mechanisms, Edc3p

stimulates decapping and degradation of the Rps28b mRNA through its 3' UTR (Badis et al., 2004).

In contrast to protein-RNA interactions, eukaryotes have evolved RNA-RNA interactions as an additional means to induce specific mRNA degradation (Bagga et al., 2005). miRNAs are derived mainly from the exonic or intronic products of class II promoters and less so from those of class III. The initial pri-miRNAs are the direct products of transcription and are truncated by the double stranded RNA-specific endonuclease activity of Drosha into ~65 nucleotide stem loop structures (Lee et al., 2004). The resultant pre-miRNA stem loop is exported into the cytoplasm by a karyopherin receptor and further truncated into the mature ~22 nucleotide RNA duplex by the double stranded RNA-specific endonuclease Dicer (Lee et al., 2002). The miRNA guide strand is loaded onto the RISC complex that bears the core Ago subfamily and directs mRNA decay or translational silencing through interaction with the 3' UTR (Jinek and Doudna, 2009). miRNAs contain a conserved six nucleotide seed region at its 5' end that base pairs perfectly with the 3' UTR, whereas siRNAs base pair perfectly throughout its length (Bartel, 2004). The Ago subfamily contains three conserved domains, namely the N-terminal PAZ domain, the central MID domain, and the C-terminal PIWI domain (Jinek and Doudna, 2009). The PAZ and MID domains contact the 3' and 5' ends of the guide strand, respectively, whereas the PIWI domain, which is structurally similar to RNase H, contains the catalytic site, if present at all (Wang et al., 2009). However, the Ago subfamily diverges evolutionarily beyond the homology criterium. Of the four human Ago members, Ago2 is the exclusive member that bears endonuclease activity. By contrast in flies, both Ago1 and Ago2 possess catalytic activity. In addition, *Drosophila*

Ago2 appears to preferentially load siRNAs rather than miRNAs. In plants, Ago1 and Ago7 possess endonuclease activity, whereas Ago4 and Ago6 induce transcriptional silencing through heterochromatin formation (Jinek and Doudna, 2009). In fission yeast, Ago1 promotes heterochromatin formation (Irvine et al., 2006). These studies show RNA-RNA interaction leads to a gene repression program that involves more than mRNA degradation.

The mechanism surrounding Ago-mediated gene repression points toward mRNA degradation and translational silencing. The Ago subfamily in the context of an miRNA-loaded RISC complex may direct the mRNA target toward mRNA degradation. In *Drosophila melanogaster*, an mRNA that is cleaved internally to produce 5' and 3' fragments are generally degraded by the 3' and 5' general mRNA decay pathways, respectively (Orban and Izaurralde, 2005). Studies in two different organism models suggest the RISC complex directs cap and poly(A) tail removal to accelerate mRNA decay. In fly miRNA systems, a reporter target accumulates upon deadenylase and Dcp2 knockdowns (Behm-Ansmant et al., 2006). Similarly, in the zebrafish model, miR-430 directs deadenylation of its target mRNA (Eulalio et al., 2007). On the other hand, at least two studies suggest the Ago subfamily may direct translational silencing by blocking the early cap-recognition step or later elongation phase. One report states Ago is a cap-binding protein that may compete for eIF4E for the 5' cap and may influence the step of translation initiation (Kiriakidou et al., 2007). Mutation of the critical residues for cap-binding counters the translational repression induced in an miRNA-mediated reporter system. Alternatively, translational silencing may occur by blocking 80S ribosome assembly or induce premature displacement of the 80S ribosome during translation

elongation. An miRNA reporter target with six cognate binding sites in its 3' UTR is more dissociated from ribosomes in the presence of translational inhibition by hippuristanol (Petersen et al., 2006). Furthermore, usage of the Hepatitis C or Cricket paralysis viral IRES-directed miRNA reporter also recapitulates the dissociation from ribosome, suggesting small RNA-mediated silencing occurs at a step subsequent to translational initiation. Therefore, the miRNA/siRNA-associated Ago subfamily adds a separate regulatory layer of complexity to post-transcriptional mechanism through RNA-RNA interactions.

Nucleoside Diphosphate Linked Moiety X (NUDIX) Decapping Enzymes

The NUDIX family is a group of nucleotide hydrolases that contain the 23 amino acid motif, GX₅EX₇REUXEEXGU, where the glutamates are essential for catalysis and X denotes any residue (Cartwright and McLennan, 1999). NUDIX decapping proteins exist from bacteria through humans. Dcp2, X29, NUDT16 are NUDIX proteins that are interspersed throughout the subcellular space. The common feature of these proteins is the presence of a prokaryote-derived NUDIX domain and a capacity to bind RNA (Bessman et al., 1996). Dcp2 is a well-defined decapping protein in terms of its function, biochemistry, and subcellular location. Dcp2 orthologs span the interspecies spectrum from yeast through humans. As mentioned previously, Dcp2 functions at the step subsequent to deadenylation in yeast and exposes the 5' end of the mRNA to Xrn1-mediated degradation (Dunckley and Parker, 1999; Wang et al., 2002). Dcp2 hydrolyzes the 5' cap of mRNA as substrate to release m⁷Gpp and RNA with a 5' monophosphate in a divalent cation-dependent manner. Dcp2 acts sufficiently on its own but also responds

to regulators, namely activators such as Edc1/2/3, Hds, Dhh1, Lsm1-7, Ge-1, p54, Pat1, and Dcp1 (Bonnerot et al., 2000; Collier and Parker, 2005; Dunckley et al., 2001; Fischer and Weis, 2002; Schwartz et al., 2003; Xu et al., 2006; Yu et al., 2005). In contrast, the roster of negative Dcp2 regulators is more modest and includes eIF4E, PABP and VCX (Jiao et al., 2006; Khanna and Kiledjian, 2004). At the subcellular level, Dcp2 is cytoplasmic and concentrates densely in areas known as P bodies, which are potential sites of 5' mRNA degradation or temporary storage of miRNA-repressed mRNAs (Behm-Ansmant et al., 2006; Fillman and Lykke-Andersen, 2005). Similarly, Dcp1 colocalizes to P bodies as well and stimulates Dcp2 catalytic activity in yeast rather than possess intrinsic decapping activity (She et al., 2008; Xu et al., 2006). X29 is a nucleolar NUDIX protein found throughout the animal kingdom from worms through humans and exists as a homodimer (Ghosh et al., 2004; Peculis et al., 2004; Scarsdale et al., 2006). X29's was initially discovered in frog, and the enzyme preferentially hydrolyzes U8 snoRNA in vitro. In contrast to Dcp2, X29 has a loose substrate preference and hydrolyzes mono- and tri-methylated 5' cap of RNA. Human X29 ortholog, Nudt16, is another nucleolar NUDIX protein that decaps U8 snoRNA (Peculis et al., 2007) as well as monomethyl 5' capped RNA. The NUDIX family is an evolutionarily diverse group of nucleotide hydrolases whose functions and substrate specificities are defined.

Histidine Triad (HIT) Hydrolases

The HIT family of nucleotide-binding and -hydrolyzing proteins span from bacteria through mammals. HIT members include FHIT, Hint, GaIT, aprataxin, and DcpS, and the five proteins share the conserved motif H-X-H-X-H-X-X where H is histidine

and X is any hydrophobic residue. These proteins typically homodimerize and exhibit nucleotide hydrolytic or transferase activities, nucleotide-binding activity, and are linked to disease. The FHIT locus has been mapped to the short arm of chromosome region 3p14.2, marked by genomic instability due to frequent deletions, integrations, and translocations (Hassan et al., 2010). This region is home to familial-kidney-cancer translocation, papilloma virus integration site, and the human genome's most unstable locus, FRA3B. Loss of FHIT itself has been linked to a variety of human tumors of lung, cervix, stomach, pancreas, and kidney origin (Ohta et al., 1996). Therapeutic correction of mice implanted with a tumorigenic cell line overexpressing FHIT indicates its tumor suppressive potency. FHIT has been understood on the biochemical level. It binds and hydrolyzes nucleotide substrates, diadenosinopolyphosphates, specifically ApppA and AppppA (Pace et al., 1998). However, FHIT hydrolytic activity is unlinked to its tumor suppressive activity. Secondly, Hint1 hydrolyzes adenosine monophosphoramides such as AMP-NH₂ and AMP-Lys (Chou and Wagner, 2007). Mice knocked out for Hint1 has led to a higher incidence of squamous tumors and thus indicated its potential tumor suppressive activity (Su et al., 2003). Hint1 is related to Hint2 and Hint3, which are less understood. Hint2 exhibits hepatic- and pancreatic-preferential tissue expression and is expressed less so in brain, heart, kidney, and lung (Martin et al., 2006). On the subcellular level, Hint2 localizes to mitochondria, whereas Hint1 localizes to both nucleus and cytoplasm. Thirdly, GalT is the causative link in a metabolic genetic disorder known as classical galactosemia. Biochemically, it catalyzes the transfer of UMP from UDP-glucose to galactose-1-P in the essential step of galactose biosynthesis (Satomi and Kishimoto, 1981). Fourthly, aprataxin has been associated with ataxia-oculomotor

aprataxia 1, a neurodegenerative disease and functions in DNA repair. An N-terminal Forkhead domain and C-terminal Zn finger domain flanks its HIT motif (Satomi and Kishimoto, 1981). Evolutionarily, it is the closest relative to FHIT, but aprataxin also exhibits 31% identity with Hint in mammals over an 86 amino acid stretch. On the subcellular level, aprataxin localizes to the nucleus and nucleolus. Aprataxin hydrolyzes FHIT substrate ApppA and as well as Hint1 substrate AMPNH₂, confirming its phylogenetic relationship with other HIT members (Seidle et al., 2005). Finally, DcpS hydrolyzes the 5' cap structure of mRNA.

Until recently, DcpS has remained the sole HIT protein without a link to a disease. New studies show a lead compound that inhibits DcpS catalytic activity and improves lifespan and motor function of a Spinal Muscular Atrophy mouse model (Singh et al., 2008). The HIT motif has its roots in a prokaryotic origin. In streptococcal pneumoniae, the Pht family is the prokaryotic ancestor to the eukaryotic HIT family and consists of four members comprised of PhtA, PhtB, PhtD, and PhtE. In contrast to eukaryotic HIT proteins, the bacterial Pht members harbor multiple HIT motifs and are transmembrane proteins (Adamou et al., 2001). The function of this family is unknown, but injection of this family of proteins in mice prevents pneumococcal infection and mortality. Therefore, the HIT genes encode an old family of nucleotide hydrolases with broad functionality and diverse clinical manifestations.

DcpS, a Catalytic Cap-Binding Protein

The identification of DcpS is a cornerstone in the study of cap-binding proteins, and its discovery marks the first cap-binding protein that exhibits enzymatic activity.

Discovery of its activity originates from an early study that has detected a nucleotide hydrolyzing activity (Nuss et al., 1975). Three decades pass prior to its identification from cytosolic extract (Liu et al., 2002; Wang and Kiledjian, 2001). Its activity is specific for the 5' cap of mRNAs albeit following degradation of the phosphodiester bonds. Unlike the monomeric Cbp20 and eIF4E cap-binding prototypes which are associated with the upregulation of gene expression, DcpS plays a role in mRNA degradation and exists natively as a homodimer that can bind two cap ligands simultaneously (Gu et al., 2004). Among interspecies distinctions, the yeast genome encodes two DcpS orthologs, whereas the genome of worms or mammals encodes one DcpS ortholog (Lall et al., 2005). Another discrepancy occurs in the subcellular aspect. In yeast and worm embryos, DcpS resides in the cytoplasm, whereas mammalian cells retain DcpS within the nucleus (Malys and McCarthy, 2006). From yeast through humans, DcpS unequivocally catalyzes a substitution reaction using a nucleophilic residue within the Histidine Triad (HIT) motif to attack the triphosphate link of cap structure at the alpha phosphate position (Liu et al., 2002). The hydrolysis of cap substrate, m⁷GpppG, by DcpS releases m⁷GMP and GDP as products. Despite its purification from cytoplasmic extract (Liu et al., 2002) and characterization with cytoplasmic factors (Cohen et al., 2004; Liu et al., 2002; van Dijk et al., 2003), DcpS is predominantly if not exclusively a nuclear protein by cytological criterium (Cougot et al., 2004; Liu et al., 2004; Salehi et al., 2002).

Broader functions of DcpS

The existent data suggests DcpS is a protein with a predominantly cytoplasmic role. Eukaryotic mRNAs are degraded by either of two cytoplasmic general decay

pathways that differ in the direction in which the exonucleases consume the mRNA. In mammals, the mRNA is degraded from the 3' end by the exosome complex (Mitchell et al., 1997) until a few nucleotides extend off the cap. DcpS hydrolyzes the 5' cap substrate (Wang and Kiledjian, 2001). A previous work also illustrates DcpS can displace eIF4E from capped RNA based on in vitro competition assay (Liu et al., 2004), suggestive of a role in cap-dependent translation. Recent experiments reveal an auto-regulatory mechanism whereby DcpS positively influences the alternative 5' to 3' mRNA degradation pathway (Liu and Kiledjian, 2005). Fourthly, from an evolutionary perspective, DcpS is a cytoplasmic protein in yeast. These four data share a common theme, and that is DcpS exerts post-transcriptional regulatory influence over the cytoplasmic compartment. However, mammalian DcpS nuclear localization contrasts starkly against these data and strongly indicates an unassigned nuclear function (Cougot et al., 2004). The present work shows DcpS is a nucleocytoplasmic shuttling protein that regulates at least two nuclear events, pre-mRNA first intron splicing and transcription. The last set of experiments indicates DcpS is an essential gene during mouse embryogenesis. The work presented in this thesis addresses the nuclear functions and biological relevance of DcpS through cell-based reporter systems and a knockout mouse model.

MATERIALS AND METHODS

Plasmid constructs

The pcDNA3-Flag-DcpS plasmid that expresses Flag-tagged DcpS in mammalian cells was made by inserting the DcpS open reading frame flanked by a BamHI site at the 5' end and an XhoI site at the 3' end into the pcDNA3-Flag vector (Fenger-Gron et al., 2005). pcDNA3-Flag-DcpS^{ΔKR} containing a deletion of amino acids 10–13 of DcpS was derived from pcDNA3-Flag-DcpS construct by using site-directed mutagenesis (Stratagene) according to the manufacturer's instructions. The pEGFP-DcpS plasmid encoding GFP-DcpS was constructed by inserting the DcpS open reading frame into the EcoRI and BamHI sites of the pEGFP-C1 (Clontech) vector. pEGFP-DcpS^{L148/150A} was made by using two rounds of site-directed mutagenesis of the parental pEGFP-DcpS vector. The DcpS-specific shRNA expression construct, pSHAG1-puro-DCPS, was generated by inserting a double-stranded shRNA that encodes the following mature RNA: 5' TGCAGTTCTCCAATGATATCTACAGCAC 3' into the BseRI and BamHI sites of the pSHAG1-puro vector (Paddison et al., 2002) modified with the addition of a puromycin selection marker. The pSHAG1 construct was kindly provided by Dr. Gregory J. Hannon (Cold Spring Harbor Laboratory, New York). The pcDNA3-Flag-Cbp20 construct was designed by inserting the Cbp20 open reading frame derived by reverse transcription and PCR-amplification from human K562 cell RNA. The PCR product containing a BamHI and EcoRI site was inserted into the same sites of the pcDNA3-Flag plasmid. pcDNA3-myc-PK-hnRNPA1 was kindly provided by Dr. Serafin Piñol-Roma (CUNY Medical School, New York) and has been previously described (Michael et al., 1995)(Siomi and Dreyfuss, 1995). The rat fibronectin reporter construct, p773B, was

kindly provided by Dr. Samuel Gunderson (Rutgers University, New Jersey) and previously described (Norton and Hynes, 1990). The His-Cbp20 construct was kindly provided by Dr. Stephen Cusack and has been previously described (Mazza et al., 2002). The Renilla-HCV IRES-Firefly luciferase was cloned between the NheI and HindIII sites of the pcDNA3.1 vector (Invitrogen) to generate the dicistronic pcDNA3.1 Renilla-HCV IRES-Firefly. The Renilla luciferase coding region was cloned between the NheI and XbaI sites of the pIRES plasmid (Clontech) to generate the pIRES-EMCV Renilla luciferase construct. The 4EBP1 clone TRCN0000040206 and 4EBP2 clone TRCN0000117812, and pLKO.1-puro MISSION shRNA constructs were purchased from Sigma Aldrich. psPAX2 and pCMV-VSV-G constructs, encoding packaging and envelope proteins, respectively, were used. Sequences for all primers are listed in Table 2.

Cell lines, transfections, lentiviral infections, D156844 stock

HeLa, NIH3T3, and 293T cell lines were grown in DMEM (Invitrogen) supplemented with 10% fetal bovine serum, penicillin–streptomycin, sodium pyruvate under 5% CO₂ at 37°C. 293T cells were grown in the presence of 80 µg/mL G418. Unless otherwise stated, all transfections were carried out with Lipofectamine 2000 (Invitrogen) according to the manufacturer's instructions. The 293T cell line stably transformed with the construct expressing an shRNA targeting DcpS (293T^{DcpS-KD}) or expressing the empty pSHAG1-puro vector were generated by transfecting pSHAG1-DcpS or pSHAG1-puro, respectively. After 48 h of transfection, cells were placed under 0.5 µg/mL G418 and 3 µg/mL puromycin selection. Clonal cell lines were isolated by plating the population into

a 96-well plate such that one colony occupied a single well under puromycin and G418 selection, and the colony with the most efficient DcpS protein level reduction was expanded and used. 4EBP1 and 4EBP2 stable 293T cell lines were produced from lentiviral infection. 293T cells were transfected with M Stable 4EBP1 and 4EBP2 were made by co-transfection of 2 μ g MISSION shRNA construct along with 2 μ g psPAX2 and 1 μ g pCMV-VSV-G constructs using Lipofectamine 2000 according to manufacturer's instructions. At 24 hours post-transfection, medium was replaced with fresh growth medium. Supernatant containing lentiviral particles was harvested at 48 hours post-transfection and used for subsequent infections. 293T cells were infected with 1/4 volume overnight, and medium was replaced at 24 hour post-transfection with fresh growth medium. At 48 hours post-transfection, cells were placed under 3 μ g/mL puromycin selection. D156844 was kindly provided by deCODE Inc. and was dissolved directly into DMSO to achieve a 10 mM stock.

Mapping of DcpS gene trap and mouse genotyping

DcpS heterozygous mice were purchased from BayGenomics. Genomic DNA was isolated from adult mouse tails using the Wizard Genomic DNA Purification Kit (Promega). Multiplex PCR used three primers to amplify a wildtype band and mutant band for genotyping. One forward primer annealed to a region upstream of the gene trap cassette in an intronic region. A second reverse primer annealed to a region within the gene trap cassette so as to amplify a 1.6 kb mutant band. A third reverse primer annealed to a region downstream of the gene trap cassette in an intronic region to amplify a 550 bp wildtype fragment. PCR products were analyzed on 1% agarose gel. Similar genotypic

analysis was implemented toward embryos as per manufacturer's instructions. Sequences for all primers are listed in Table 2.

Heterokaryon assay

Heterokaryon assays were carried out as described (Pinol-Roma and Dreyfuss, 1992) with minor modifications. Briefly, HeLa cells were co-transfected with 4 μ g pcDNA-Flag-DcpS and 4 μ g pcDNA3-myc-PK-hnRNPA1 in 60-mm plates. 3T3 cells were seeded onto coverslips in a six-well plate on the same day. At 24 h post-transfection, HeLa cells were trypsinized and seeded onto 3T3 cells at a density 2 times that of the mouse cells. Cell attachment to the coverslip was allowed for 5 h, followed by addition of 100 μ g/mL cycloheximide 1 h prior to cell fusion. Human and mouse cells were fused by 50% PEG 3350 (Sigma) for 90 sec. Cells were washed of residual PEG and incubated for an additional 4 h in the presence of cycloheximide prior to visualization by indirect immunofluorescence. Where indicated, 20 ng/mL Leptomycin B (LMB) was added to the cell during the seeding following trypsinization and maintained in LMB throughout the duration of the experiment.

Immunofluorescence, westerns, mouse tissue, and X-gal staining embryos

Mouse anti-Flag (Sigma) was used at a dilution of 1:10,000 for Western and 1:500 for immunofluorescence. Rabbit anti-myc (Santa Cruz) was used at a dilution of 1:200 for immunofluorescence. Secondary anti-rabbit and anti-mouse (ImmunoJackson) were used at a dilution of 1:200 for immunofluorescence. Cells were fixed and permeabilized as previously described (Liu et al., 2004) and visualized using the Axiovision 4.1 software

and an Olympus 100 M Axiovert microscope. Rabbit anti-4EBP1 (Cell Signal), rabbit anti-4EBP2 (Cell Signal), anti-beta-actin (Santa Cruz), Goat anti-beta-tubulin (Sigma Aldrich) were used at a dilution of 1:1000. Mouse anti-GAPDH (Abcam) was used at a dilution of 1:2000. Mouse tissues were isolated from adult mice euthanized by cervical dislocation. 1X PBS was added to each sample and sonicated to homogeneity at 4°C and resolved on 15% SDS-PAGE. Proteins were transferred onto nitrocellulose membrane (BioRad) by semi-dry procedure. Secondary anti-rabbit, anti-mouse, and anti-goat (ImmunoJackson) were used at a dilution of 1:10000 for western blot.

UV cross-linking, EMSA, decapping assay

UV cross-linking reactions were carried out as described (Liu et al., 2004). Briefly, 30 pmol of His-CBP20 were preincubated with ³²P-labeled cap structure (2–5K cpm) in IVDA buffer on ice for 10 min, followed by the addition of the indicated catalytically inactive DcpS mutant containing histidine 277 to asparagine substitution (His-DcpS^{mH}). Following a 10-min incubation, the samples were covalently cross-linked by exposure to a 15 W germicidal UV lamp for 10 min, and the consequent cross-linking samples were resolved on a 12.5% SDS-PAGE and visualized by autoradiography. EMSA was conducted using ³²P-labeled-cap RNA with a G16 tract (2–5K cpm) and recombinant eIF4E as previously described (Liu et al., 2004) with the exception that protein was optionally preincubated with 500 nM D156844 or equivalent vehicle for 10 min at 4°C. Decapping assay was performed as previously described (Liu et al., 2008) except for the 5 min duration and the presence of 20 µg of extract derived from 293T cells treated with D156844 or equivalent vehicle for three days.

Splicing reporter assay

293T^{DcpS-KD} cells were transfected with the p773B rat reporter construct with Lipofectamine 2000 in G418. Cells were harvested 36 h post-transfection and total RNA isolated with Trizol Reagent (Invitrogen). cDNA was generated with MMLV reverse transcriptase (Promega) according to the manufacturer's instructions. Real time PCR was performed with iTaq Supermix (Biorad) according to the manufacturer's instructions. Data was computed by the comparative Ct method as explained previously (Livak and Schmittgen, 2001). Sequences for all primer sets are listed in Table 2.

Dicistronic reporter assay

293T cells were treated with 500 nM D156844 or equivalent vehicle for three days prior to transfection with dicistronic construct. At eight hours post-transfection in D156844 presence, cells were harvested and assayed for Renilla and Firefly Luciferase activities using the Dual Luciferase Reporter Assay System (Promega) based on Bradford protein quantitation (Biorad). Cap-dependent translation efficiency was defined as the ratio of Renilla to Firefly Luciferases. Similar experiments were conducted in the 293T^{DcpS-KD} and 293T^{vector-KD} cell lines. Analogous experiments replaced the dicistronic reporter construct with pcDNA3.1-Firefly and pIRES-Renilla Luciferase constructs.

mRNA decay and nuclear run on assays

293T cells were treated with 500 nM D156844 or equivalent vehicle for three days prior to actinomycin D treatment (Sigma Aldrich). Cells were harvested for 0 h, 4 h, and 8 h timepoints post-actinomycin D treatment. Total RNA was extracted by Trizol Reagent

(Invitrogen), and quantitative PCR analysis was performed as in the splicing reporter assay except gene-specific primers against 4EBP1, 4EBP2, and beta actin were used. For nuclear run on assay, 293T cells were treated with 500 nM D156844 or equivalent vehicle for three days prior to nuclei isolation as previously described (Patrone et al., 2000) except quantitative PCR was used using gene-specific primers against 4EBP1, 4EBP2, beta actin, and beta tubulin. Sequences for all primer sets are listed in Table 2.

CHAPTER I: DcpS in Nuclear pre-mRNA Processing

Summary

A cell-based mRNA assay reveals a novel nuclear function of DcpS. Characterization of DcpS primary sequence shows it contains a nuclear localization signal and nuclear export sequence in the N-terminal and central hinge regions, respectively. Secondly, a cell-based mRNA reporter assay shows DcpS is required for first intron splicing. DcpS and Cbp20 partially and completely rescue the splicing defect of the first intron, respectively. Thirdly, two endogenous transcripts recapitulate the splicing defects observed in the reporter assay upon DcpS knockdown. This work shows DcpS is a nucleocytoplasmic protein that regulates a nuclear process in addition to its previously characterized role in cytoplasmic mRNA degradation.

Introduction

DcpS Primary Structure

The sequence of DcpS has been characterized with respect to the HIT motif but also serves as the most informative starting point in reconciling between its nuclear presence and cytoplasmic function. The N-terminus contains a stretch of positively charged basic amino acids that appear to be a putative nuclear localization sequence (Lange et al., 2007). The basic stretch stands alone as an island, and therefore qualifies as a monopartite subtype that attracts the alpha importin receptor in association with the GDP-bound Ran complex. These chaperones act as universal adaptors that assist large proteins bearing the nuclear localization sequence to traverse across the nuclear bilayer and into the nucleus. Similarly, a putative nuclear export sequence exists in the central

loop region of DcpS. The central loop bears the mark of a stretch of leucines that attract the Crm1 receptor and association of GTP-bound Ran (Kudo et al., 1999). This ternary complex exploits its cognate components as a passport to gain passage from the nuclear face to the cytoplasmic side. In this prediction, DcpS has two functional localization signals that provide a basis for its nucleocytoplasmic shuttling property.

DcpS and Nuclear Cap-Dependent Processes

As a cap-binding protein, DcpS can potentially influence pre-mRNA splicing through its homeostatic regulation of the intracellular cap structure concentration. Aberrant events that lead to an accumulation of inhibitory cap structure in the nuclear compartment may impede cap-dependent events. One scenario is an accumulation of the effective cap concentration may rise to hazardous levels in the nucleus to sequester the cap-binding component Cbp20 from its normal function. Early extract-based reporter system indicates depletion of CBC, composed of a Cbp20/80 heterodimer, leads to first intron splicing deficiency (Izaurralde et al., 1994). According to the exon definition model, an intron would not undergo splicing should either of its two adjacent exons be not properly demarcated (Robberson et al., 1990). Each exon is defined by the consensus 3' and 5' splice sites that attract common spliceosomal components. An exception to this guideline pertains to the leading and final exons whose traditional 3' and 5' splice sites are replaced by the cap and poly(A) tail, respectively. In these special cases, Cbp20/80 and PABP help define the cap-proximal and poly(A) tail-proximal exons in order for proper splicing to occur. Cbp20 sequestration from the 5' cap would lead to an undefined first exon and subsequently unspliced first intron. In this prediction, DcpS would

positively regulate cap-dependent pre-mRNA splicing through its ability to maintain homeostasis of intracellular cap levels.

Results

DcpS is a Shuttling Protein

Previous immunofluorescent data have shown the subcellular localization of DcpS to be nuclear (Liu et al., 2004; van Dijk et al., 2003). The observation was surprising given that DcpS has been purified and identified from mammalian cytosolic S130 extract, and its proposed hydrolytic function follows mRNA degradation by the cytoplasmic resident exosome (Liu et al., 2002; Wang and Kiledjian, 2001). The nuclear localization of DcpS and its known cytoplasmic function suggested that DcpS is a nucleocytoplasmic shuttling protein with a dynamic subcellular distribution. To experimentally test this possibility, we utilized a construct expressing GFP-tagged DcpS that localizes to the nucleus at steady state (Fig. 1A) analogous to the endogenous protein (Liu et al., 2004). Interspecies heterokaryon assay that provides a qualitative assessment of a protein's mobility between nuclear and cytoplasmic compartments was used (Pinol-Roma and Dreyfuss, 1992). This assay relies on distinct fluorescence properties between human and mouse nuclei, which enable tracking of any tagged protein expressed in one cell type to be detected if localized in another following cell membrane fusion. Constructs expressing GFP-tagged DcpS were transfected into human HeLa cells exclusively followed by fusion with mouse 3T3 cells in the presence of cycloheximide to

cease ongoing translation. The resulting interspecies heterokaryons (human-mouse fused cells) were further incubated to allow active protein transport to proceed. A construct encoding the well-characterized shuttling hnRNP A1 protein (Piñol-Roma and Dreyfuss 1992) was co-transfected to serve as a positive control for the heterokaryon assay. Similar to the shuttling observed with myc-hnRNP A1, the GFP-DcpS signal appears in both the human and mouse nuclei in Fig. 1A. The presence of the tagged proteins in the mouse nuclei is an outcome originating from protein exported from the human nucleus and subsequently imported into the mouse nucleus. Therefore, DcpS is a shuttling protein that can be exported from the nucleus.

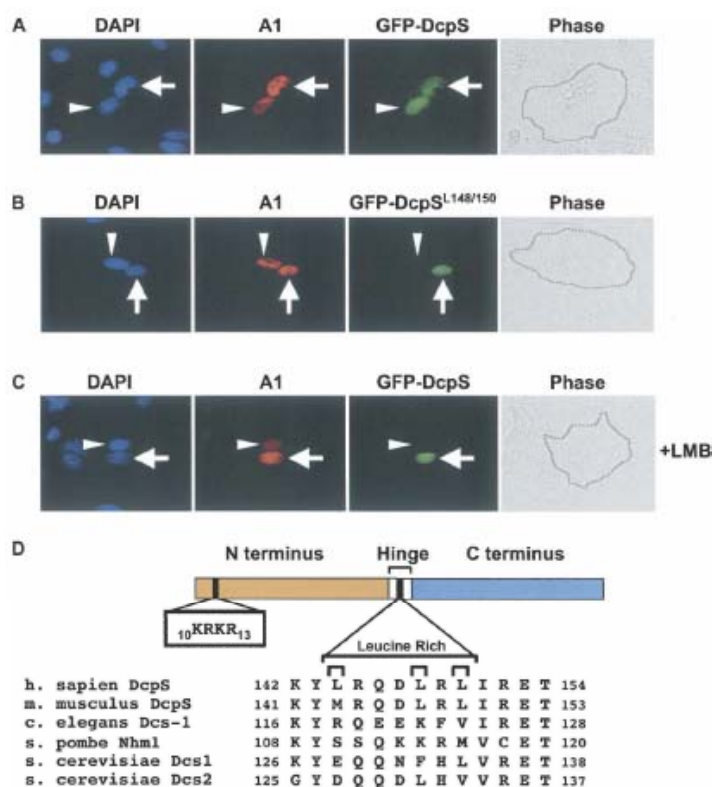


FIGURE 1. DcpS was a nucleocytoplasmic shuttling protein that required a leucine-rich Nuclear Export Sequence (NES).

Human Hela cells co-transfected with constructs expressing GFPDcpS and the shuttling myc-hnRNPA1 positive control were fused to mouse NIH3T3 cells. The nuclei are designated by DAPI staining. The Hela cell nuclei is denoted by the arrow and the punctate nuclei indicative of mouse cells is shown by the arrow head. The red staining denotes localization of the myc-hnRNPA1 while the green signal represents GFP-DcpS. The phase contrast of the cells is shown on the right panel with the black dotted lines indicating the fused plasma membrane of the heterokaryons. (A) Similar to the myc-hnRNPA1, GFP-DcpS can exit the human nucleus and be re-imported into the mouse nucleus. (B) A similar interspecies heterokaryon assay is shown except a mutant GFP-DcpS containing substitutions of leucine 148 and 150 to alanines (GFP-DcpSL148/150A) was used. (C) Heterokaryon assay carried out in the presence of leptomycin B (+LMB) is shown. DcpS requires the leucine-rich region for nuclear export in a LMB sensitive manner. (D) A schematic of DcpS is shown with the distinct N- and C-terminal fragments separated by a hinge region. The relative position of the putative N-terminal NLS from amino acids 10 through 13 and putative leucine-rich NES from amino acids 144 through 150 in the hinge region are bracketed with the corresponding sequences expanded. Alignment of the leucine-rich region of DcpS homologs across different species with characterized subcellular localizations are shown at the bottom. The resulting interspecies heterokaryons (human-mouse fused cells) were further incubated to allow active protein transport to proceed. A construct encoding the well-characterized shuttling hnRNP A1 protein (Pinol-Roma and Dreyfuss, 1992) was co-transfected to serve as a positive control for the heterokaryon assay. Similar to the shuttling observed with myc-hnRNP A1, the GFP-DcpS signal appears in both the human and mouse nuclei (Fig. 1A). The presence of the tagged proteins in the mouse nuclei is an outcome originating from protein exported from the human nucleus and subsequently imported into the mouse nucleus. Therefore, DcpS is a shuttling protein that can be exported from the nucleus.

DcpS Contains a Canonical Nuclear Export Signal

Our demonstration that DcpS is a shuttling protein indicated that this protein contains a nuclear export sequence. Consistent with this property, a putative leucine-rich nuclear export signal was detected at the central hinge domain of the protein (Fig. 1D). To experimentally test the functional relevance of the leucine-rich region in nuclear export, we designed a GFP-tagged DcpS harboring double alanine substitutions of two leucine residues at amino acid positions 148 and 150 (DcpSL148/150A) that are critical for nuclear export function of previously characterized leucine-rich regions (Wen et al., 1995). Figure 1B shows that in contrast to the shuttling exhibited by myc-tagged hnRNP A1, the GFP-DcpSL148/150A signal was exclusively detected in the human cell nucleus of the same heterokaryon, denoting a defect in protein nuclear export. To further substantiate the significance of the leucine-rich region in export, we tested DcpS shuttling in the presence of leptomycin B (LMB) treatment. LMB is an antagonist of Crm1, a protein that recognizes leucine-rich nuclear export sequences and transports them out of the nuclear compartment (Kudo et al., 1999). As shown in Figure 1C, DcpS fails to shuttle within the heterokaryon assay in the presence of LMB and remains in the HeLa nucleus similar to the result observed with the DcpSL148/150A leucine mutant. As expected of the control protein, myc-tagged hnRNP A1 was unaffected by LMB due to its noncanonical nuclear export sequence (Michael et al., 1995). Interestingly, an alignment of the leucine-rich nuclear export signal from several different species where the localization of DcpS has been tested reveals a conservation of this region in the nuclear human and mouse DcpS proteins but diverges in the *Caenorhabditis elegans* DCS-1 and *Saccharomyces cerevisiae* Dcs1p, orthologs of DcpS, as well as the

catalytically inactive paralog of Dcs1p in *S. cerevisiae*, Dcs2p (Fig. 1D), that appear to be exclusively cytoplasmic (Lall et al., 2005; Malys et al., 2004). Curiously, the *Schizosaccharomyces pombe* homolog, Nhm1, is nuclear (Salehi et al., 2002) but also lacks a clear conservation of the leucine-rich sequence (Fig. 1D). Collectively, the data demonstrate that human DcpS is a shuttling protein and supports a role for DcpS in the Crm1-mediated export pathway via its leucine-rich nuclear export signal located in the central hinge domain of the protein and suggest acquisition of the leucine-rich element may be a more recent evolutionary event.

DcpS Contains a Basic Region Nuclear Localization Signal (NLS)

To address the means by which DcpS is imported into the nucleus, we identified its NLS. Inspection of the N-terminal region of DcpS reveals a stretch of basic amino acids (KRKR) that are suggestive of a previously defined nuclear localization signal (Fig. 1D) (Lange et al., 2007). To validate this prediction, we designed a construct expressing a Flag tagged DcpS containing the four basic amino acid deletion within the N terminus, specifically amino acids 10 through 13 (DcpS^{ΔKR}). Consistent with localization of endogenous DcpS (Liu et al., 2004), Flag-tagged DcpS is detected predominantly in the nucleus of HeLa cells transfected with the epitope tagged DcpS expression plasmid (Fig. 2A). In contrast, epitope tagged DcpS^{ΔKR} staining was predominantly cytoplasmic, demonstrating that this region is necessary for nuclear localization (Fig. 2B). Therefore, similar to other proteins that utilize a conventional NLS, human DcpS relies on a region of basic amino acids located in the N-terminal domain of the protein for nuclear protein import. Interestingly, the basic NLS and hydrophobic-rich NES of the scavenger

decapping protein are conserved exclusively in human and mouse (Gu and Lima, 2005).

The cytoplasmic *C. elegans* DcpS

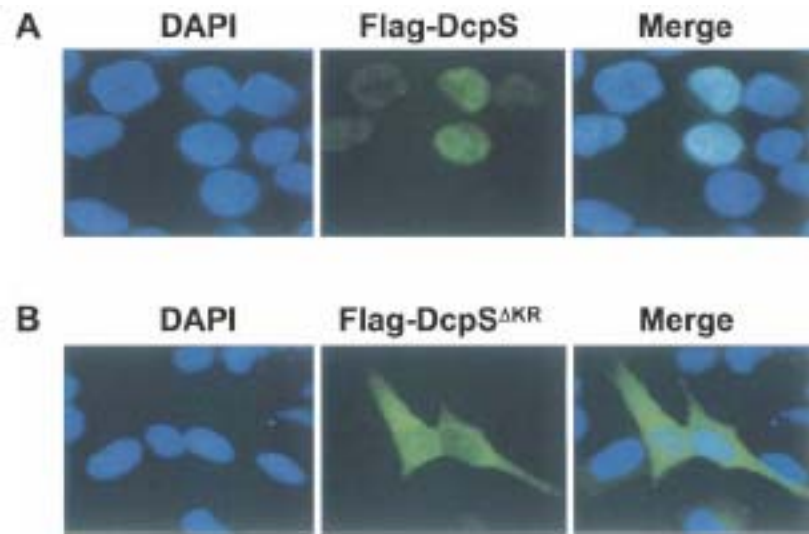


FIGURE 2. Identification of the DcpS nuclear import sequences.

Hela cells transfected with either (A) wild-type Flag-DcpS or the (B) mutant construct containing a four amino acid truncation of amino acids 10–13 Flag-DcpS Δ KR. The left panel demarcates the position of the nuclei with DAPI staining and the DcpS localization is denoted by the green fluorescence and identified with the use of the anti-Flag monoclonal antibody. A merge of the two panels is shown on the *right*.

homolog Dcs-1 (Lall et al., 2005) and *S. cerevisiae* DcpS homolog Dcs1 (Malys et al., 2004), lack the first 30 and 31 amino acids, respectively, corresponding to human DcpS, which includes the NLS. In the case of the catalytically inactive *S. cerevisiae* Dcs2, the NLS region is not conserved, and we are unable to decipher another putative NLS (data not shown). The *S. pombe* homolog of DcpS, Nhm1, is predominantly nuclear but also present in the cytoplasm (Salehi et al., 2002); however, neither an NLS nor NES could be readily discerned based on examination of the amino acid sequence (Gu and Lima, 2005).

A Nuclear Role for DcpS in Facilitating First Intron mRNA Splicing

To begin addressing the cellular function of DcpS, we generated a proliferative cell line that was readily transfectable that could be constitutively knocked down for DcpS. Human kidney 293T cells were stably transformed with a shRNA expression plasmid specific for DcpS transcribed by a Pol III-directed U6 promoter. Single colonies were expanded and tested for their efficiency of DcpS protein and activity knockdown, and the most significantly silenced clonal cell line was expanded (293T^{DcpS-KD}). As shown in Figure 3A, DcpS levels are reduced in the 293T^{DcpS-KD} cells greater than 90% relative to 293T cells expressing the shRNA empty vector by Western blot (cf. lanes 1–3). Similarly, an in vitro decapping assay confirmed that scavenger decapping activity detected from extract obtained from the knockdown cells was reduced by greater than 80% relative to the control extract (cf. lanes 4–6) in Figure 3B. Aside from its tendency to grow as discrete cells in a nonaggregated form, the 293T^{DcpS-KD} cell line does not pose an additional unique phenotype in comparison to the empty vector cell line. These data demonstrate that the 293T^{DcpS-KD} clonal cell line contains reduced DcpS expression and a corresponding reduction in cap hydrolytic activity. In an effort to begin addressing potential nuclear function(s) of DcpS, we reasoned that the ability of DcpS to hydrolyze cap structure would be essential in modulating the activity of cap-binding proteins since inhibitory cap structure would otherwise accumulate in the absence of DcpS. Having previously demonstrated that DcpS can efficiently displace eIF4E from cap structure (Liu et al., 2004), we tested whether the same was also true with the nuclear CBC. To begin addressing the relationship between

CBC and DcpS, we initially used UV cross-linking to determine whether DcpS could compete the cap-binding potential of the Cbp20 cap-binding component of CBC.

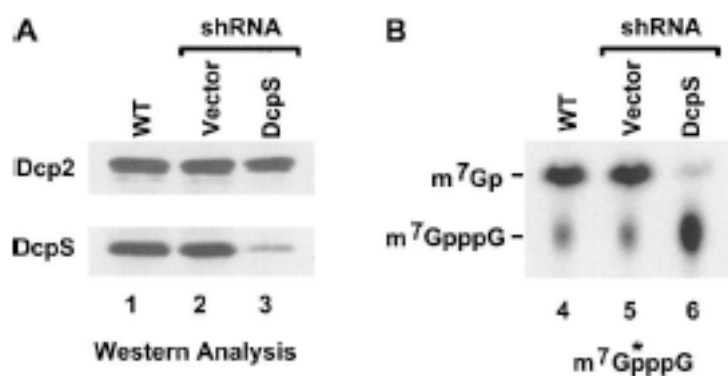


FIGURE 3. A knockdown clonal cell line is diminished in DcpS expression and catalysis.

A clonal 293T cell line stably transformed with pShag-DcpS expressing shRNA specific to DcpS was used in a western assay (A) and decapping activity assay (B). 293T cells not expressing an shRNA (lane 1), expressing the shRNA vector (lane 2), or shRNA to DcpS (lane 3) are shown with antibodies to either the human Dcp2 protein or DcpS as indicated. DcpS protein levels are reduced in the 293T cells expressing the DcpS-specific shRNA. The right panel shows a decapping assay of labeled cap structure incubated with wild-type 293T cell extract (lane 4), 293T cell extract expressing the empty shRNA vector (lane 5), or 293T cell extract from cells expressing the DcpS-specific shRNA (lane 6). Reaction products were resolved on PEI TLC plates. Standards were developed on the TLC simultaneously, visualized by ultraviolet shadowing and their migration indicated on the left. The labeled cap structure used in the reaction is schematically depicted on the bottom, where the asterisks denote the labeled phosphate.

Analogous to the ability of DcpS to displace eIF4E from cap structure (Liu et al., 2004), DcpS could readily outcompete Cbp20 from the cap structure (Fig. 4, lanes 2–8) while a control RNA-binding protein, alphaCP1, could not (lane 9). Although this is an *in vitro* study with the Cbp20 monomer in the absence of the Cbp80 component, it is suggestive that DcpS activity could be a modulator of CBC access to the cap and, in turn, its function. CBC has been shown to serve multiple functions in the nucleus, including facilitation of first intron splicing (Edery and Sonenberg, 1985; Izaurralde et al., 1994; Konarska et al., 1984). Exons are defined nucleotide sequences flanked by spliceosomal complexes that assemble at the upstream 3' and downstream 5' splice sites. One minor deviation concerns the first exon in which the absence of an upstream spliceosomal component is compensated by the presence of CBC cap recognition (Berget, 1995). Depletion of CBC in HeLa extract has been shown to reduce splicing of the cap proximal intron (Lewis et al., 1996). Given DcpS activity in cap hydrolysis and its ability to displace Cbp20 from cap structure, we reasoned that a reduction of DcpS levels could also result in an accumulation of inhibitory cap in the nucleus, which, in turn, could sequester CBC and reduce splicing of the first intron. To assess whether a reduction of DcpS levels can impact first intron splicing, a rat fibronectin minigene reporter construct that expresses a pre-mRNA consisting of three exons and two introns was transfected into 293T^{DcpS-KD} cells to assess the *in vivo* splicing efficiency of the first intron relative to the second intron. Following a 36-h post-transfection period, RNA was isolated and splicing analyzed by reverse transcription PCR. A primer pair that anneals to the first and second exons was used to detect the unspliced and spliced RNA forms of the first intron.

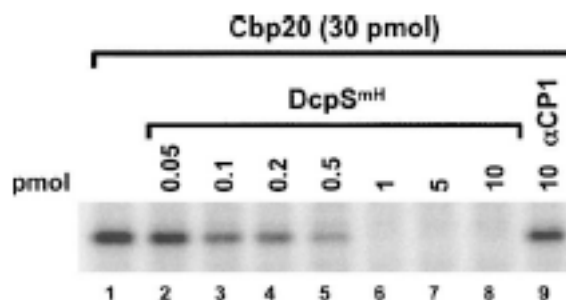


FIGURE 4. DcpS can displace Cbp20 from cap structure.

The ability of DcpS to displace Cbp20 from the cap structure was tested. Thirty picomoles of histidine tagged Cbp20 were prebound to ³²P-labeled cap structure on ice for 10 min, followed by addition of the indicated amounts of catalytically inactive histidine tagged DcpS^{mh} for an additional 10 min (lanes 2–8). The reactions were subsequently UV cross-linked and resolved by SDS-polyacrylamide gel. The aCP1 RNA-binding protein was used as a control (lane 9). DcpS can efficiently displace Cbp20 from the cap structure at substoichiometric concentrations. Result was provided by Dr. Hudan Liu.

As shown in Figure 5A, a qualitative difference is detected where a noticeable accumulation of unspliced RNA is detected in the splicing of the first intron in 293T^{DcpS-KD} cells in contrast to that of the control cell line (cf. lanes 3 and 5). However, the splicing reaction in the second intron appears to be largely unaffected between the two cell lines (cf. lanes 8 and 10). To obtain a quantitative assessment of the DcpS effect on differential splicing of the reporter pre-mRNA, quantitative real-time PCR was carried out with primer pairs that anneal to an exon and an immediately downstream intron (Fig. 5B). Reverse transcribed RNA from cells transfected with the rat fibronectin reporter construct was monitored to determine first intron splicing efficiency in the 293T^{DcpS-KD} cells or control cells. Relative unspliced RNA levels of the first intron (exon–intron junction 1; EIJ1) were measured in reference to the relative unspliced RNA amount of the second intron, exon–intron junction 2 (EIJ2). Therefore the EIJ1/EIJ2 ratio reflects the fold splicing defect observed of the first intron normalized to that of the second intron upon reduction of DcpS. The data illustrate that splicing of the reporter transcript exhibited a twofold greater splicing defect of the first intron in the 293T^{DcpS-KD} cells relative to the vector control cell line (Fig. 5B). In order to confirm that the effect on splicing is attributed to DcpS, we cotransfected along with the reporter a construct expressing Flag-tagged DcpS to rectify the processing defect. Flag- DcpS is expressed at sufficient levels to overcome the knockdown effect of the DcpS-specific shRNA (Fig. 5C). DcpS overexpression partially corrects the splicing defect in the first intron (Fig. 5B, lane 4) while expression of a control plasmid failed to complement (lane 3). Moreover, Cbp20 overexpression was able to completely reverse the splicing defect (lane 5), indicating that the reduced splicing of intron one was due to the limiting

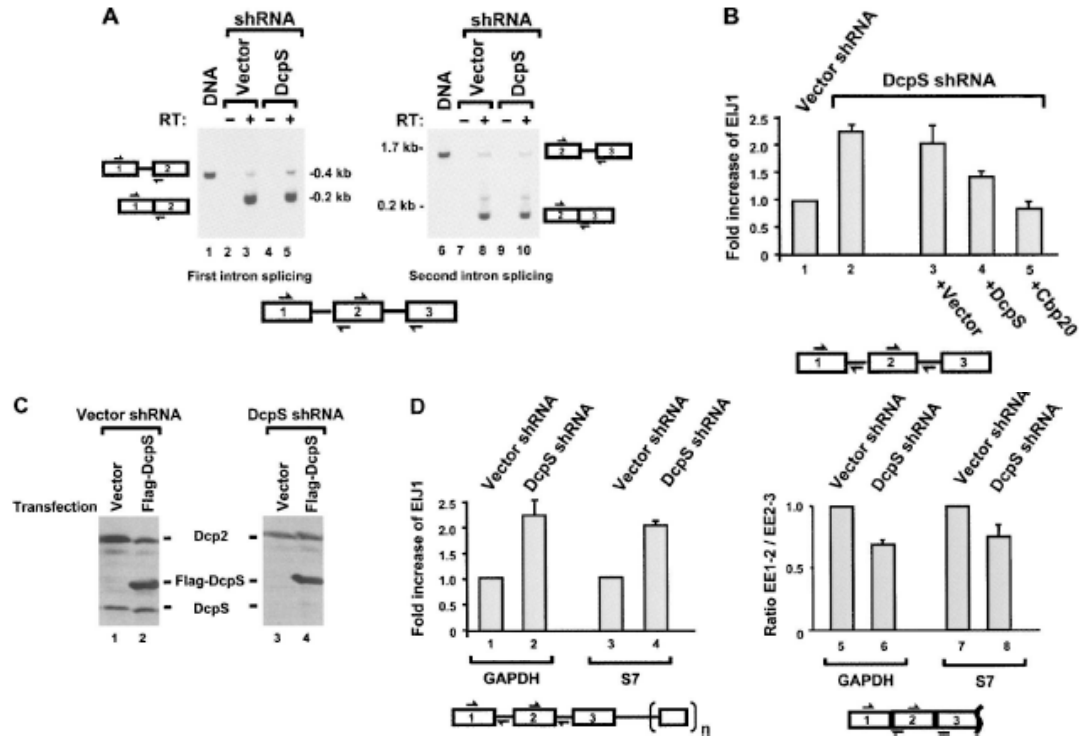


FIGURE 5. DcpS can influence splicing of the first intron in cells.

(A) DcpS affects the splicing efficiency of the rat fibronectin minigene reporter pre-mRNA first intron. Stable 293T cell line of either control empty shRNA or DcpS shRNA background was transfected with the rat fibronectin minigene and was analyzed 36 h post-transfection by reverse transcription PCR assays. Qualitative presence of intron 1 splicing (left panel) or intron 2 splicing (right panel) was determined with primer pairs that monitor the splicing status as shown in the schematic on the side of each panel and summarized at the bottom. The boxes with the numbers denote the exons and the lines represent the introns. DNA size markers are shown to the side of each panel. PCR products corresponding to the unspliced intron 1 and unspliced intron 2 obtained from amplification of the plasmid expressing the rat fibronectin transcript are shown in lanes 1 and 6, respectively. (B) Splicing reactions analogous to A were analyzed by quantitative real-time PCR using the primer sets that span the exon-intron junctions shown schematically below the panel. The EIJ1/EIJ2 ratio obtained from the control shRNA vector was arbitrarily set to one (lane 1) and all other values are presented relative to this control. A twofold increase in the detection of EIJ1 relative to that of EIJ2 is observed in the 293T-DcpSKD cells (lane 2), an indication of a preferential splicing defect in the first intron. Complementation with either the empty vector (lane 3) or vector expressing DcpS (lane 4) or Cbp20 (lane 5) is shown. Quantization of three independent experiments performed in duplicate and the corresponding standard deviation denoted by the error bars are shown. (C) Expression of Flag-DcpS in 293T-DcpSKD cells. Control and 293T-DcpSKD cells were transfected with either a vector construct or Flag-DcpS expression construct as indicated and expression of both endogenous and exogenous DcpS detected by Western analysis using a DcpS antibody. The level of Dcp2 was tested as a control. Expression of exogenous Flag-DcpS is high enough to overcome the DcpS shRNA. (D, left panel) Quantitative real-time PCR was carried out to detect the EIJ1 fold increase relative to that of EIJ2 as in B for the indicated endogenous genes from RNA obtained from the control or DcpS-specific shRNA expressing 293T cell lines. The exons and introns are schematically shown on the bottom with $n = 6$ for GAPDH and $n = 4$ for S7. GAPDH and S7 genes exhibit a twofold preferential increase of EIJ1 in 293T-DcpSKD cells (lanes 2,4) relative to control cells (lanes 1,3). (Right panel) Quantitative real-time PCR analysis was carried out analogous to that above except primers that spanned exon-exon 1-2 (EE1-2) and exon-exon 2-3 (EE2-3) were used as indicated in the schematic below and short elongation times were used such that the spliced form was exclusively detected. Quantitation of three independent experiments carried out in duplicate and corresponding standard deviation denoted by the error bars are shown. Western result was provided by Dr. Shin-Wu Liu.

availability of Cbp20 in the DcpS knockdown cells. Taken together, the in vivo splicing experiments consistently suggest that DcpS influences proper first intron splicing of an exogenously expressed gene.

The chimeric rat fibronectin minigene used above contains three exons and two introns. To determine if an influence on first intron splicing could also be seen for an endogenous multi-intron-containing gene, we compared the relative splicing of the first and second introns of two endogenous genes. For this purpose, two relatively abundant mRNAs were used to enable more efficient detection of the pre-mRNA species, GAPDH and the ribosomal S7 genes. The same quantitative real-time PCR strategy was carried out to determine the splicing defect about the first intron in reference to that of the second. Similar to the results obtained with the rat fibronectin minigene, an approximate twofold-splicing defect was observed for the splicing of the first intron relative to the second intron for both genes in the 293T^{DcpS-KD} cells (Fig. 5D, cf. lanes 1–2 and 3–4). The above analyses were carried out by comparing the relative proportions of EIJ1 to EIJ2. To rule out the formal possibility that higher levels of EIJ1 relative to EIJ2 in the DcpS knockdown cell line reflected increased aberrant pausing or abortive transcription in the 293T^{DcpS-KD} cells, we alternatively conducted real-time PCR on the levels of spliced exonic boundaries. Quantitative real-time PCR was carried out as above except that the primers and PCR parameters were designed to detect the spliced exon–exon junctions exclusively. The fold change of spliced exon–exon 1–2 (EE1–2) mRNA levels relative to spliced exon–exon 2–3 (EE2–3) mRNA levels were determined by real-time PCR. If reduction of DcpS levels results in an increased incidence of transcriptional pauses or termination, a greater level of the upstream spliced exon–exon junction would

be detected relative to the next downstream spliced exon– exon junction; that is, the ratio of EE1–2 to EE2–3 would be greater than one. Consistent with a regulation at the level of splicing, rather than transcription pausing, a relative decrease in EE1–2 in relation to EE2–3 was observed (Fig. 5D, cf. lanes 6–5 and 8–7). However, the decrease is not as dramatic as that observed when measuring the pre-mRNA in lanes 1–4 since the abundance of the spliced products in the latter analysis would skew the results relative to the less abundant pre-mRNA. Collectively, these data provide evidence for a novel nuclear function for DcpS in maintaining proper pre-mRNA splicing.

DISCUSSION

The current study demonstrates that DcpS, the scavenger decapping protein previously thought to exclusively function in mRNA turnover, is a nucleocytoplasmic shuttling protein with broader functionality as a modulator of capbinding proteins. Heterokaryon assays show that DcpS is a shuttling protein and relies on an N-terminal NLS for import and leucine-rich consensus NES located in the central hinge region for nuclear export. The presence of functional NLS and NES provides a clear explanation of a nuclear protein extending its influence over cytoplasmic events. We show that DcpS can compete Cbp20 from cap structure at substoichiometric concentrations. A splicing reporter assay confirmed the expectation that DcpS modulates CBC-associated functions where splicing activity was notably reduced in the DcpS knockdown cell line 293T^{DcpS-KD}. Rescue experiments show that both DcpS and Cbp20 overexpression can restore the defect, supporting the idea that DcpS positively modulates pre-mRNA processing. More specifically, DcpS regulation preferentially influences the first intron, a result consistent

with previous findings of CBC's preferential regulation on the cap-proximal intron. This study extends the primary scope of DcpS regulation beyond mRNA degradation to earlier events involved in RNA maturation. Furthermore, it is interesting that Cbp20 was able to completely restore splicing in the 293T^{DcpS-KD} cell line while DcpS partially restored the splicing defect. The reason for this intriguing discrepancy is not clear but may appear to be due to the limiting Cbp20 concentration in relation to overexpressed DcpS.

Our demonstration that the primarily nuclear localized DcpS is a shuttling protein with cytoplasmic residency addresses an apparent paradox for the function of DcpS. We, and others, have previously reported a cytoplasmic scavenger-decapping activity (Liu and Kiledjian, 2005; Liu et al., 2002; Liu et al., 2004; van Dijk et al., 2003) from a protein residing mainly in the nucleus. The shuttling capacity of DcpS has been confirmed based on the identification of its amino acid sequence and by immunocytochemistry using an interspecies heterokaryon assay (Fig. 1). Nuclear import of DcpS requires a short stretch of basic amino acids at the N terminus of the protein (Fig. 2) consistent with the canonical SV40 large T antigen basic NLS (Kalderon et al., 1984). Interestingly, the DcpS NLS falls within an unstructured N terminus of the protein (Gu et al., 2004) that is dispensable for hydrolytic activity (Liu et al. 2004).

Conforming to the shuttling property of DcpS, a nuclear export signal consisting of a leucine-rich region (Wen et al., 1995) closely matching the consensus leucine-rich NES, LXXXLXL is present in the protein (L denotes leucine and X any amino acid (Kutay and Guttinger, 2005). Confirmation for the functional significance of this region in nuclear export is provided by the substitution of the two highly conserved leucine residues to alanines (L148/150A) that perturbed export (Fig. 1B). As expected for this

class of export signals, the exit of DcpS from the nucleus is inhibited by LMB, indicating that DcpS export is Crm1 mediated. Positioning of the leucine-rich export signal lies notably within the hinge region connecting the N- and C-terminal domains of DcpS. One possible consequence for positioning of the NES to the hinge is that the central region provides an interface for protein interaction that would likely lock the N-terminal segment of the DcpS homodimer with respect to the C terminus to inhibit catalytic activity and could be a mechanism to modulate hydrolytic activity during nucleocytoplasmic transport.

The current findings reveal that the predominantly nuclear residency and shuttling capacity of DcpS in mammals are driven by the classical NLS and NES located in the N-terminal and central hinge domains, respectively. However, the absence of a corresponding NLS and NES in the *C. elegans* and *S. cerevisiae* orthologs of the human DcpS protein are consistent with the cytoplasmic localization of these proteins (Lall et al., 2005; Malys et al., 2004) and suggest that a nuclear DcpS function may not be uniformly conserved throughout all species. Other than the mammalian DcpS, the exception thus far is the *S. pombe* Nhm1, which is also nuclear (Salehi et al., 2002). The absence of a leucine-rich NES in Nhm1 suggests this protein either does not shuttle or uses another element to fulfill this function. Whether certain species have evolved to confine the DcpS orthologs in one compartment to restrict its influence while mammals have adapted to utilize DcpS in both compartments remains to be more thoroughly addressed.

The ability of DcpS to hydrolyze the resulting cap structure end product of 3' to 5' exonucleolytic mRNA decay that would otherwise accumulate (Fig. 3B; (Liu and

Kiledjian, 2005) and potentially sequester cap-binding proteins implicates DcpS in cellular functions beyond mRNA decay. We propose DcpS is essential to relieve CBC from cap sequestration to maintain normal levels of protein synthesis and mRNA maturation by maintaining cellular homeostasis by buffering against the potentially adverse effects of inhibitory cap accumulation. Normally, mRNAs that are targeted into the 3' to 5' mRNA decay pathway become degraded to a short oligo-cap structure or cap structure by the exosome (Liu et al., 2002), a product which in turn serves as a substrate for the subsequent hydrolytic activity of DcpS (Wang and Kiledjian, 2001). A model can be envisioned whereby DcpS depletion leads to the aberrant accumulation of effective cap concentration, which otherwise would have been hydrolyzed or captured by DcpS. Consequently, excess cap structure in the nucleus could serve to compete and sequester CBC from their mRNA substrates (Fig. 6, right panel). The net effect of DcpS depletion would be a reduction in the active pool of cap-binding proteins leading to altered phenotypes of cap-binding protein-dependent processes, including pre-mRNA splicing. The established role of CBC in mRNA transport out of the nucleus suggests this process could also be affected by DcpS activity, although this still remains to be tested. Furthermore, the significance of the cap and eIF4E in mRNA translation suggests translation may also be impacted by DcpS through the modulation of eIF4E. Therefore, DcpS could be a modulator of cap structure concentrations in a cell, and this activity could in turn impinge on multiple posttranscriptional processes. Further support for this premise is provided with the demonstration that disruption of the DcpS homolog in yeast, Dcs1, leads to an accumulation of inhibitory cap structure (Liu et al., 2002) and a marked reduction of 5' to 3' exonucleolytic activity (Liu and Kiledjian, 2005).

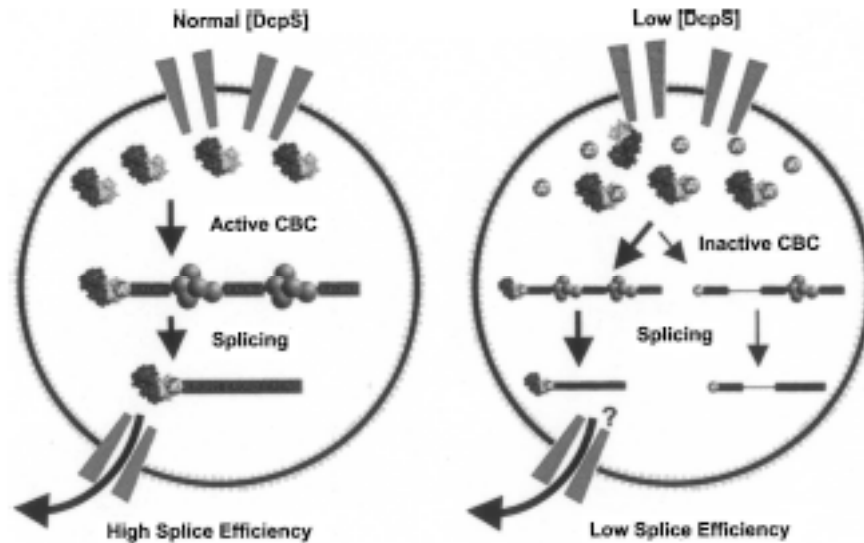


FIGURE 6. Model depicting consequence on nuclear splicing in the presence or reduction of DcpS.

A cartoon of a nucleus containing wild-type levels of DcpS is shown on the left panel and a nucleus with reduced DcpS is shown on the right. DcpS reduction leads to an increase in the level of inhibitory cap structure (sphere). The inhibition by cap structure leads to a reduction in the active pool of nuclear CBC (heterodimer subunits) through sequestration, and promotes a splicing defect of the first intron in a subset of mRNAs possibly through incomplete spliceosomal complex (pentamer spheres) assembly on the pre-mRNA.

To our knowledge, the regulatory function of DcpS on splicing presented in this study provides the first cell-based confirmation in mammalian cells for the significance of CBC in splicing of the cap-proximal intron. These results extend previous studies with mammalian *in vitro* splicing (Edery and Sonenberg, 1985; Izaurralde et al., 1994; Konarska et al., 1984) and suggest the regulation of cap structure could be a natural means to influence splicing. The results also provide a framework for future studies to address the potential broader impact on alternative utilization of the first intron in splicing and raise numerous new questions. Approximately 60% of human genes are predicted to contain their translation start site in the first exon (Davuluri et al., 2001). Alterations in the efficiency of intronic inclusion or exclusion could dramatically affect expression from these genes since failure to remove the intron would most likely result in the ribosome encountering a premature stop codon within the intron and subsequent decay of the mRNA by the nonsense-mediated decay pathway (Chang et al., 2007; Lejeune et al., 2002; Lejeune et al., 2003). The demonstration that GAPDH and S7 splicing are affected indicates that DcpS can influence endogenous pre-mRNA splicing, and this might be a general function of DcpS. However, it remains to be determined whether all pre-mRNAs are equally impacted by cap structure or whether a certain subset is more susceptible. Further studies are necessary to test the global impact of this previously unanticipated role of DcpS in the potential regulation of first intron splicing.

Although the functional assignment of DcpS extends from general mRNA degradation to pre-mRNA splicing, the importance of the prevalent nuclear signal of DcpS remains to be addressed. Identification of a functional role for DcpS in splicing provides a novel avenue to pursue nuclear functions for this protein. An additional

function postulated for this family of proteins includes the removal of methylated nucleotides within the nucleus to prevent their misincorporation into RNA during transcription (Malys et al., 2004; van Dijk et al., 2003), although this has yet to be demonstrated. Maintaining the idea of DcpS influence over cap-mediated processes, eIF4E-dependent mRNA translation as well as miRNA-guided translational repression may be additional points of regulatory interest for the cap-hydrolyzing protein. Cytoplasmic sequestration of eIF4E as a consequence of cap structure accumulation would be expected to result in a decrease of mRNA translation. Alternatively, DcpS repression may increase mRNA translation if less DcpS sequesters the 5' cap of mRNA from eIF4E. The ability of DcpS to effectively compete eIF4E from cap structure and capped mRNA (Liu et al., 2004) supports both hypotheses

Although the precise mechanism of translational repression by miRNAs is still unclear, inhibition of translation initiation is one likely possibility (Pillai et al., 2005). Interestingly, the recent demonstration that Argonaute 2 (Ago2) is a cap-binding protein raises important questions for the role of DcpS in miRNA-mediated translational suppression. One model posits that the nucleation of Ago2 onto the 3' UTR of an mRNA through its guide miRNA provides a wider window of opportunity for its cap-binding domain to access the upstream 5' cap and thus prevent eIF4E from initializing subsequent rounds of ribosome loading (Kiriakidou et al., 2007). Whether the DcpS activity could also influence the cap-binding property of Argonaute 2 and miRNA-mediated translation inhibition remains to be determined.

Collectively, the data support a multifunctional role for the methyl-guanosine cap hydrolyzing human DcpS enzyme at several levels of mRNA metabolism. An important

future area to address involves what additional cellular functions are modulated by DcpS and how DcpS activity is regulated. Studies in *C. elegans* and *S. cerevisiae* provide initial insight into potential regulation of DcpS. DcpS orthologs in both these organisms are induced in response to stress (Gasch et al., 2000; Kwasnicka et al., 2003; Malys et al., 2004), raising the appealing possibility that DcpS and its downstream functions react to environmental conditions of cellular stress.

CHAPTER II: DcpS in Nuclear Transcription and its New Genetic Interaction

Summary

The current work reveals DcpS function downregulates cap-dependent protein synthesis and stimulates 4EBP1 and 4EBP2 transcription rates. DcpS repression causes a two fold stimulation of cap-dependent translation in a protein reporter assay and decreases endogenous 4EBP1 protein level in 293T cells. The former result is unexpected and demonstrates cap-dependent translation behaves oppositely to pre-mRNA splicing in terms of response to DcpS depletion. On the other hand, the latter result correlates with a decrease in endogenous 4EBP1 and 4EBP2 transcription rates. Individual knockdown of 4EBP1 and 4EBP2 does not fully recapitulate the two fold stimulation of cap-dependent translation, opening the possibility of an unidentified DcpS target. This is the first demonstration that DcpS influences nuclear transcription of two specific gene targets.

Introduction

DcpS and Cytoplasmic Cap-Dependent Processes

If DcpS repression leads to an intracellular accumulation of inhibitory cap structure in both subcellular compartments, cap-dependent translation may exhibit less efficiency due to a shift toward the pool of inactive eIF4E. Several studies attest to this hypothesis albeit to a less physiological degree in which cap structure and derivatives negate in vitro cap-dependent translation (Hickey et al., 1976; Sasavage et al., 1979; Suzuki, 1976). The decrease in the translational output is generally a correlate of the ribosome's inability to associate with capped mRNA (Adams et al., 1978; Roman et al.,

1976). eIF4E exists in an initiation complex known as eIF4F (Etchison et al., 1982; Grifo et al., 1982; Grifo et al., 1983; Sonenberg et al., 1978) along with two other subunits, eIF4A and eIF4G, and facilitates ribosome 5' entry and 5' UTR scanning (Kozak, 1980; Ray et al., 1985). Accumulation of inhibitory cap would predictably sequester eIF4E from the 5' cap and lead to a block in translation initiation. eIF4E is also sensitive to the intracellular concentration of the 4EBPs. These proteins are analogous to cap structure in the sense that both regulators negatively affect translation (Lin et al., 1994; Pause et al., 1994). However, unlike cap analogs which are competitive inhibitors of eIF4E's nucleotide-binding site, the 4EBPs bind to an allosteric site that is recognized by eIF4G. The goal of this work is to provide experimental validation that DcpS positively influences cap-dependent translation through a cell-based protein reporter assay.

Results

DcpS Is Required for Normal Cap-dependent Translation

A previous report showed that a potential therapeutic compound for spinal muscular atrophy termed, D156844 is a competitive inhibitor of DcpS catalytic activity in extract (Singh et al., 2008). As a step toward incorporating this inhibitor in the development of an assay that efficiently repressed DcpS activity, proliferating 293T cells were grown in the presence of D156844 for three days. The cells were harvested and washed extensively prior to assaying for *in vitro* decapping activity. In Figure 7, compound-treated cells efficiently repressed decapping activity compared to those of DMSO-treated. The result confirmed D156844 was a potent DcpS inhibitor and

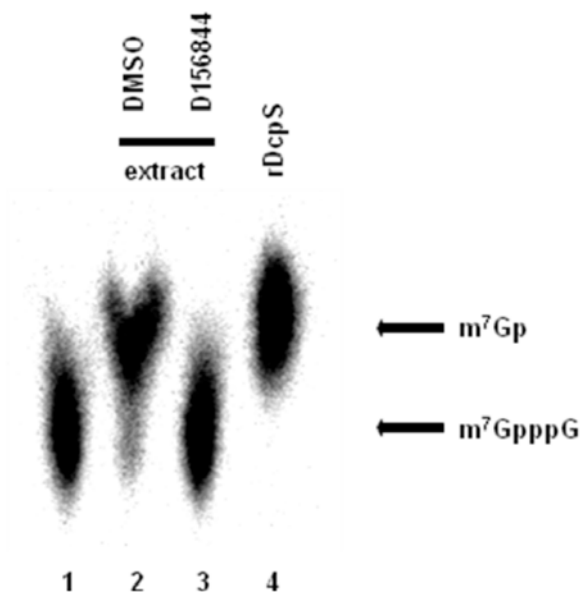


FIGURE 7. D156844 repressed DcpS activity.

Pretreated 293T cells were harvested and washed. Whole cell extract was assayed for decapping activity, and products were resolved on TLC in 0.45M $\text{NH}_4(\text{SO}_4)_2$. Recombinant DcpS was used as positive control (lane 4). D156844 repressed DcpS activity (compare lanes 2 and 3). Result was provided by Dr. Sophie Bail.

suggested the compound remained bound to the enzyme's active site throughout the extract preparative process.

In order to address DcpS requirement in cap-dependent translation, a dicistronic reporter construct encoding a transcript bearing two coding regions was transfected into compound-treated 293T cells. The upstream cistron encoded Renilla Luciferase whose translation was driven cap-dependently, is shown in Figure 8A. Contrarily, the downstream cistron encoded the Firefly Luciferase whose protein synthesis was driven through a hepatitis C viral Internal Ribosomal Entry Site (HCV IRES) that recruited the ribosome directly via its secondary structure (Jang et al., 1988; Tsukiyama-Kohara et al., 1992). The ratio of Renilla to Firefly Luciferases provided a quantifiable measure of the cap-dependent translational efficiency. After three days of treatment, cells were transfected and grown for eight hours prior to harvest. D156844 clearly stimulated cap-dependent translation by two fold over that of DMSO as shown in Figure 8B. This suggested DcpS normally downregulated cap-dependent translation. Analysis of the individual Renilla and Firefly components revealed the stimulatory effect on cap-dependent translation was not due to a negative response from the HCV IRES Firefly reporter component (Figure 8C). Similarly, in Figure 8B, a previously characterized DcpS shRNA cell line (Shen et al., 2008) exhibited higher cap-dependent translation than that of control shRNA cell line, confirming the compound-induced translational stimulation was mediated specifically through DcpS.

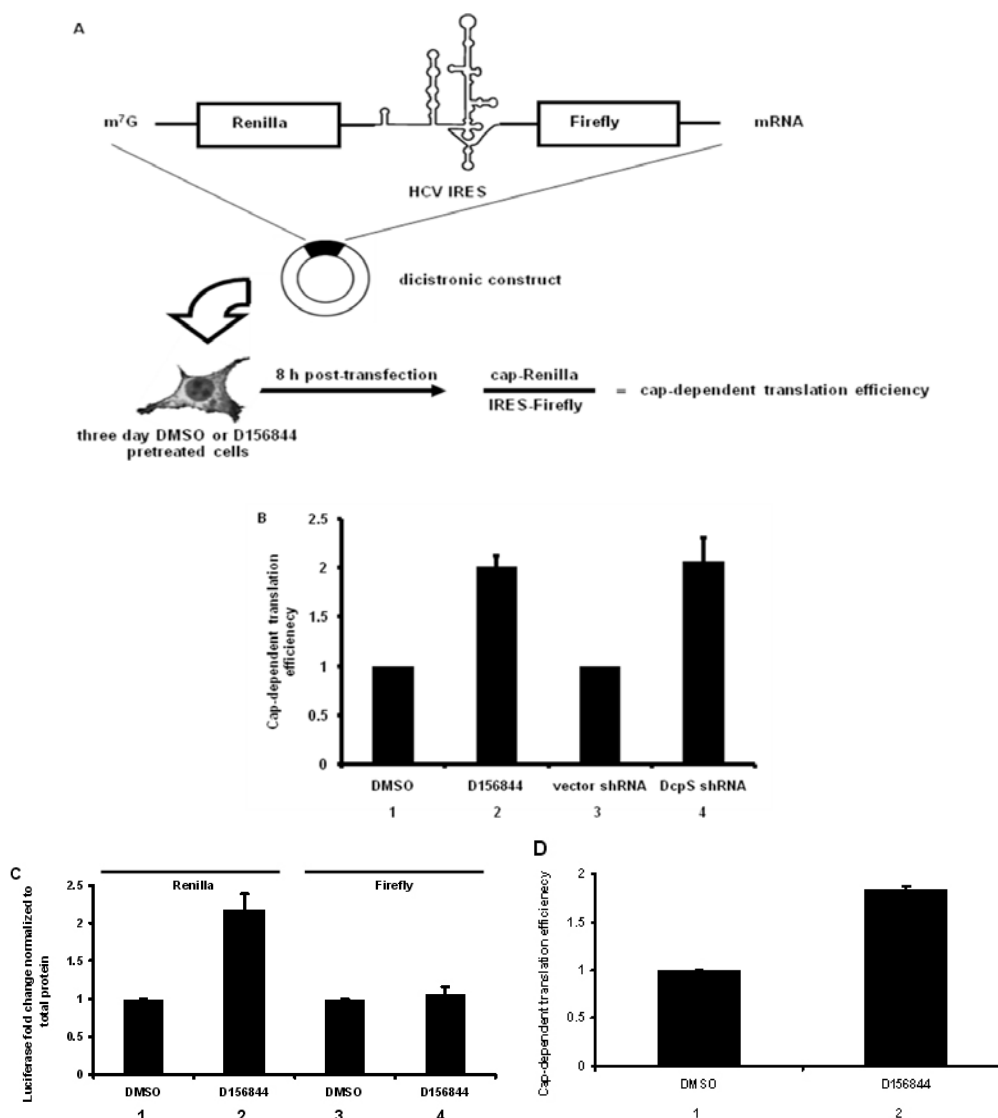


FIGURE 8. DcpS repression stimulated cap-dependent translation.

Schematic diagram showed the dicistronic reporter transcript that translated Renilla Luciferase cap-dependently and Firefly Luciferase HCV IRES-dependently. The m^7G represented the 5' cap. Open boxes denoted coding regions, and thin lines denoted untranslated regions. Pretreated or DcpS shRNA 293T cells were transfected with the dicistronic construct for eight hours prior to harvest and assayed for Renilla and Firefly activities with DMSO and control shRNA cells. Renilla activity was normalized to Firefly activity. (B) Cap-dependent translation was stimulated upon DcpS repression (compare lanes 1 and 2; compare lanes 3 and 4). Error bars denoted standard errors for three data sets ($n=3$). (C) Cap-dependent translational efficiencies were separated into individual Renilla and Firefly Luciferase activities. Compound treatment stimulated Renilla luciferase (compare lanes 1 and 2) but did not affect Firefly luciferase (compare lanes 3 and 4). (D) Pretreated 293T cells were co-transfected with constructs expressing cap-dependent Firefly Luciferase and EMCV-IRES-dependent Renilla Luciferase. Firefly activity was normalized to Renilla activity. Cap-dependent translation was stimulated upon DcpS repression (compare lanes 1 and 2). Error bars denoted standard error for three data sets ($n=3$).

eIF4G Is Not a Direct Target of DcpS

The Encephalomyocarditis Viral (EMCV) IRES was employed to address the target of DcpS in its effect on cap-dependent translation (Jang et al., 1988). In contrast to the HCV IRES that did not rely on any subunit of the eIF4F complex, the EMCV IRES required the eIF4G subunit for ribosomal recruitment during translation initiation (Kolupaeva et al., 1998; Lomakin et al., 2000; Pestova et al., 1996). If eIF4G was not a target of DcpS, replacement of the HCV IRES with EMCV IRES would not alter the results of the cell-based protein reporter assay. Two reporter constructs encoding either a cap-dependent Firefly Luciferase or EMCV-driven Renilla Luciferase were co-transfected into 293T cells after three days of D156844 pretreatment. Consistent with the preceding observation, DcpS repression stimulated cap-dependent translation by two fold irrespective of the IRES swap shown in Figure 8D. This result suggested DcpS repression did not stimulate protein synthesis through this particular translation initiation factor and influenced an earlier step than eIF4G recruitment. Furthermore, these results demonstrate that the observed increase in luciferase activity was not a result of DcpS acting at the level of the protein activity since similar results were obtained irrespective of the positioning of the luciferase cistrons.

DcpS Is Required for Normal 4EBP Expression.

A previous report showed DcpS and eIF4E competed for the 5' cap of mRNA (Liu et al., 2004). Another explanation behind cap-dependent translational stimulation was DcpS repression led to a preferential shift in mRNAs bound to eIF4E. Cells in which DcpS was chemically repressed or knocked down by shRNA were harvested and tested

for endogenous eIF4E levels by western blot. Figures 9A and 9B showed DcpS repression did not substantially change eIF4E protein levels. The rare event that D156844 enhanced eIF4E-binding to the 5' cap was also ruled out when

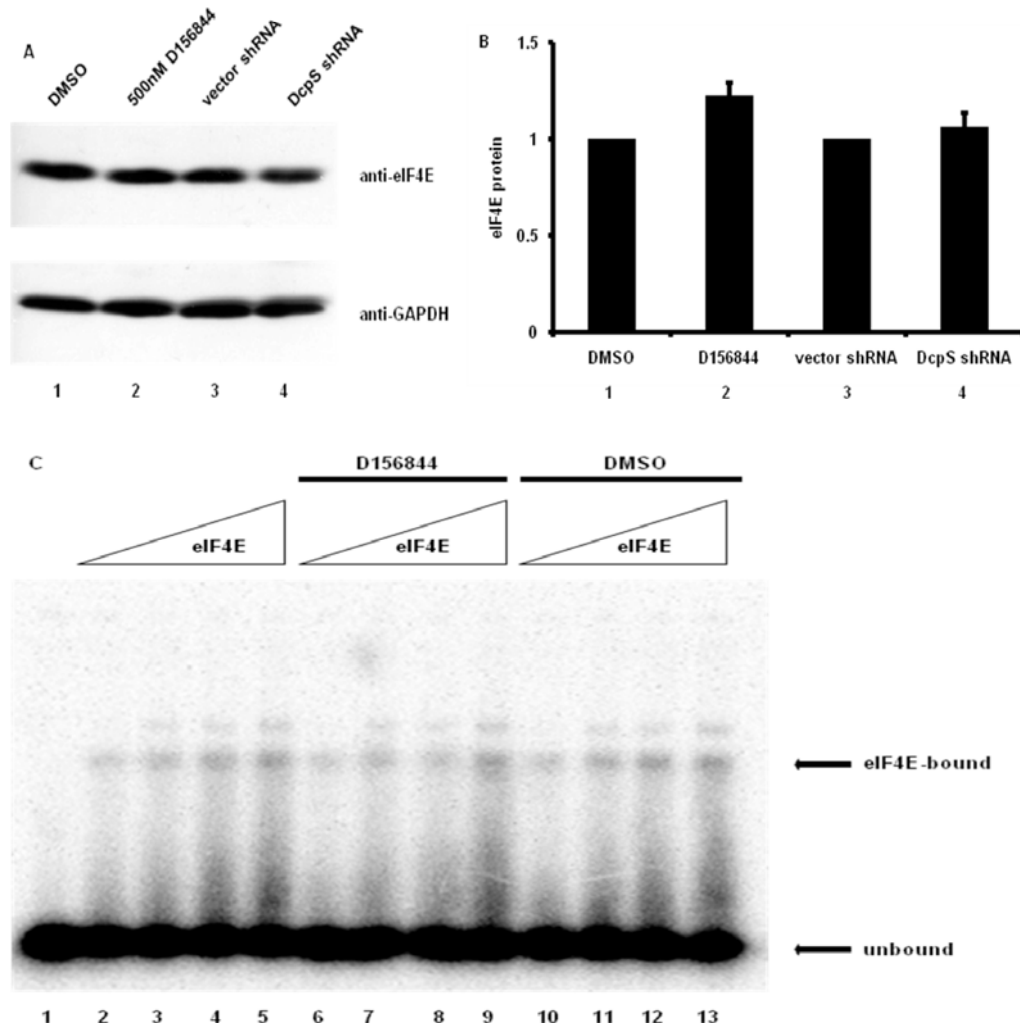


FIGURE 9. eIF4E did not account for translational stimulation.

(A) Pretreated or DcpS shRNA 293T cells were harvested with DMSO and control shRNA cells. Whole cell extract was resolved on SDS PAGE and analyzed by western blot with eIF4E- and GAPDH-specific antibodies. D156844 stimulated eIF4E slightly (compare lanes 1 and 2). However, eIF4E protein did not change upon DcpS repression (compare lanes 3 and 4). GAPDH was used as reference gene. (B) Western blot was quantitatively confirmed. Error bars denoted standard error for three data sets (n=3). (C) Recombinant human eIF4E and 32 P-alpha-GTP cap-labeled RNA were incubated, in the presence of D156844 or DMSO to form protein-RNA complexes. After UV crosslinking and nuclease treatment, bound complexes were resolved on denaturing urea PAGE and analyzed by autoradiography. D156844 did not affect eIF4E-capped RNA interaction (lanes 6-9) compared to no treatment (lanes 2-5) or DMSO treatment (lanes 10-13). Western result was provided by Dr. Xinfu Jiao.

compound addition failed to elicit any response from recombinant eIF4E's interaction with capped mRNA (Figure 9C). Therefore, these results suggested DcpS did not stimulate cap-dependent translation through eIF4E.

A third possible explanation was cap-dependent translational stimulation occurred through an influence on 4EBP1 and 4EBP2, two well-known translational inhibitors of the eIF4F complex. These proteins were assessed by western blot with specific antibodies that recognized one but not the other protein. Three days of D156844 pretreatment of 293T cells reduced 4EBP1 steady state protein level by 31% and 4EBP2 by 8% in Figure 10A. However, the reduction in 4EBP2 was statistically insignificant. Similarly, in Figure 10A, DcpS shRNA repressed 4EBP1 protein level by 13% relative to those of control shRNA, indicating DcpS repression by chemical inhibitor specifically downregulated 4EBP1 protein levels. DcpS shRNA also repressed 4EBP2 protein level by 15%. In short, the western analysis pointed to 4EBP1 and 4EBP2 as potential targets of DcpS.

To address the manner by which DcpS repression may reduce 4EBP1 and 4EBP2 protein levels, RNA was extracted from 293T cells grown for three days in the presence of D156844 or DMSO and reverse transcribed for quantitative PCR (qPCR) analysis with primer pairs specifically toward either 4EBP1 or 4EBP2. In Figure 11A, D156844 reduced 4EBP1 and 4EBP2 mRNA steady state levels by ~50%, suggesting a deterioration in mRNA stability or transcriptional rates. In order to address the mRNA stability issue, D156844- or DMSO-treated cells were subjected to actinomycin D treatment to shut down ongoing transcription and harvested at 0, 4 and 8 hour post-actinomycin D timepoints to assess mRNA decay rates by qPCR. Figure 11B showed that

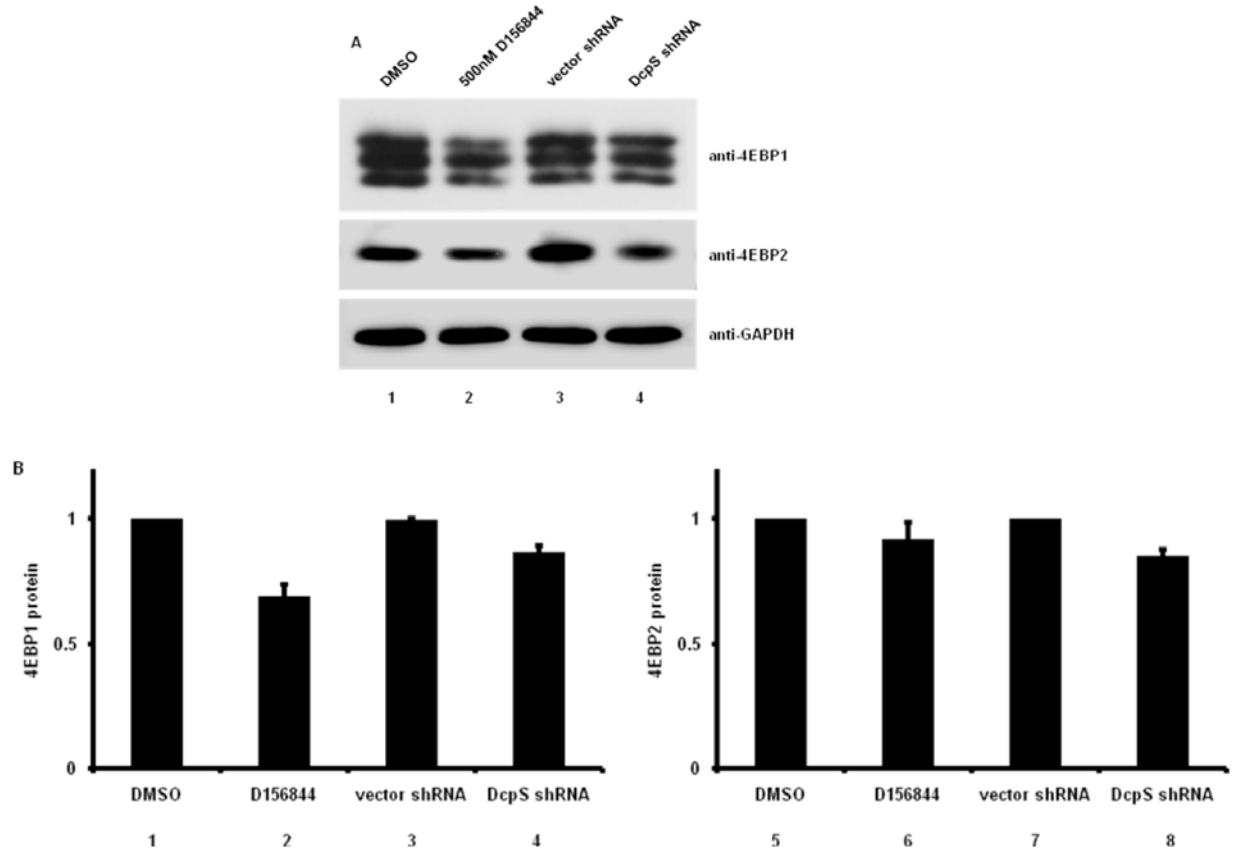


FIGURE 10. DcpS repression reduced 4EBP1 protein level.

(A) Pretreated or DcpS shRNA 293T cells were harvested with DMSO and control shRNA cells. Whole cell extract was run on SDS PAGE and analyzed by western blot with 4EBP1, 4EBP2, and GAPDH antibodies. 4EBP1 protein was reduced by D156844 addition and DcpS repression by shRNA (top panel: compare lanes 1 and 2; compare lanes 3 and 4). 4EBP2 protein reduction was statistically insignificant by D156844 addition (middle panel: compare lanes 1 and 2). 4EBP2 protein reduced upon DcpS repression by shRNA (middle panel: compare lanes 3 and 4). GAPDH was used as the reference gene. (B) Western blot was quantitatively confirmed. Error bars denoted standard errors for three data sets (n=3). Result was provided by Dr. Xinfu Jiao.

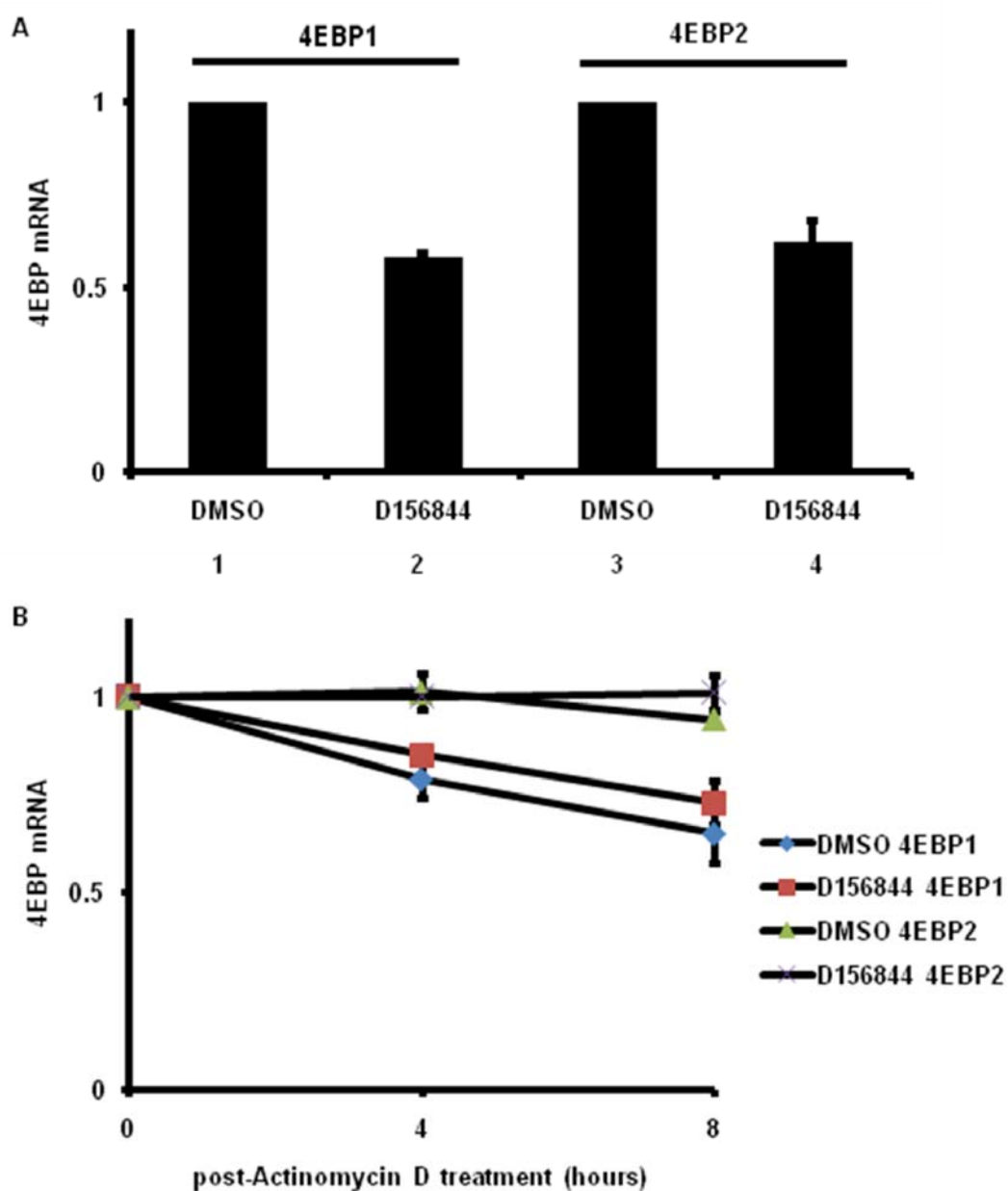


FIGURE 11. D156844 reduced endogenous 4EBP1 and 4EBP2 mRNA levels.

(A) Pretreated 293T cells were harvested. RNA was isolated for qPCR analysis with 4EBP1- and 4EBP2-specific primer pairs. Beta-actin was used as the reference gene. 4EBP1 and 4EBP2 mRNAs reduced upon D156844 addition (compare lanes 1 and 2; compare lanes 3 and 4). (B) Pretreated 293T cells were transcriptionally blocked with actinomycin D, after which cells were harvested at 0 h, 4 h, 8 h timepoints. RNA was isolated and detected by qPCR. 4EBP1 and 4EBP2 mRNA stabilities did not change upon D156844 addition (compare slopes of square and diamond lines; compare slopes of cross and triangle lines). Error bars denoted standard errors for three data sets (n=3).

D156844 led to equivalent 4EBP1 and 4EBP2 transcript decay rates when compared to their respective DMSO-treated counterparts. qPCR analysis implicated DcpS repression reduced 4EBP1 and 4EBP2 mRNA steady state levels but did not affect transcript decay rates, suggesting regulation of both 4EBPs occurred at the transcriptional level.

Next, in order to assess D156844's effect on the translational repressors at the transcriptional level through a quantitative method, nuclear run-on assay coupled with qPCR (Patrone et al., 2000) was used to measure the transcriptional rates of endogenous 4EBP1 and 4EBP2. D156844- or DMSO-treated cells were immersed in hypotonic solution to extract the intact nuclei. RNA polymerase II complexes that remained associated along the endogenous promoter and coding regions were primed for elongation with ATP, GTP, CTP, and biotinylated UTP. Biotinylated nascent transcripts were purified from total RNA via streptavidin beads and reverse transcribed for qPCR analysis. In Figure 12, DcpS repression led to a ~50% reduction in both 4EBP1 and 4EBP2 transcriptional rates that correlated with the respective steady state mRNA levels. In contrast, beta-tubulin transcriptional rates remained unresponsive in the treatment and control samples.

One possible model based on these findings suggested DcpS repression reduced 4EBP1 and 4EBP2 protein levels to alleviate the cytoplasmic translation machinery. As a step toward bypassing DcpS, 293T cells were stably infected with lentivirus that induced the expression of either 4EBP1 or 4EBP2 shRNAs in an effort to reconstitute cap-dependent translational stimulation. Quantitations indicated 4EBP1 and 4EBP2 were knocked down by 43% and 16%, respectively, relative to that of control shRNA as shown in Figure 13B. The cells were transfected with the dicistronic

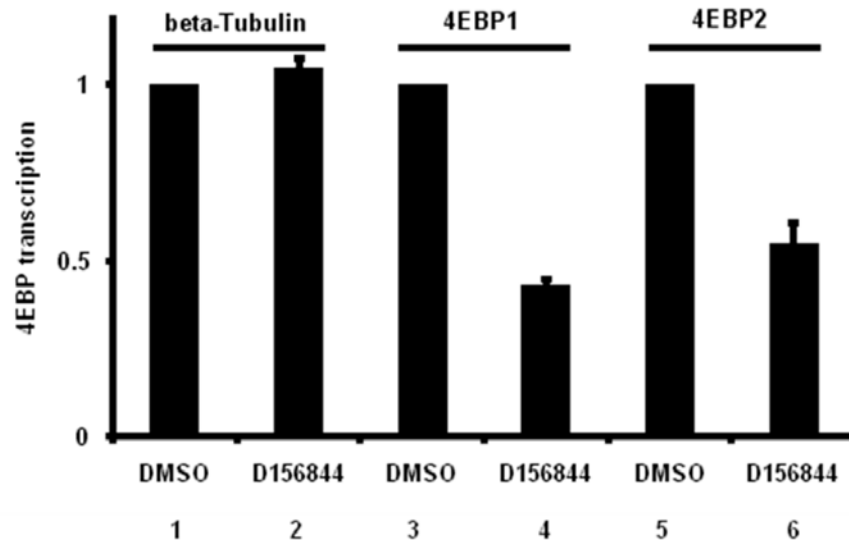


FIGURE 12. D156844 stimulated endogenous 4EBP1 and 4EBP2 transcriptions.

Nuclei of pretreated 293T cells were isolated and subjected to nuclear runon assay. Nascent transcripts were detected by qPCR with beta-tubulin-, 4EBP1-, and 4EBP2-specific primers. Beta-actin was used as the reference gene. Beta-tubulin transcription did not change upon DcpS repression (compare lanes 1 and 2). 4EBP1 and 4EBP2 transcriptions reduced upon D156844 addition (compare lanes 3 and 4; compare lanes 5 and 6). Error bars denoted standard errors for three data sets (n=3).

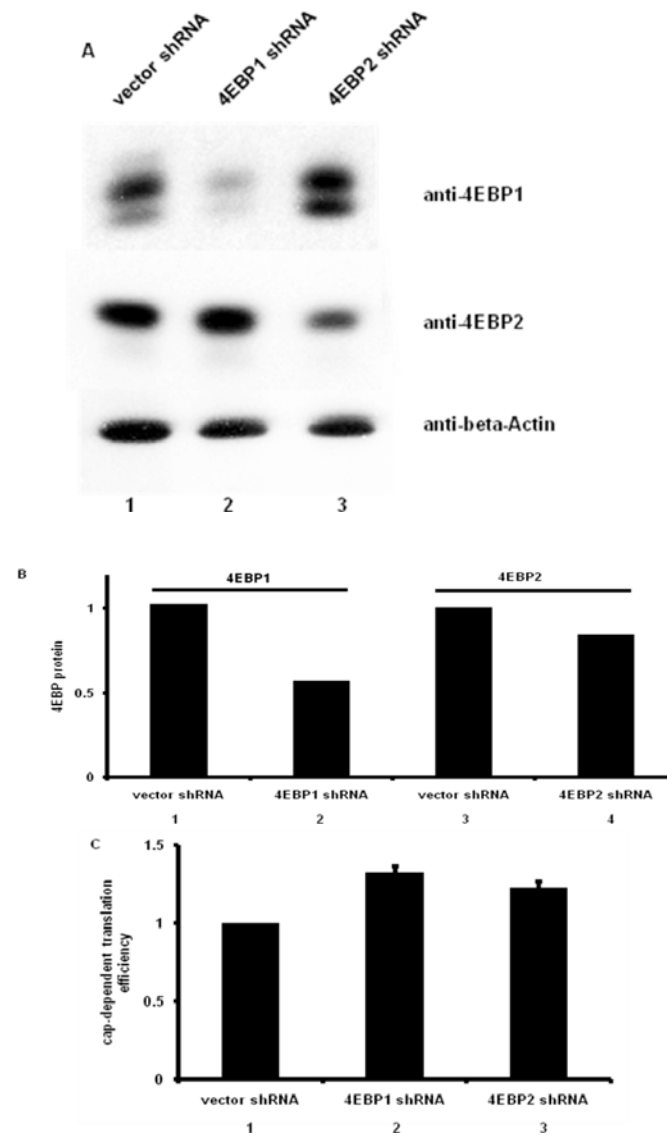


FIGURE 13. 4EBP1 and 4EBP2 knockdown stable cell lines.

(A) Stable 4EBP1 and 4EBP2 knockdown cell lines were harvested and tested for knockdown efficiency using western blot with 4EBP1- and 4EBP2-specific antibodies. Beta-actin was used as reference gene. (B) Western blots were quantitatively confirmed. 4EBP1 and 4EBP2 were knocked down by 43% and 16% (top panel: compare lanes 1 and 2; middle panel: compare lanes 2 and 3). (C) Stable 4EBP1 and 4EBP2 knockdown cell lines were transfected with the dicistronic reporter construct, harvested eight hours later, and assayed for Luciferase activities. Renilla activity was normalized to Firefly activity. Cap-dependent translations were stimulated slightly upon 4EBP1 repression (compare lanes 1 and 2) and 4EBP2 repression (compare lanes 1 and 3). Error bars denoted standard errors for three data sets (n=3).

reporter construct and assayed for Luciferase activities. Repression of either 4EBP1 or 4EBP2 led to the expected stimulation of cap-dependent translation in Figure 13C. However, each individual knock down experiment produced a partial stimulation on the order of 33% and 23% increases, respectively. These data suggested the redundant nature of 4EBP1 and 4EBP2 required both simultaneous knock down to recapitulate the full magnitude of cap-dependent translational stimulation. Alternatively, DcpS-mediated translational stimulation extends beyond the modulation of the 4EBPs. Thus far, generation of an efficient dual knock down cell line to distinguish the two possibilities had not been successful.

Discussion

Prior to the current work, DcpS has been shown to be involved in mRNA degradation and pre-mRNA splicing (Liu and Kiledjian, 2005; Shen et al., 2008; Wang and Kiledjian, 2001). One working model predicts DcpS repression would lead to an intracellular accumulation of inhibitory cap structure which can potentially negate cap-dependent translation similarly to pre-mRNA splicing. Contrary to the prediction, DcpS repression stimulates cap-dependent translation in the cell-based protein reporter assay, and this opposite result contends the model is not viable in the cytoplasmic context as opposed to the nucleus. Secondly, DcpS repression leads to an accompanied decrease in 4EBP1 and 4EBP2 protein and mRNA levels. The precise manner in which these consequences occur and are related is unclear at this moment. The novel finding of this work indicates DcpS stimulates transcription of specific target genes.

The present report maps the first functional interaction between DcpS and two related translational repressors. Previous studies have supported roles for DcpS in gene expression without referring to specific gene targets (Liu and Kiledjian, 2005; Shen et al., 2008; Wang and Kiledjian, 2001). In contrast, this work defines two specific genes that operate downstream of DcpS. Upon DcpS repression, 4EBP transcriptional rates are clearly reduced by ~50%, whereas their respective protein levels are reduced to a less degree. The changes in transcriptional rates and steady state mRNA levels do not proportionately reflect the changes at the protein levels. For example, the ~8-30% reduction in 4EBP protein levels amidst 50% reduction of transcriptional rates indicates an unknown compensatory event in the gene expression paradigm. In a more extreme example, the observation that D156844 does not statistically significantly reduce 4EBP2 protein level, while simultaneously reducing 4EBP2 transcript levels, hints an underlying compensatory event. These discrepancies may involve any combination of an enhanced step during mRNA export, mRNA stability, protein synthesis, or protein stability. Analysis of endogenous 4EBP transcript decay has ruled out any likelihood of enhanced mRNA stability. However, the other candidate steps are still potential causes of the mismatched throughput of gene expression between the mRNA and protein levels. On the other hand, the relative 4EBP1 and 4EBP2 steady state mRNA levels correlate quantitatively with their respective transcriptional rates. In short, these results indicate DcpS promotes 4EBP1 and 4EBP2 transcription.

This study provides additional support for DcpS role in cap-dependent processes. The reversal of the expected relationship between DcpS and protein synthesis compels re-evaluation of a model that may not be as broadly applicable as previously thought. In the

dicistronic reporter assay, DcpS repression preferentially stimulates cap-dependent translation over HCV IRES-directed protein synthesis. In a second demonstration, DcpS repression stimulates cap-dependent Firefly Luciferase translation preferentially over EMCV IRES-directed Renilla Luciferase activity but does not activate global protein synthesis according to ^{35}S -methionine metabolic labeling in cells. These collective results suggest DcpS repression stimulates cap-dependent translation of a subset of genes, but the mechanism behind the translational response to DcpS is elusive. The responsive event appears to take place during translation initiation, the step in which cap recognition occurs. Translational stimulation may occur through the activation of the eIF4F cap-binding complex or inactivation of the 4EBP translational repressors. Two lines of evidence indicate eIF4F is not activated with regards to eIF4E and eIF4G. Western blot shows DcpS repression does not dramatically change endogenous eIF4E protein level. Secondly, DcpS repression does not alter EMCV IRES-directed translation, a system that utilizes eIF4G. A more stringent test calls upon the empirical assessment of DcpS influence over eIF4E-cap interaction. However, the technical feat of detecting endogenous eIF4E in whole cell extract and its cap-binding capacity in response to DcpS repression poses a challenge for this type of functional analysis. Of secondary note, the minor population of cytoplasmic DcpS partially explains why translational inhibition has not been observed upon DcpS repression. For instance, there may not be ample DcpS molecules, to alter, in the cytoplasmic compartment to observe translational inhibition. In this scenario, cytoplasmic DcpS level does not fluctuate sufficiently in terms of bulk molecule. On the contrary, the nuclear compartment is a different environment and may very well exhibit an accumulation of inhibitory cap structure due to a substantial

reduction of the bulk DcpS population in the nucleus. Moreover, the unobserved translational inhibition indicates the nuclear envelope serves as an effective barrier against inhibitory cap structure diffusion from nucleus to cytoplasm. However, the establishment of a quantitative method to measure subcellular cap levels would provide the most accurate answer to this last unknown variable. Despite the imprecise mechanistic details surrounding the link between DcpS and early protein synthesis, the current study clearly shows DcpS can readily influence cap-dependent processes.

The incomplete stimulation of cap-dependent translation by 4EBP1 and 4EBP2 individual knockdowns suggests either the genes are functionally redundant or at least one unidentified DcpS target remains to be identified. Their isolated inability to reconstitute the complete two fold stimulation in translation supports these two likely scenarios. 4EBP1 and 4EBP2 are functionally redundant in terms of translational repression and eIF4E-binding capacity. A 4EBP1/2 double knockdown cell line would address whether their repressions are sufficient to mimic cap-dependent translational stimulation by DcpS repression. Alternatively, 4EBP1/2 double knockdown may not be sufficient to recapitulate the two fold cap-dependent translational stimulation, and this outcome would be consistent with the idea of an unidentified gene.

A more detailed mapping of the genetic interactions between DcpS and the translational repressors in regards to cap-dependent protein synthesis requires epistatic analysis. The current results indicate DcpS lies upstream of 4EBP1 and 4EBP2 with respect to cap-dependent translation. Past studies also indicate 4EBP1 and 4EBP2 are regulators of cap-dependent translation (Pause et al., 1994). Redundancy between 4EBP1 and 4EBP2 can be confirmed by analysis of the severities on translational output between

single and 4EBP1/2 double knockouts. However, no such report or evidence to date has addressed whether DcpS and 4EBPs act in series or parallel. This can be determined by using the *Irf7* gene, a validated endogenous target of the 4EBPs, as a measure of translational readout (Erickson and Gale, 2008). Individual knockouts and combined DcpS/4EBP knockouts can be analyzed with respect to *Irf7* output. If DcpS and 4EBPs act in parallel, the double DcpS/4EBP knockouts would exhibit higher translational stimulation of *Irf7* than that of either single knockout. On the other hand if DcpS and 4EBPs act in series, the double DcpS/4EBP knockouts would exhibit similar translational stimulation of *Irf7* to that of either individual knockout. Although the collective studies infer to position DcpS, 4EBP1, and 4EBP2 within the same regulatory pathway of cap-dependent translation, epistatic analysis is essential to build a more detailed genetic model. In the present state, two genetic regulatory models exist and involve either DcpS and 4EBPs acting in parallel pathways or DcpS and 4EBPs acting in series in cap-dependent protein synthesis. The observation that 4EBP mRNAs are reduced expands the notion that DcpS regulates nuclear activities other than pre-mRNA splicing through an indirect role.

CHAPTER III: DcpS in Mouse Development

Summary

A beta-galactosidase-neomycin fusion cassette has been randomly inserted into the mouse genome and disrupts the *DcpS* gene. PCR-based genotyping shows the cassette inserts into the second intron of the locus. *DcpS* heterozygous mice are normal with respect to viability and fertility. This indicates the ablated allele is recessive to that of the wildtype. Heterzygous intercrosses produce two heterzygotes per wildtype pup, indicating homozygotes are embryonic lethal. *DcpS* recessive homozygotes cannot be detected as early as E6 and confirms the essential role which *DcpS* plays during early mouse development. Western blot shows *DcpS* expression is ubiquitous throughout the brain, heart, liver, and kidney throughout the adult stage. In contrast, mouse embryo shows preferential *DcpS* wholemount staining in the forebrain. Expression analysis shows *DcpS* is regulated in a spatial and temporal manner. This is the first work that demonstrates the essential role of *DcpS* in an organism.

Introduction

DcpS Biological Function in Mouse

Despite extensive efforts in the characterization of *DcpS* biochemical and subcellular properties, the systemic contribution of *DcpS* has never been addressed in mammalian development and has been studied over a limited range of organisms comprised of yeast and worms. In yeast, two separate loci, *Dcs1* and *Dcs2*, encode the decapping scavenger protein although the latter is catalytically inactive, whereas in worms, the genome encodes one decapping scavenger enzyme (Lall et al., 2005; Liu et al.,

2002). In addition, worm DcpS is not essential for development (Lall et al., 2005; Liu and Kiledjian, 2005). Although the systemic consequence of DcpS function in mammals has not been addressed directly, a recent study raises the possibility of a link between DcpS and SMN (Singh et al., 2008), in which a molecule that rescues Spinal Muscular Atrophy (SMA) mice from embryonic lethality also inhibits decapping activity,. In this case, DcpS would appear to promote the affected phenotype since its reduction correlates with the amelioration of SMA. In humans, SMN2 is a duplicated locus that contains a missense that reduces splicing efficiency and thus produces a higher proportion of the inactive truncated protein (Monani et al., 1999). Eight copies of human SMN2 reverses the SMA phenotype in mice (Monani et al., 2000b). The biological function of DcpS in a mammalian model is unknown, and therefore, the present goal is to address the systemic contribution of DcpS during mouse development.

Results

DcpS Is Essential and Ubiquitous in Adults

In order to address the biological significance of DcpS, we set out to generate mice with a homozygous disruption of the *DcpS* gene. A 129/Ola-derived mouse embryonic stem (ES) cell line, CSH092 (Baygenomics), containing a gene-trap cassette within exon 2 of *DcpS* was injected into blastocysts obtained from pregnant C57BL/6 female mice (Jackson Laboratory). These blastocysts were introduced into surrogate mothers to produce chimeric progeny which indicated germline transmission of the modified ES cell. The male chimeras were screened for presence of the targeted allele and mated with the C57BL/6 females to produce DcpS heterozygotes. The precise

insertion site was mapped by PCR reactions that walked a series of non-overlapping forward primers across the chromosome and relied on a common reverse primer that annealed to the cassette. As shown in Figure 14A, chromosomal walking produced a step-like pattern of amplicons in decreasing sizes as the forward primer approached closer to the insertion site. The gene-trap cassette was inserted near the 6679th nucleotide of the second intron by random chance and contained a cistronic fusion that encoded beta-galactosidase and neomycin selection marker as shown in Figure 14B. The fused cistron was flanked by an upstream 3' splice site and downstream poly(A) signal which promoted its ligation to the second exon to produce a truncated transcript. Multiplex PCR genotyping of adult tails using three primers identified heterozygotes on the basis of the presence of the mutant allele and the wildtype allele. The higher mutant PCR product was amplified by a common forward primer and reverse primer that annealed to an upstream intronic region and cassette, respectively. On the other hand, the lower mutant amplicon was generated by the same forward primer and a distinct reverse primer that annealed to a downstream intronic region. DcpS heterozygotes were intercrossed to an effort to obtain recessive homozygotes.

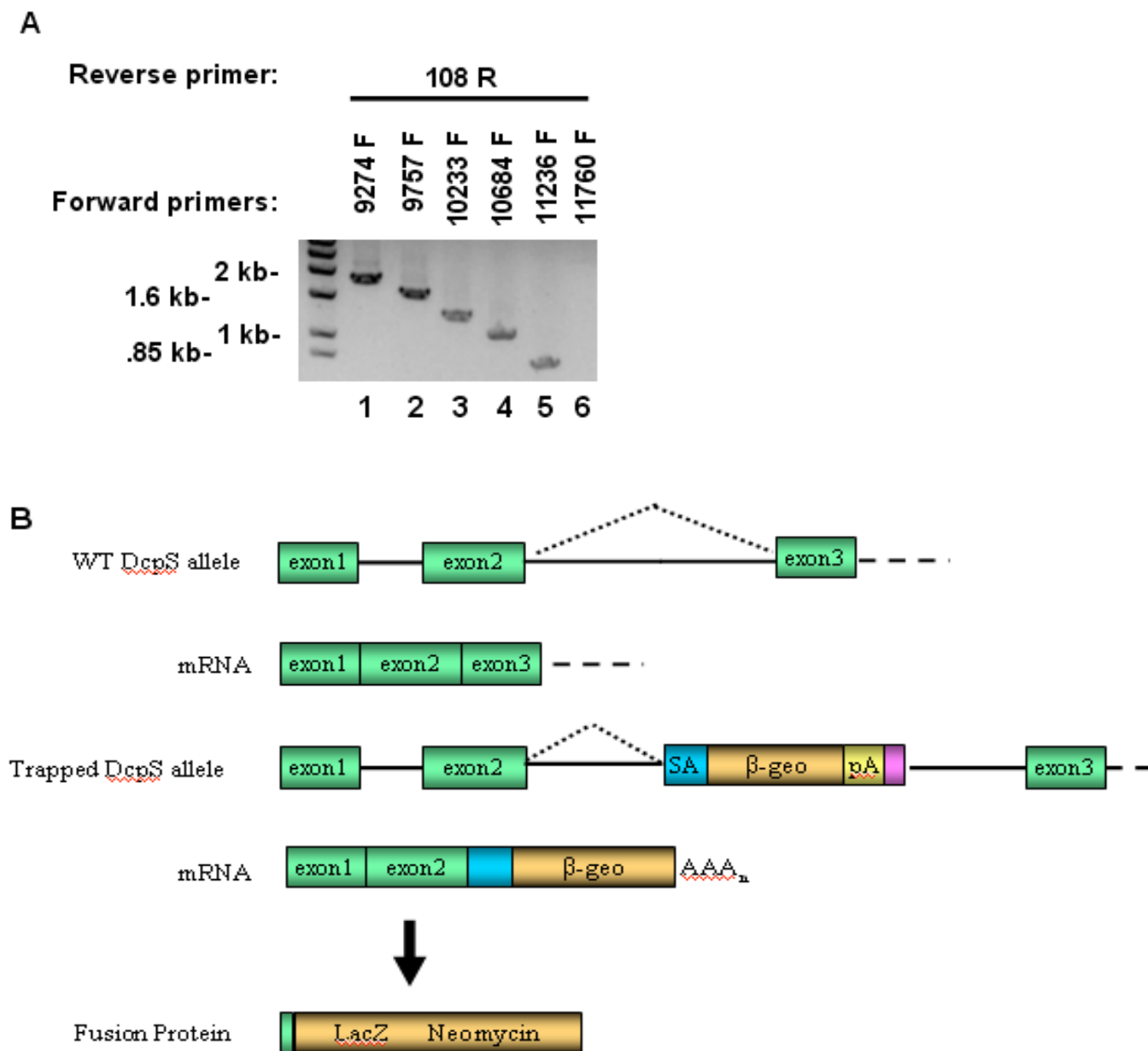


FIGURE 14. A gene-trap cassette randomly inserted into the second intron of *DcpS* locus.

(A) Non-overlapping forward primers were walked across intron 2 with a common reverse primer to map the beta-geo cassette insertion site. Detection of products were visible (lanes 1-5) until forward primer annealed past the reverse primer, and no product was detected (lane 6). Reverse primer annealed to the beta-geo cassette. (B) Beta-geo cassette which encoded beta-galactosidase and neomycin was randomly inserted into the second intron of the *DcpS* locus. The cassette contains a strong splice acceptor (SA) site that spliced into exon 2, generating a truncated gene product.

The ablated allele was recessive to the wildtype DcpS allele since heterozygous adults were indistinguishable from their wildtype counterparts in terms of viability and fertility. Heterozygotes successfully interbred to produce progeny in proportions of two heterozygotes for every wildtype pup, suggestive of a lethal autosomal recessive inheritance pattern as shown in Table 1. Differences between proportions of heterozygous intercross progeny and Mendelian expected proportions were statistically significant at the levels of the pup and 9.5 dpc embryos. The failure to detect recessive homozygotes as early as 6 days post coitum (dpc) suggested DcpS gene dosage was essential during the first third of embryogenesis. In Figure 15, wholemount X-gal staining of 12.5 dpc embryos showed prevalent DcpS presence in the forebrain but was completely absent or severely diminished in the midbrain and hindbrain. Saggital cryosections were used to refine DcpS spatial expression with respect to anatomical landmarks, but the post-seven hour stain intensity was deemed too weak to assess even for the strong signal in the forebrain. Expression analysis was carried out on tissue samples of later age as well. In Figure 16, western blot of adult tissues showed DcpS was ubiquitously expressed in brain, liver, kidney, and heart in wildtype and heterozygous tissues. The main findings clearly indicated DcpS was essential for mouse embryogenesis before 6 dpc, and its expression did not exhibit preferential tissue restriction in the present panel of adult mouse tissue.

genotype	pup numbers	9.5 dpc embryo numbers
+/+	29	16
+/-	55	26
-/-	0	0
total:	84	42

Table 1. DcpS was essential in early mouse development.

Pup tails were genotyped using multiplex PCR. Chi square test indicated a two-tailed p value of 0.0001, indicating a statistically significant deviation from the expected ratios. 9.5 dpc embryos were genotyped using the same multiplex PCR. Chi square test indicated a two-tailed p value of 0.0007, indicating a statistically significant deviation from the expected proportions. The absence of DcpS homozygotes indicated an embryonic lethal phenotype.

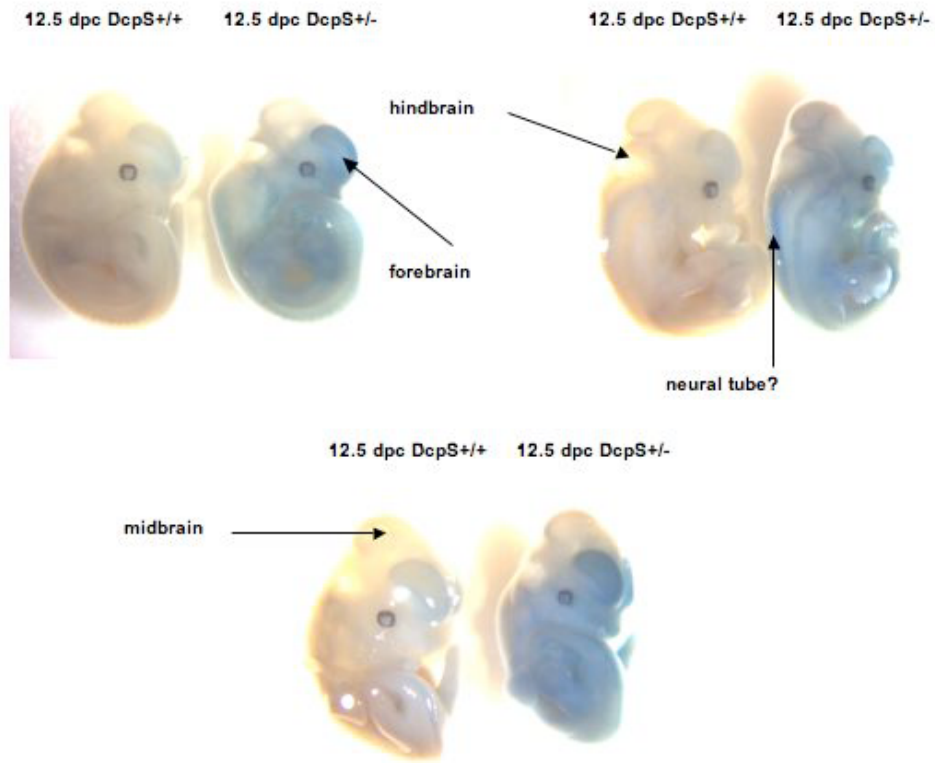


FIGURE 15. DcpS was expressed in the embryonic forebrain. 12.5 dpc embryos from a heterozygous intercross were stained with X-gal substrate for seven hours at 37°C. Arrows indicated forebrain, midbrain, hindbrain, and putative neural tube staining.

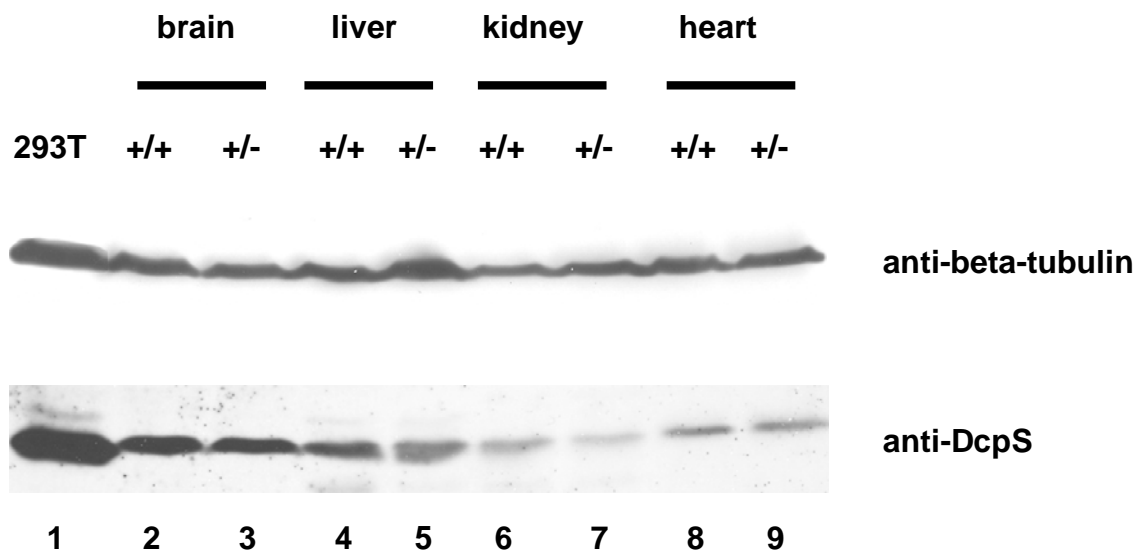


FIGURE 16. DcpS was express ubiquitously in various adult organs.

Organs were isolated from wildtype and DcpS heterozygous mice and homogenized to prepare extract to be run on SDS PAGE. Western analysis with DcpS and beta-tubulin antibodies showed DcpS appeared ubiquitously expressed in brain (lanes 2 and 3), liver (lanes 4 and 5), kidney (lanes 6 and 7), and heart (lanes 8 and 9). 293T whole cell extract was included as a positive control (lane 1). Beta-tubulin was used as a reference gene.

Discussion

The inability to detect DcpS homozygous embryos demonstrates the requirement of scavenger decapper in early mouse development. The 2:1 Mendelian proportion of heterozygotes to wildtypes recovered from heterozygous intercrosses indicates production of functional sperm and oocyte were normal. The absence of homozygotes as early as 6 dpc indicates the earliest essential function of DcpS resides somewhere from fertilization through implantation. In retrospect of cell line data that show an association between DcpS and SMN through a drug compound (Singh et al., 2008), the common embryonic lethal phenotype shared by the loss of either gene may be due to coincidence or may reflect a functional link. An essential DcpS role during implantation, for example, is not far-fetched in light of the peri-implantation defects found in SMN knockout embryos that die around a similar developmental stage (Hsieh-Li et al., 2000; Schrank et al., 1997). SMN heterozygous intercrosses yield normal proportions of homozygous recessive blastocysts at 3.5 dpc. However, mouse development exhibit abnormally pleiotropic events as early as morula compaction around 3 dpc, blastocyst cavity formation by 4 dpc, and subsequent blastocyst implantation by 5.5 dpc. The cells of the SMN deficient blastocyst at 4 dpc undergo extensive apoptosis based on a morphology and TUNEL staining, incapacitating the blastocyst's affinity for the uterine wall. Whether DcpS knockout blastocysts may exhibit a similar phenotype is not currently clear. Additional DcpS requirement may reside in mid-late stages of embryogenesis. The results in the current work clearly illustrates DcpS is required for early mouse embryogenesis, but the precise stage at which this gene is required is unknown. Alternatively, DcpS may mimic SMN's role in facilitating axonal growth toward target tissue in later development.

During zebrafish embryogenesis, for example, SMN knockdown leads to partial failure of axonal growth to reach the ventrally located muscular target (Boon et al., 2009). The associative tie between DcpS and SMN provides an insightful clue into the scavenger decapping enzyme's function during early mouse embryogenesis and can be suggestive of a role in peri-implantation development, which if true, would intimate a common pathway.

Although the biological relevance of the relationship between DcpS and SMN through a lead compound is not clear (Singh et al., 2008), recent results support the notion of shifting the therapeutic momentum toward non-traditional targets that show promise for an SMA cure. The reversal of the affected phenotype in SMA mouse models with a human transgene has been the primary push behind SMN2 as the traditional SMA therapeutic target (Monani et al., 2000a). Coincidentally, human SMN and SMN2 reside on the same chromosome and thus attention has focused predominantly exclusively on the SMN locus. However, three studies indicate the need to broaden the scope of SMA therapeutics beyond the traditional genetic marker in order to diversify the medicinal SMA portfolio, which has yet to produce its first federally approved drug. One of the clearest yet intriguing reports to suggest additional SMA determinants that exist beyond the SMN locus has been the unaffected individuals who harbor homozygous SMN deletions (Hahnen et al., 1995). These individuals belong to four families, and they have siblings who share identical SMN flanking sequences, implying the existence of unlinked SMA determinants. Another study has shown similar unaffected females of six families who have higher plastin 3 protein levels compared to that of their siblings (Oprea

et al., 2008). Plastin 3 locus is a potential X-linked SMA determinant, and its expression correlates with the unaffected phenotype. Finally, the most recent work shows SMN2 is linked to DcpS through a lead compound in a screen for an SMA drug candidate (Singh et al., 2008). The lead compound, D156844, activates SMN2 but inhibits DcpS, illustrating a putative autosomal SMA determinant. Not one of these instances on its own indicates cause-effect relationships in the context of a genetic disorder, but they represent independent cases that urge the necessity to seek novel determinants that are causally related to the SMA phenotype and that are not necessarily linked to the SMN locus. A collective band of research efforts that converge from sparse nodes of truly unrelated scientific inquiry can gain farther progress in the therapeutic search for a cure of an infantile disease for which the pathological cause is still poorly understood.

Final Summary on the Current Work

DcpS is a protein whose canonical role has been rooted in cytoplasmic mRNA degradation. Cytoplasmic assignment of DcpS is supported by several biochemical experiments. The cytoplasmic fraction provides a rich soluble source of its potent activity (Wang and Kiledjian, 2001). In terms of substrate specificity, DcpS exclusively hydrolyzes the 5' cap end of mRNA after the 3' to 5' exoribonuclease activity has degraded the majority of the phosphodiester bonds. The prerequisite for 3' to 5' exoribonuclease activity can be explained by the physical association between DcpS and the exosome complex (Wang and Kiledjian, 2001). In vitro binding study indicates DcpS competes with eIF4E for the mRNA 5' cap (Liu et al., 2004), providing a link between a decapping protein and a cytoplasmic cap-dependent process. Yeast and worm DcpS reside mainly in the cytoplasm (Lall et al., 2005; Malys et al., 2004), but the nuclear residence of mammalian DcpS is the single physiological data that hints of an unknown nuclear assignment. The broad findings of the current work focus on mammalian DcpS and address its nuclear presence in light of an unknown nuclear function. The first work reveals identification of DcpS nuclear import and export signals that account for its nucleocytoplasmic shuttling capability. Providing one explanation for its prevalent nuclear signal, Figure 17 shows DcpS regulates cap-proximal pre-mRNA splicing. In support of an additional role in a cap-dependent process, evidence indicates DcpS represses cap-dependent translation and concomitantly stimulates specific transcription of translation inhibition factors. Therefore, the crucial findings of the first two works confirm a general role for DcpS in cap-dependent processes and unveil its dual nuclear roles in pre-mRNA splicing and transcription for specific target genes. The third work

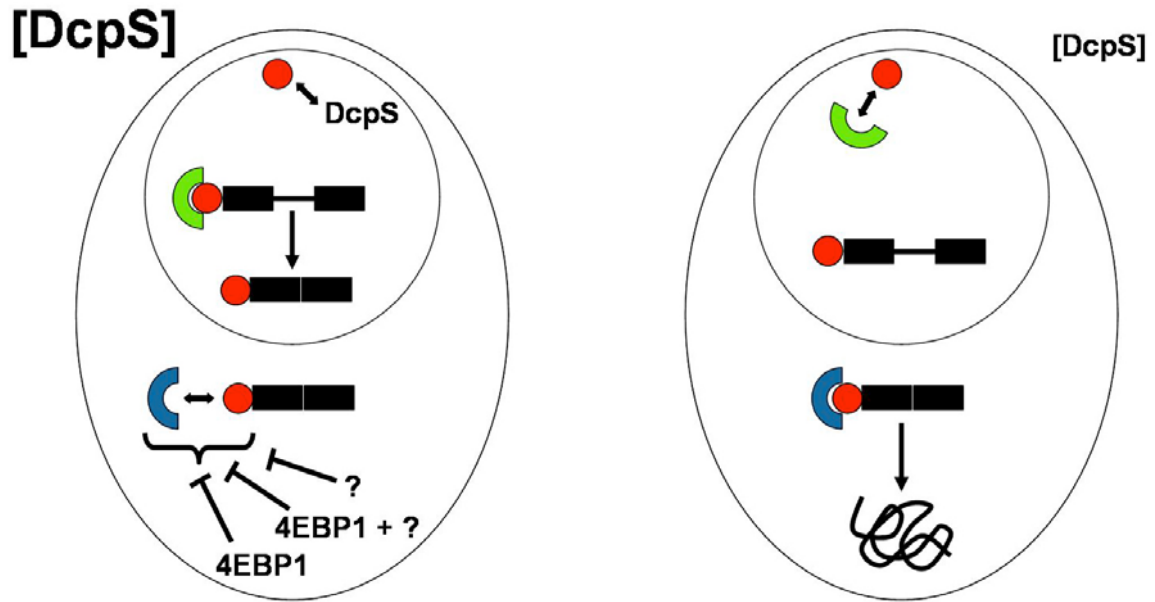


FIGURE 17. DcpS regulated cap-dependent processes.

(Left panel) Under normal DcpS levels, pre-mRNA splicing occurs normally in the nucleus. However, cap-dependent translation is repressed through an unknown mechanism. The manner by which this cytoplasmic event may occur through 4EBP1 enhancement with or without an associated factor(s). Alternatively, translational repression may be independent of 4EBP1. The enhancement of 4EBP1 may occur potentially through an upregulation of its nuclear transcription (not shown). (Right panel) When DcpS is depleted, nuclear splicing about the first intron is defective, but cytoplasmic cap-dependent translation occurs normally. Red ball denotes cap-structure. Green and blue shapes denote Cbp20 and eIF4E, respectively. Black rectangle and intermediate black lines represent the exons and introns of pre-mRNA. Squiggly line denotes protein. Oval lines denote the phospholipids bilayer.

addresses the biological significance of mammalian DcpS for the first time and indicates DcpS is essential for mouse development. In summary, the novel contributions of the present DcpS work entail identifications of its nuclear import and export sequences, dual nuclear roles in cap-proximal splicing and transcription, and an unforeseen essential function in mouse development.

DcpS function is becoming increasingly nuclear-oriented and essential than its previous characterizations as a cytoplasmic decapping protein. DcpS performs two previously undefined nuclear functions with regard to pre-mRNA splicing and transcription in a subset of genes. The present evidence shows DcpS is a positive effector of both nuclear processes. In the case of pre-mRNA splicing, the outcomes are consistent with the idea that DcpS keeps cap structure concentrations in check for a nuclear cap-dependent event to occur normally. Previous work suggests DcpS provides an intracellular signal in 5' to 3' mRNA degradation. Its substrate and products may be signaling molecules given the common guanine structural feature and its ubiquitous role as a universal building block found in the phospholipids bilayer, post-translational modifications, molecular switches, and genetic code. The idea that DcpS and its bound nucleotide operate as a molecular switch analogous to G proteins is an attractive possibility that requires identification of GAP- or GEF-like activities that regulate its enzymology. The notion that DcpS can take on non-canonical functions is not new and has been addressed by at least two other sources. One work suggests DcpS is a repressor of bHLH transcription factor MITF (Chou and Wagner, 2007). Considering its new found involvement in a genetic circuit, the notion that DcpS is a transcription factor is attractive, but a DNA-binding motif or transcriptional potential has yet to be shown. Still, another

work points to DcpS as a bifunctional protein with hydrolase and phosphate addition activities (Guranowski et al., 2010), reminiscent of the dual triphosphatase and guanylyltransferase properties of human capping enzyme. This idea is also tempting, but mapping of the sequence responsible for its phosphate addition activity is required. Although the exact mechanism behind its dual nuclear roles in cap-proximal splicing and transcription is unknown, the present results are in line with the idea that DcpS keeps intracellular cap concentrations at a level that is permissive toward nuclear events. DcpS plays an increasingly important role in normal development and has moved up the evolutionary ladder with regard to biological significance. Worm DcpS is non-essential, whereas in mammals, DcpS appears to have assumed more essential roles. On a second note, the decapping proteins may serve as an anti-viral defense regimen against infection. This is perceivable in light of the observation that at least one component of the interferon response pathway may lie downstream of DcpS. Decapping proteins can convert its cellular capped oligonucleotides into distinct biosynthetic camouflage that evades detection by the viral machinery. Hydrolysis of capped oligonucleotides would prevent them from being partially recycled onto the 5' diphosphate ends of bamboo mosaic viral transcripts for example. Similarly, cleavage of capped oligonucleotides would eliminate their usage as primers for RNA synthesis by the influenza virus. Viral replication would thus be hampered by this cellular decapping proteins. In this final respect, DcpS serves to insulate the flow of genetic information, and it does so by ensuring the faithful and exclusive transmission of information from cellular genome to cellular gene products.

TABLE 2. Primer Sequences

RT-PCR (real time PCR)

Primer name	Primer pair listed as forward followed by reverse
Flag-DcpS PCR	5' AGGATCCCGCCTCCGCGGCAGCATG 3' 5' TCTCGAGTCAGCTTTGCTGAGCCTCCTG 3'
DcpS ^{ΔKR} PCR	5' GCAGCTCCTCAACTAGGCGAATTGGA 3' 5' CTCCTCCACGTCCAATTCGCCTAGTTG 3'
GFP-DcpS PCR	5' ATATGAATTCTATGGCGGACGCAGCTCCTC 3' 5' GCATGGATCCTCAGCTTTGCTGAGCCTCCTG 3'
DcpS ^{L148A} PCR	5' GTACCTGCGCCAGGACGCCCCGCCTGATCCGAGAG 3' 5' CTCTCGGATCAGGCGGGCGTCCTGGCGCAGGTAC 3'
DcpS ^{L150A} PCR	5' CGCCAGGACGCCCCGCGCGATCCGAGAGACGGGAG 3' 5' CTCCCGTCTCTCGGATCGCGCGGGCGTCCTGGCG 3'
Flag-Cbp20 PCR	5' AAGCTTGGATCCATGTCGGGTGGCCTCCTGAAGG 3' 5' CTCGAGGAATCCTCACTGGTTCTGTGCCAGTTTTC 3'
Fibronectin EE1-2 PCR	5' ATGCCGATCAGAGTTCCTGCACTT 3' 5' TCAGGCCGATGCTTGAGTCAGTTA 3'
Fibronectin EE2-3 PCR	5' ATGCCGATCAGAGTTCCTGCACTT 3' 5' TCAGGCCGATGCTTGAGTCAGTTA 3'
Fibronectin EIJ1 RT-PCR	5' ATGCCGATCAGAGTTCCTGCACTT 3' 5' CTGCTACTCAAACCTGCCTCTCTGA 3'
Fibronectin EIJ2 RT-PCR	5' TGGAACCCGGCATTGACTATGACA 3' 5' GGCTTCTCCTTGGCAACATCCAAA 3'
GAPDH EIJ1 RT-PCR	5' AAATTGAGCCCGCAGCCTC 3' 5' TTTCTCTCCGCCCCGTCTTCAC 3'
GAPDH EE1-2 RT-PCR	forward primer same as for EIJ1 5' CGTTGACTCCGACCTTCACCTT 3'

GAPDH EIJ2 RT-PCR	5' CCGAGCCACATCGCTCAGAC 3' 5' ATACGACTGCAAAGACCCGGAG 3'
GAPDH EE2-3 RT-PCR	forward primer same as for EIJ2 5' AGGCGCCCAATACGACCAAAT 3'
S7 EIJ1 RT-PCR	5' GCTGTTTCCGCCTCTTGCCTTC 3' 5' AAAGTTCTGTCCGAGAGCAGG 3'
S7 EE1-2 RT-PCR	forward primer same as for EIJ1 5' AACTGAACATGGCTTTCTCCTGGG 3'
S7 EIJ2 RT-PCR	5' TCCCAGGAGAAAGCCATGTTTCAGT 3' 5' CCCCAGGGAAACCCTCTCAC 3'
S7 EE2-3 RT-PCR	forward primer same as for EIJ2 5' AGCTGCCGTAATATTCAGCTCCCT 3'
4EBP1 PCR	5' CGGGGACTACAGCACGAC 3' 5' AGTTCCGACACTCCATCAGG 3'
4EBP2 PCR	5' TCATGACTATTGCACCACGC 3' 5' GAGAATTGCGACGATCCAAC 3'
4EBP3 PCR	5' TCGCTATGTCAACGTCCACT 3' 5' CGGTCGTAGATGATCCTGGT 3'
BACTIN PCR	5' GGCATCCTCACCCCTGAAGTA 3' 5' CCACACGCAGCTCATTGTA 3'
TUBB PCR	5' TAACCATGAGGGAAATCGTG 3' 5' TCGATGCCATGTTCATCACT 3'
mDcpS PCR	5' ACGGGTTCCAACCCACTGAGATAAG 3' (F intron) 5' CCTGGCCTGTGGCTAAAGTCCTGAG 3' (R intron) 5' GGATCCTCTAGAGTCCAGATCTGCCGA 3' (R trap)

REFERENCES

- Adamou, J.E., Heinrichs, J.H., Erwin, A.L., Walsh, W., Gayle, T., Dormitzer, M., Dagan, R., Brewah, Y.A., Barren, P., Lathigra, R., *et al.* (2001). Identification and characterization of a novel family of pneumococcal proteins that are protective against sepsis. *Infect Immun* 69, 949-958.
- Adams, B.L., Morgan, M., Muthukrishnan, S., Hecht, S.M., and Shatkin, A.J. (1978). The effect of "cap" analogs on reovirus mRNA binding to wheat germ ribosomes. Evidence for enhancement of ribosomal binding via a preferred cap conformation. *J Biol Chem* 253, 2589-2595.
- Altmann, M., Edery, I., Trachsel, H., and Sonenberg, N. (1988). Site-directed mutagenesis of the tryptophan residues in yeast eukaryotic initiation factor 4E. Effects on cap binding activity. *J Biol Chem* 263, 17229-17232.
- Altmann, M., Handschin, C., and Trachsel, H. (1987). mRNA cap-binding protein: cloning of the gene encoding protein synthesis initiation factor eIF-4E from *Saccharomyces cerevisiae*. *Mol Cell Biol* 7, 998-1003.
- Amberg, D.C., Goldstein, A.L., and Cole, C.N. (1992). Isolation and characterization of RAT1: an essential gene of *Saccharomyces cerevisiae* required for the efficient nucleocytoplasmic trafficking of mRNA. *Genes Dev* 6, 1173-1189.
- Atasoy, U., Curry, S.L., Lopez de Silanes, I., Shyu, A.B., Casolaro, V., Gorospe, M., and Stellato, C. (2003). Regulation of eotaxin gene expression by TNF-alpha and IL-4 through mRNA stabilization: involvement of the RNA-binding protein HuR. *J Immunol* 171, 4369-4378.
- Badis, G., Saveanu, C., Fromont-Racine, M., and Jacquier, A. (2004). Targeted mRNA degradation by deadenylation-independent decapping. *Mol Cell* 15, 5-15.
- Bagga, S., Bracht, J., Hunter, S., Massirer, K., Holtz, J., Eachus, R., and Pasquinelli, A.E. (2005). Regulation by let-7 and lin-4 miRNAs results in target mRNA degradation. *Cell* 122, 553-563.
- Ban, N., Nissen, P., Hansen, J., Moore, P.B., and Steitz, T.A. (2000). The complete atomic structure of the large ribosomal subunit at 2.4 Å resolution. *Science* 289, 905-920.
- Barbas, A., Matos, R.G., Amblar, M., Lopez-Vinas, E., Gomez-Puertas, P., and Arraiano, C.M. (2008). New insights into the mechanism of RNA degradation by ribonuclease II: identification of the residue responsible for setting the RNase II end product. *J Biol Chem* 283, 13070-13076.
- Bartel, D.P. (2004). MicroRNAs: genomics, biogenesis, mechanism, and function. *Cell* 116, 281-297.

- Beaudoing, E., Freier, S., Wyatt, J.R., Claverie, J.M., and Gautheret, D. (2000). Patterns of variant polyadenylation signal usage in human genes. *Genome Res* 10, 1001-1010.
- Behm-Ansmant, I., Rehwinkel, J., Doerks, T., Stark, A., Bork, P., and Izaurralde, E. (2006). mRNA degradation by miRNAs and GW182 requires both CCR4:NOT deadenylase and DCP1:DCP2 decapping complexes. *Genes Dev* 20, 1885-1898.
- Behrens, S.E., and Luhrmann, R. (1991). Immunoaffinity purification of a [U4/U6.U5] tri-snRNP from human cells. *Genes Dev* 5, 1439-1452.
- Berget, S.M. (1995). Exon recognition in vertebrate splicing. *J Biol Chem* 270, 2411-2414.
- Bessman, M.J., Frick, D.N., and O'Handley, S.F. (1996). The MutT proteins or "Nudix" hydrolases, a family of versatile, widely distributed, "housecleaning" enzymes. *J Biol Chem* 271, 25059-25062.
- Bonneau, F., Basquin, J., Ebert, J., Lorentzen, E., and Conti, E. (2009). The yeast exosome functions as a macromolecular cage to channel RNA substrates for degradation. *Cell* 139, 547-559.
- Bonnerot, C., Boeck, R., and Lapeyre, B. (2000). The two proteins Pat1p (Mrt1p) and Spb8p interact in vivo, are required for mRNA decay, and are functionally linked to Pab1p. *Mol Cell Biol* 20, 5939-5946.
- Boon, K.L., Xiao, S., McWhorter, M.L., Donn, T., Wolf-Saxon, E., Bohnsack, M.T., Moens, C.B., and Beattie, C.E. (2009). Zebrafish survival motor neuron mutants exhibit presynaptic neuromuscular junction defects. *Hum Mol Genet* 18, 3615-3625.
- Bringmann, P., Rinke, J., Appel, B., Reuter, R., and Luhrmann, R. (1983). Purification of snRNPs U1, U2, U4, U5 and U6 with 2,2,7-trimethylguanosine-specific antibody and definition of their constituent proteins reacting with anti-Sm and anti-(U1)RNP antisera. *EMBO J* 2, 1129-1135.
- Brown, J.W., Feix, G., and Frendewey, D. (1986). Accurate in vitro splicing of two pre-mRNA plant introns in a HeLa cell nuclear extract. *EMBO J* 5, 2749-2758.
- Bushell, M., and Sarnow, P. (2002). Hijacking the translation apparatus by RNA viruses. *J Cell Biol* 158, 395-399.
- Carballo, E., Lai, W.S., and Blackshear, P.J. (1998). Feedback inhibition of macrophage tumor necrosis factor- α production by tristetraprolin. *Science* 281, 1001-1005.
- Carr-Schmid, A., Durko, N., Cavallius, J., Merrick, W.C., and Kinzy, T.G. (1999). Mutations in a GTP-binding motif of eukaryotic elongation factor 1A reduce both translational fidelity and the requirement for nucleotide exchange. *J Biol Chem* 274, 30297-30302.

Cartwright, J.L., and McLennan, A.G. (1999). The *Saccharomyces cerevisiae* YOR163w gene encodes a diadenosine 5', 5'''-P₁,P₆-hexaphosphate (Ap₆A) hydrolase member of the MutT motif (Nudix hydrolase) family. *J Biol Chem* 274, 8604-8610.

Chang, Y.F., Imam, J.S., and Wilkinson, M.F. (2007). The nonsense-mediated decay RNA surveillance pathway. *Annu Rev Biochem* 76, 51-74.

Chapman, R.D., Heidemann, M., Albert, T.K., Mailhammer, R., Flatley, A., Meisterernst, M., Kremmer, E., and Eick, D. (2007). Transcribing RNA polymerase II is phosphorylated at CTD residue serine-7. *Science* 318, 1780-1782.

Chen, J., Chiang, Y.C., and Denis, C.L. (2002). CCR4, a 3'-5' poly(A) RNA and ssDNA exonuclease, is the catalytic component of the cytoplasmic deadenylase. *Embo J* 21, 1414-1426.

Chiara, M.D., Gozani, O., Bennett, M., Champion-Arnaud, P., Palandjian, L., and Reed, R. (1996). Identification of proteins that interact with exon sequences, splice sites, and the branchpoint sequence during each stage of spliceosome assembly. *Mol Cell Biol* 16, 3317-3326.

Chinali, G., and Parmeggiani, A. (1980). The coupling with polypeptide synthesis of the GTPase activity dependent on elongation factor G. *J Biol Chem* 255, 7455-7459.

Choi, K.M., McMahon, L.P., and Lawrence, J.C., Jr. (2003). Two motifs in the translational repressor PHAS-I required for efficient phosphorylation by mammalian target of rapamycin and for recognition by raptor. *J Biol Chem* 278, 19667-19673.

Chou, T.F., and Wagner, C.R. (2007). Lysyl-tRNA synthetase-generated lysyl-adenylate is a substrate for histidine triad nucleotide binding proteins. *J Biol Chem* 282, 4719-4727.

Clapier, C.R., and Cairns, B.R. (2009). The biology of chromatin remodeling complexes. *Annu Rev Biochem* 78, 273-304.

Cohen, L.S., Mikhli, C., Friedman, C., Jankowska-Anyszka, M., Stepinski, J., Darzynkiewicz, E., and Davis, R.E. (2004). Nematode m⁷GpppG and m³(2,2,7)GpppG decapping: activities in *Ascaris* embryos and characterization of *C. elegans* scavenger DcpS. *Rna* 10, 1609-1624.

Coller, J., and Parker, R. (2005). General translational repression by activators of mRNA decapping. *Cell* 122, 875-886.

Connelly, S., and Manley, J.L. (1988). A functional mRNA polyadenylation signal is required for transcription termination by RNA polymerase II. *Genes Dev* 2, 440-452.

Cougot, N., Babajko, S., and Seraphin, B. (2004). Cytoplasmic foci are sites of mRNA decay in human cells. *J Cell Biol* 165, 31-40.

- Custodio, N., Carvalho, C., Condado, I., Antoniou, M., Blencowe, B.J., and Carmo-Fonseca, M. (2004). In vivo recruitment of exon junction complex proteins to transcription sites in mammalian cell nuclei. *RNA* 10, 622-633.
- D'Alessio, J.A., Wright, K.J., and Tjian, R. (2009). Shifting players and paradigms in cell-specific transcription. *Mol Cell* 36, 924-931.
- Dantonel, J.C., Murthy, K.G., Manley, J.L., and Tora, L. (1997). Transcription factor TFIID recruits factor CPSF for formation of 3' end of mRNA. *Nature* 389, 399-402.
- Davuluri, R.V., Grosse, I., and Zhang, M.Q. (2001). Computational identification of promoters and first exons in the human genome. *Nat Genet* 29, 412-417.
- Dias, A., Bouvier, D., Crepin, T., McCarthy, A.A., Hart, D.J., Baudin, F., Cusack, S., and Ruigrok, R.W. (2009). The cap-snatching endonuclease of influenza virus polymerase resides in the PA subunit. *Nature* 458, 914-918.
- Dominski, Z., Sumerel, J., Hanson, R.J., Whitfield, M.L., and Marzluff, W.F. (1995). The polyribosomal protein bound to the 3' end of histone mRNA can function in histone pre-mRNA processing. *Nucleic Acids Symp Ser*, 234-236.
- Dreher, T.W., Uhlenbeck, O.C., and Browning, K.S. (1999). Quantitative assessment of EF-1 α .GTP binding to aminoacyl-tRNAs, aminoacyl-viral RNA, and tRNA shows close correspondence to the RNA binding properties of EF-Tu. *J Biol Chem* 274, 666-672.
- Dunckley, T., and Parker, R. (1999). The DCP2 protein is required for mRNA decapping in *Saccharomyces cerevisiae* and contains a functional MutT motif. *Embo J* 18, 5411-5422.
- Dunckley, T., Tucker, M., and Parker, R. (2001). Two related proteins, Edc1p and Edc2p, stimulate mRNA decapping in *Saccharomyces cerevisiae*. *Genetics* 157, 27-37.
- Dvir, A., Conaway, J.W., and Conaway, R.C. (2001). Mechanism of transcription initiation and promoter escape by RNA polymerase II. *Curr Opin Genet Dev* 11, 209-214.
- Edery, I., and Sonenberg, N. (1985). Cap-dependent RNA splicing in a HeLa nuclear extract. *Proc Natl Acad Sci U S A* 82, 7590-7594.
- Egloff, S., O'Reilly, D., Chapman, R.D., Taylor, A., Tanzhaus, K., Pitts, L., Eick, D., and Murphy, S. (2007). Serine-7 of the RNA polymerase II CTD is specifically required for snRNA gene expression. *Science* 318, 1777-1779.
- Erickson, A.K., and Gale, M., Jr. (2008). Regulation of interferon production and innate antiviral immunity through translational control of IRF-7. *Cell Res* 18, 433-435.
- Etchison, D., Milburn, S.C., Edery, I., Sonenberg, N., and Hershey, J.W. (1982). Inhibition of HeLa cell protein synthesis following poliovirus infection correlates with

the proteolysis of a 220,000-dalton polypeptide associated with eucaryotic initiation factor 3 and a cap binding protein complex. *J Biol Chem* 257, 14806-14810.

Eulalio, A., Behm-Ansmant, I., Schweizer, D., and Izaurralde, E. (2007). P-body formation is a consequence, not the cause, of RNA-mediated gene silencing. *Mol Cell Biol* 27, 3970-3981.

Fenger-Gron, M., Fillman, C., Norrild, B., and Lykke-Andersen, J. (2005). Multiple processing body factors and the ARE binding protein TTP activate mRNA decapping. *Mol Cell* 20, 905-915.

Fillman, C., and Lykke-Andersen, J. (2005). RNA decapping inside and outside of processing bodies. *Curr Opin Cell Biol* 17, 326-331.

Fischer, N., and Weis, K. (2002). The DEAD box protein Dhh1 stimulates the decapping enzyme Dcp1. *Embo J* 21, 2788-2797.

Fortner, D.M., Troy, R.G., and Brow, D.A. (1994). A stem/loop in U6 RNA defines a conformational switch required for pre-mRNA splicing. *Genes Dev* 8, 221-233.

Franks, T.M., and Lykke-Andersen, J. (2007). TTP and BRF proteins nucleate processing body formation to silence mRNAs with AU-rich elements. *Genes Dev* 21, 719-735.

Fraser, C.S., and Doudna, J.A. (2007). Structural and mechanistic insights into hepatitis C viral translation initiation. *Nat Rev Microbiol* 5, 29-38.

Frolova, L., Le Goff, X., Rasmussen, H.H., Cheperegin, S., Drugeon, G., Kress, M., Arman, I., Haenni, A.L., Celis, J.E., Philippe, M., *et al.* (1994). A highly conserved eukaryotic protein family possessing properties of polypeptide chain release factor. *Nature* 372, 701-703.

Furneaux, H.M., Perkins, K.K., Freyer, G.A., Arenas, J., and Hurwitz, J. (1985). Isolation and characterization of two fractions from HeLa cells required for mRNA splicing in vitro. *Proc Natl Acad Sci U S A* 82, 4351-4355.

Gasch, A.P., Spellman, P.T., Kao, C.M., Carmel-Harel, O., Eisen, M.B., Storz, G., Botstein, D., and Brown, P.O. (2000). Genomic expression programs in the response of yeast cells to environmental changes. *Mol Biol Cell* 11, 4241-4257.

Gherzi, R., Lee, K.Y., Briata, P., Wegmuller, D., Moroni, C., Karin, M., and Chen, C.Y. (2004). A KH domain RNA binding protein, KSRP, promotes ARE-directed mRNA turnover by recruiting the degradation machinery. *Mol Cell* 14, 571-583.

Ghosh, T., Peterson, B., Tomasevic, N., and Peculis, B.A. (2004). Xenopus U8 snoRNA Binding Protein Is a Conserved Nuclear Decapping Enzyme. *Mol Cell* 13, 817-828.

Gnirke, A., Geigenmuller, U., Rheinberger, H.J., and Nierhaus, L.H. (1989). The allosteric three-site model for the ribosomal elongation cycle. Analysis with a heteropolymeric mRNA. *J Biol Chem* 264, 7291-7301.

Grentzmann, G., and Kelly, P.J. (1997). Ribosomal binding site of release factors RF1 and RF2. A new translational termination assay in vitro. *J Biol Chem* 272, 12300-12304.

Grifo, J.A., Tahara, S.M., Leis, J.P., Morgan, M.A., Shatkin, A.J., and Merrick, W.C. (1982). Characterization of eukaryotic initiation factor 4A, a protein involved in ATP-dependent binding of globin mRNA. *J Biol Chem* 257, 5246-5252.

Grifo, J.A., Tahara, S.M., Morgan, M.A., Shatkin, A.J., and Merrick, W.C. (1983). New initiation factor activity required for globin mRNA translation. *J Biol Chem* 258, 5804-5810.

Gu, M., Fabrega, C., Liu, S.W., Liu, H., Kiledjian, M., and Lima, C.D. (2004). Insights into the structure, mechanism, and regulation of scavenger mRNA decapping activity. *Mol Cell* 14, 67-80.

Gu, M., and Lima, C.D. (2005). Processing the message: structural insights into capping and decapping mRNA. *Curr Opin Struct Biol* 15, 99-106.

Guranowski, A., Wojdyla, A.M., Zimny, J., Wypijewska, A., Kowalska, J., Jemielity, J., Davis, R.E., and Bieganski, P. (2010). Dual activity of certain HIT-proteins: A. thaliana Hint4 and C. elegans DcpS act on adenosine 5'-phosphosulfate as hydrolases (forming AMP) and as phosphorylases (forming ADP). *FEBS Lett* 584, 93-98.

Haghighat, A., Mader, S., Pause, A., and Sonenberg, N. (1995). Repression of cap-dependent translation by 4E-binding protein 1: competition with p220 for binding to eukaryotic initiation factor-4E. *Embo J* 14, 5701-5709.

Hahnen, E., Forkert, R., Marke, C., Rudnik-Schoneborn, S., Schonling, J., Zerres, K., and Wirth, B. (1995). Molecular analysis of candidate genes on chromosome 5q13 in autosomal recessive spinal muscular atrophy: evidence of homozygous deletions of the SMN gene in unaffected individuals. *Hum Mol Genet* 4, 1927-1933.

Hansen, J.L., Schmeing, T.M., Moore, P.B., and Steitz, T.A. (2002). Structural insights into peptide bond formation. *Proc Natl Acad Sci U S A* 99, 11670-11675.

Harper, J.E., and Manley, J.L. (1991). A novel protein factor is required for use of distal alternative 5' splice sites in vitro. *Mol Cell Biol* 11, 5945-5953.

Hassan, M.I., Naiyer, A., and Ahmad, F. (2010). Fragile histidine triad protein: structure, function, and its association with tumorigenesis. *J Cancer Res Clin Oncol* 136, 333-350.

Hausmann, S., and Shuman, S. (2005). Specificity and mechanism of RNA cap guanine-N2 methyltransferase (Tgs1). *J Biol Chem* 280, 4021-4024.

Hernandez, N., and Keller, W. (1983). Splicing of in vitro synthesized messenger RNA precursors in HeLa cell extracts. *Cell* 35, 89-99.

Hickey, E.D., Weber, L.A., and Baglioni, C. (1976). Inhibition of initiation of protein synthesis by 7-methylguanosine-5'-monophosphate. *Proc Natl Acad Sci U S A* 73, 19-23.

Ho, C.K., Martins, A., and Shuman, S. (2000). A yeast-based genetic system for functional analysis of viral mRNA capping enzymes. *J Virol* 74, 5486-5494.

Ho, C.K., Schwer, B., and Shuman, S. (1998). Genetic, physical, and functional interactions between the triphosphatase and guanylyltransferase components of the yeast mRNA capping apparatus. *Mol Cell Biol* 18, 5189-5198.

Ho, C.K., and Shuman, S. (1999). Distinct roles for CTD Ser-2 and Ser-5 phosphorylation in the recruitment and allosteric activation of mammalian mRNA capping enzyme. *Mol Cell* 3, 405-411.

Ho, L., and Crabtree, G.R. (2010). Chromatin remodelling during development. *Nature* 463, 474-484.

Hsieh-Li, H.M., Chang, J.G., Jong, Y.J., Wu, M.H., Wang, N.M., Tsai, C.H., and Li, H. (2000). A mouse model for spinal muscular atrophy. *Nat Genet* 24, 66-70.

Huang, H.K., Yoon, H., Hannig, E.M., and Donahue, T.F. (1997). GTP hydrolysis controls stringent selection of the AUG start codon during translation initiation in *Saccharomyces cerevisiae*. *Genes Dev* 11, 2396-2413.

Irvine, D.V., Zaratiegui, M., Tolia, N.H., Goto, D.B., Chitwood, D.H., Vaughn, M.W., Joshua-Tor, L., and Martienssen, R.A. (2006). Argonaute slicing is required for heterochromatic silencing and spreading. *Science* 313, 1134-1137.

Izaurrealde, E., Lewis, J., McGuigan, C., Jankowska, M., Darzynkiewicz, E., and Mattaj, I.W. (1994). A nuclear cap binding protein complex involved in pre-mRNA splicing. *Cell* 78, 657-668.

Jang, S.K., Krausslich, H.G., Nicklin, M.J., Duke, G.M., Palmenberg, A.C., and Wimmer, E. (1988). A segment of the 5' nontranslated region of encephalomyocarditis virus RNA directs internal entry of ribosomes during in vitro translation. *J Virol* 62, 2636-2643.

Jiao, X., Wang, Z., and Kiledjian, M. (2006). Identification of an mRNA-Decapping Regulator Implicated in X-Linked Mental Retardation. *Mol Cell* 24, 713-722.

Jinek, M., and Doudna, J.A. (2009). A three-dimensional view of the molecular machinery of RNA interference. *Nature* 457, 405-412.

Juven-Gershon, T., Hsu, J.Y., Theisen, J.W., and Kadonaga, J.T. (2008). The RNA polymerase II core promoter - the gateway to transcription. *Curr Opin Cell Biol* 20, 253-259.

- Kalderon, D., Richardson, W.D., Markham, A.F., and Smith, A.E. (1984). Sequence requirements for nuclear location of simian virus 40 large-T antigen. *Nature* *311*, 33-38.
- Kataoka, N., and Dreyfuss, G. (2004). A simple whole cell lysate system for in vitro splicing reveals a stepwise assembly of the exon-exon junction complex. *J Biol Chem* *279*, 7009-7013.
- Khanna, R., and Kiledjian, M. (2004). Poly(A)-binding-protein-mediated regulation of hDcp2 decapping in vitro. *Embo J* *23*, 1968-1976.
- Kieft, J.S. (2008). Viral IRES RNA structures and ribosome interactions. *Trends Biochem Sci* *33*, 274-283.
- Kiriakidou, M., Tan, G.S., Lamprinaki, S., De Planell-Saguer, M., Nelson, P.T., and Mourelatos, Z. (2007). An mRNA m(7)G Cap Binding-like Motif within Human Ago2 Represses Translation. *Cell* *129*, 1141-1151.
- Kolev, N.G., Yario, T.A., Benson, E., and Steitz, J.A. (2008). Conserved motifs in both CPSF73 and CPSF100 are required to assemble the active endonuclease for histone mRNA 3'-end maturation. *EMBO Rep* *9*, 1013-1018.
- Kolossova, I., and Padgett, R.A. (1997). U11 snRNA interacts in vivo with the 5' splice site of U12-dependent (AU-AC) pre-mRNA introns. *RNA* *3*, 227-233.
- Kolupaeva, V.G., Pestova, T.V., Hellen, C.U., and Shatsky, I.N. (1998). Translation eukaryotic initiation factor 4G recognizes a specific structural element within the internal ribosome entry site of encephalomyocarditis virus RNA. *J Biol Chem* *273*, 18599-18604.
- Konarska, M.M., Padgett, R.A., and Sharp, P.A. (1984). Recognition of cap structure in splicing in vitro of mRNA precursors. *Cell* *38*, 731-736.
- Konarska, M.M., Vilardeell, J., and Query, C.C. (2006). Repositioning of the reaction intermediate within the catalytic center of the spliceosome. *Mol Cell* *21*, 543-553.
- Kozak, M. (1980). Influence of mRNA secondary structure on binding and migration of 40S ribosomal subunits. *Cell* *19*, 79-90.
- Kozak, M. (1986). Point mutations define a sequence flanking the AUG initiator codon that modulates translation by eukaryotic ribosomes. *Cell* *44*, 283-292.
- Krainer, A.R., Maniatis, T., Ruskin, B., and Green, M.R. (1984). Normal and mutant human beta-globin pre-mRNAs are faithfully and efficiently spliced in vitro. *Cell* *36*, 993-1005.
- Kramer, A. (1996). The structure and function of proteins involved in mammalian pre-mRNA splicing. *Annu Rev Biochem* *65*, 367-409.

- Kudo, N., Matsumori, N., Taoka, H., Fujiwara, D., Schreiner, E.P., Wolff, B., Yoshida, M., and Horinouchi, S. (1999). Leptomycin B inactivates CRM1/exportin 1 by covalent modification at a cysteine residue in the central conserved region. *Proc Natl Acad Sci U S A* 96, 9112-9117.
- Kutay, U., and Guttinger, S. (2005). Leucine-rich nuclear-export signals: born to be weak. *Trends Cell Biol* 15, 121-124.
- Kwasnicka, D.A., Krakowiak, A., Thacker, C., Brenner, C., and Vincent, S.R. (2003). Coordinate expression of NADPH-dependent flavin reductase, Fre-1, and Hint-related 7meGMP-directed hydrolase, DCS-1. *J Biol Chem* 278, 39051-39058.
- Lai, W.S., Carballo, E., Strum, J.R., Kennington, E.A., Phillips, R.S., and Blackshear, P.J. (1999). Evidence that tristetraprolin binds to AU-rich elements and promotes the deadenylation and destabilization of tumor necrosis factor alpha mRNA. *Mol Cell Biol* 19, 4311-4323.
- Lai, W.S., Carballo, E., Thorn, J.M., Kennington, E.A., and Blackshear, P.J. (2000). Interactions of CCCH zinc finger proteins with mRNA. Binding of tristetraprolin-related zinc finger proteins to AU-rich elements and destabilization of mRNA. *J Biol Chem* 275, 17827-17837.
- Lall, S., Piano, F., and Davis, R.E. (2005). *Caenorhabditis elegans* decapping proteins: localization and functional analysis of Dcp1, Dcp2, and DcpS during embryogenesis. *Mol Biol Cell* 16, 5880-5890.
- Lange, A., Mills, R.E., Lange, C.J., Stewart, M., Devine, S.E., and Corbett, A.H. (2007). Classical nuclear localization signals: definition, function, and interaction with importin alpha. *J Biol Chem* 282, 5101-5105.
- Larimer, F.W., Hsu, C.L., Maupin, M.K., and Stevens, A. (1992). Characterization of the XRN1 gene encoding a 5'-->3' exoribonuclease: sequence data and analysis of disparate protein and mRNA levels of gene- disrupted yeast cells. *Gene* 120, 51-57.
- Lau, C.K., Diem, M.D., Dreyfuss, G., and Van Duyne, G.D. (2003). Structure of the Y14-Magoh core of the exon junction complex. *Curr Biol* 13, 933-941.
- Lee, Y., Jeon, K., Lee, J.T., Kim, S., and Kim, V.N. (2002). MicroRNA maturation: stepwise processing and subcellular localization. *EMBO J* 21, 4663-4670.
- Lee, Y., Kim, M., Han, J., Yeom, K.H., Lee, S., Baek, S.H., and Kim, V.N. (2004). MicroRNA genes are transcribed by RNA polymerase II. *EMBO J* 23, 4051-4060.
- Legrand, P., Pinaud, N., Minvielle-Sebastia, L., and Fribourg, S. (2007). The structure of the CstF-77 homodimer provides insights into CstF assembly. *Nucleic Acids Res* 35, 4515-4522.

Lejeune, F., Ishigaki, Y., Li, X., and Maquat, L.E. (2002). The exon junction complex is detected on CBP80-bound but not eIF4E-bound mRNA in mammalian cells: dynamics of mRNP remodeling. *Embo J* 21, 3536-3545.

Lejeune, F., Li, X., and Maquat, L.E. (2003). Nonsense-mediated mRNA decay in mammalian cells involves decapping, deadenylating, and exonucleolytic activities. *Mol Cell* 12, 675-687.

Lewis, J.D., Izaurralde, E., Jarmolowski, A., McGuigan, C., and Mattaj, I.W. (1996). A nuclear cap-binding complex facilitates association of U1 snRNP with the cap-proximal 5' splice site. *Genes Dev* 10, 1683-1698.

Li, W., Belsham, G.J., and Proud, C.G. (2001a). Eukaryotic initiation factors 4A (eIF4A) and 4G (eIF4G) mutually interact in a 1:1 ratio in vivo. *J Biol Chem* 276, 29111-29115.

Li, Y., Chen, Z.Y., Wang, W., Baker, C.C., and Krug, R.M. (2001b). The 3'-end-processing factor CPSF is required for the splicing of single-intron pre-mRNAs in vivo. *RNA* 7, 920-931.

Li, Y., Song, M.G., and Kiledjian, M. (2008). Transcript-specific decapping and regulated stability by the human Dcp2 decapping protein. *Mol Cell Biol* 28, 939-948.

Lin, T.A., Kong, X., Haystead, T.A., Pause, A., Belsham, G., Sonenberg, N., and Lawrence, J.C., Jr. (1994). PHAS-I as a link between mitogen-activated protein kinase and translation initiation. *Science* 266, 653-656.

Linker, K., Pautz, A., Fechir, M., Hubrich, T., Greeve, J., and Kleinert, H. (2005). Involvement of KSRP in the post-transcriptional regulation of human iNOS expression-complex interplay of KSRP with TTP and HuR. *Nucleic Acids Res* 33, 4813-4827.

Liu, H., and Kiledjian, M. (2005). Scavenger decapping activity facilitates 5' to 3' mRNA decay. *Mol Cell Biol* 25, 9764-9772.

Liu, H., Rodgers, N.D., Jiao, X., and Kiledjian, M. (2002). The scavenger mRNA decapping enzyme DcpS is a member of the HIT family of pyrophosphatases. *EMBO J* 21, 4699-4708.

Liu, Q., Greimann, J.C., and Lima, C.D. (2006). Reconstitution, activities, and structure of the eukaryotic RNA exosome. *Cell* 127, 1223-1237.

Liu, S.W., Jiao, X., Liu, H., Gu, M., Lima, C.D., and Kiledjian, M. (2004). Functional analysis of mRNA scavenger decapping enzymes. *RNA* 10, 1412-1422.

Liu, S.W., Rajagopal, V., Patel, S.S., and Kiledjian, M. (2008). Mechanistic and kinetic analysis of the DcpS scavenger decapping enzyme. *J Biol Chem* 283, 16427-16436.

Livak, K.J., and Schmittgen, T.D. (2001). Analysis of relative gene expression data using real-time quantitative PCR and the 2(-Delta Delta C(T)) Method. *Methods* 25, 402-408.

Lomakin, I.B., Hellen, C.U., and Pestova, T.V. (2000). Physical association of eukaryotic initiation factor 4G (eIF4G) with eIF4A strongly enhances binding of eIF4G to the internal ribosomal entry site of encephalomyocarditis virus and is required for internal initiation of translation. *Mol Cell Biol* 20, 6019-6029.

Lorentzen, E., Walter, P., Fribourg, S., Evguenieva-Hackenberg, E., Klug, G., and Conti, E. (2005). The archaeal exosome core is a hexameric ring structure with three catalytic subunits. *Nat Struct Mol Biol* 12, 575-581.

Malys, N., Carroll, K., Miyan, J., Tollervey, D., and McCarthy, J.E. (2004). The 'scavenger' m7GpppX pyrophosphatase activity of Dcs1 modulates nutrient-induced responses in yeast. *Nucleic Acids Res* 32, 3590-3600.

Malys, N., and McCarthy, J.E. (2006). Dcs2, a novel stress-induced modulator of m7GpppX pyrophosphatase activity that locates to P bodies. *J Mol Biol* 363, 370-382.

Mandel, C.R., Kaneko, S., Zhang, H., Gebauer, D., Vethantham, V., Manley, J.L., and Tong, L. (2006). Polyadenylation factor CPSF-73 is the pre-mRNA 3'-end-processing endonuclease. *Nature* 444, 953-956.

Manley, J.L. (1983). Accurate and specific polyadenylation of mRNA precursors in a soluble whole-cell lysate. *Cell* 33, 595-605.

Mao, X., Schwer, B., and Shuman, S. (1996). Mutational analysis of the *Saccharomyces cerevisiae* ABD1 gene: cap methyltransferase activity is essential for cell growth. *Mol Cell Biol* 16, 475-480.

Martin, J., Magnino, F., Schmidt, K., Piguet, A.C., Lee, J.S., Semela, D., St-Pierre, M.V., Ziemiecki, A., Cassio, D., Brenner, C., *et al.* (2006). Hint2, a mitochondrial apoptotic sensitizer down-regulated in hepatocellular carcinoma. *Gastroenterology* 130, 2179-2188.

Mazza, C., Segref, A., Mattaj, I.W., and Cusack, S. (2002). Large-scale induced fit recognition of an m(7)GpppG cap analogue by the human nuclear cap-binding complex. *Embo J* 21, 5548-5557.

Meininghaus, M., Chapman, R.D., Horndasch, M., and Eick, D. (2000). Conditional expression of RNA polymerase II in mammalian cells. Deletion of the carboxyl-terminal domain of the large subunit affects early steps in transcription. *J Biol Chem* 275, 24375-24382.

Michael, W.M., Choi, M., and Dreyfuss, G. (1995). A nuclear export signal in hnRNP A1: a signal-mediated, temperature- dependent nuclear protein export pathway. *Cell* 83, 415-422.

Mitchell, P., Petfalski, E., Shevchenko, A., Mann, M., and Tollervey, D. (1997). The exosome: a conserved eukaryotic RNA processing complex containing multiple 3'→5' exoribonucleases. *Cell* 91, 457-466.

Moazed, D., and Noller, H.F. (1989). Intermediate states in the movement of transfer RNA in the ribosome. *Nature* 342, 142-148.

Monani, U.R., Lorson, C.L., Parsons, D.W., Prior, T.W., Androphy, E.J., Burghes, A.H., and McPherson, J.D. (1999). A single nucleotide difference that alters splicing patterns distinguishes the SMA gene SMN1 from the copy gene SMN2. *Hum Mol Genet* 8, 1177-1183.

Monani, U.R., Sendtner, M., Coover, D.D., Parsons, D.W., Andreassi, C., Le, T.T., Jablonka, S., Schrank, B., Rossol, W., Prior, T.W., *et al.* (2000a). The human centromeric survival motor neuron gene (SMN2) rescues embryonic lethality in *Smn*(^{-/-}) mice and results in a mouse with spinal muscular atrophy. *Hum Mol Genet* 9, 333-339.

Monani, U.R., Sendtner, M., Coover, D.D., Parsons, D.W., Andreassi, C., Le, T.T., Jablonka, S., Schrank, B., Rossol, W., Prior, T.W., *et al.* (2000b). The human centromeric survival motor neuron gene (SMN2) rescues embryonic lethality in *Smn*(^{-/-}) mice and results in a mouse with spinal muscular atrophy. *Hum Mol Genet* 9, 333-339.

Moser, M.J., Holley, W.R., Chatterjee, A., and Mian, I.S. (1997). The proofreading domain of Escherichia coli DNA polymerase I and other DNA and/or RNA exonuclease domains. *Nucleic Acids Res* 25, 5110-5118.

Nissen, P., Hansen, J., Ban, N., Moore, P.B., and Steitz, T.A. (2000). The structural basis of ribosome activity in peptide bond synthesis. *Science* 289, 920-930.

Norton, P.A., and Hynes, R.O. (1990). In vitro splicing of fibronectin pre-mRNAs. *Nucleic Acids Res* 18, 4089-4097.

Nuss, D.L., Furuichi, Y., Koch, G., and Shatkin, A.J. (1975). Detection in HeLa cell extracts of a 7-methyl guanosine specific enzyme activity that cleaves m7GpppNm. *Cell* 6, 21-27.

O'Brien, T., Hardin, S., Greenleaf, A., and Lis, J.T. (1994). Phosphorylation of RNA polymerase II C-terminal domain and transcriptional elongation. *Nature* 370, 75-77.

Ohlmann, T., Rau, M., Pain, V.M., and Morley, S.J. (1996). The C-terminal domain of eukaryotic protein synthesis initiation factor (eIF) 4G is sufficient to support cap-independent translation in the absence of eIF4E. *EMBO J* 15, 1371-1382.

Ohta, M., Inoue, H., Cotticelli, M.G., Kastury, K., Baffa, R., Palazzo, J., Siprashvili, Z., Mori, M., McCue, P., Druck, T., *et al.* (1996). The FHIT gene, spanning the chromosome 3p14.2 fragile site and renal carcinoma-associated t(3;8) breakpoint, is abnormal in digestive tract cancers. *Cell* 84, 587-597.

Oprea, G.E., Krober, S., McWhorter, M.L., Rossol, W., Muller, S., Krawczak, M., Bassell, G.J., Beattie, C.E., and Wirth, B. (2008). Plastin 3 is a protective modifier of autosomal recessive spinal muscular atrophy. *Science* 320, 524-527.

Orban, T.I., and Izaurralde, E. (2005). Decay of mRNAs targeted by RISC requires XRN1, the Ski complex, and the exosome. *RNA* 11, 459-469.

Pace, H.C., Garrison, P.N., Robinson, A.K., Barnes, L.D., Draganescu, A., Rosler, A., Blackburn, G.M., Siprashvili, Z., Croce, C.M., Huebner, K., *et al.* (1998). Genetic, biochemical, and crystallographic characterization of Fhit-substrate complexes as the active signaling form of Fhit. *Proc Natl Acad Sci U S A* 95, 5484-5489.

Paddison, P.J., Caudy, A.A., Bernstein, E., Hannon, G.J., and Conklin, D.S. (2002). Short hairpin RNAs (shRNAs) induce sequence-specific silencing in mammalian cells. *Genes Dev* 16, 948-958.

Parrish, S., Resch, W., and Moss, B. (2007). Vaccinia virus D10 protein has mRNA decapping activity, providing a mechanism for control of host and viral gene expression. *Proc Natl Acad Sci U S A* 104, 2139-2144.

Patrone, G., Puppo, F., Cusano, R., Scaranari, M., Ceccherini, I., Puliti, A., and Ravazzolo, R. (2000). Nuclear run-on assay using biotin labeling, magnetic bead capture and analysis by fluorescence-based RT-PCR. *Biotechniques* 29, 1012-1014, 1016-1017.

Pause, A., Belsham, G.J., Gingras, A.C., Donze, O., Lin, T.A., Lawrence, J.C., Jr., and Sonenberg, N. (1994). Insulin-dependent stimulation of protein synthesis by phosphorylation of a regulator of 5'-cap function. *Nature* 371, 762-767.

Peculis, B.A., Reynolds, K., and Cleland, M. (2007). Metal determines efficiency and substrate specificity of the nuclear nudix decapping proteins X29 and H29K(NUDT16). *J Biol Chem*.

Peculis, B.A., Scarsdale, J.N., and Wright, H.T. (2004). Crystals of X29, a *Xenopus laevis* U8 snoRNA-binding protein with nuclear decapping activity. *Acta Crystallogr D Biol Crystallogr* 60, 1668-1669.

Perez Canadillas, J.M., and Varani, G. (2003). Recognition of GU-rich polyadenylation regulatory elements by human CstF-64 protein. *EMBO J* 22, 2821-2830.

Pestova, T.V., Borukhov, S.I., and Hellen, C.U. (1998). Eukaryotic ribosomes require initiation factors 1 and 1A to locate initiation codons. *Nature* 394, 854-859.

Pestova, T.V., Kolupaeva, V.G., Lomakin, I.B., Pilipenko, E.V., Shatsky, I.N., Agol, V.I., and Hellen, C.U. (2001). Molecular mechanisms of translation initiation in eukaryotes. *Proc Natl Acad Sci U S A* 98, 7029-7036.

Pestova, T.V., Lomakin, I.B., Lee, J.H., Choi, S.K., Dever, T.E., and Hellen, C.U. (2000). The joining of ribosomal subunits in eukaryotes requires eIF5B. *Nature* 403, 332-335.

Pestova, T.V., Shatsky, I.N., and Hellen, C.U. (1996). Functional dissection of eukaryotic initiation factor 4F: the 4A subunit and the central domain of the 4G subunit are

sufficient to mediate internal entry of 43S preinitiation complexes. *Mol Cell Biol* *16*, 6870-6878.

Petersen, C.P., Bordeleau, M.E., Pelletier, J., and Sharp, P.A. (2006). Short RNAs repress translation after initiation in mammalian cells. *Mol Cell* *21*, 533-542.

Petfalski, E., Dandekar, T., Henry, Y., and Tollervy, D. (1998). Processing of the precursors to small nucleolar RNAs and rRNAs requires common components. *Mol Cell Biol* *18*, 1181-1189.

Phillips, S., and Butler, J.S. (2003). Contribution of domain structure to the RNA 3' end processing and degradation functions of the nuclear exosome subunit Rrp6p. *RNA* *9*, 1098-1107.

Pillai, R.S., Bhattacharyya, S.N., Artus, C.G., Zoller, T., Cougot, N., Basyuk, E., Bertrand, E., and Filipowicz, W. (2005). Inhibition of translational initiation by Let-7 MicroRNA in human cells. *Science* *309*, 1573-1576.

Pinol-Roma, S., and Dreyfuss, G. (1992). Shuttling of pre-mRNA binding proteins between nucleus and cytoplasm. *Nature* *355*, 730-732.

Poulin, F., Gingras, A.C., Olsen, H., Chevalier, S., and Sonenberg, N. (1998). 4E-BP3, a new member of the eukaryotic initiation factor 4E-binding protein family. *J Biol Chem* *273*, 14002-14007.

Ranu, R.S., and London, I.M. (1979). Regulation of protein synthesis in rabbit reticulocyte lysates: additional initiation factor required for formation of ternary complex (eIF-2.GTP.Met-tRNA^f) and demonstration of inhibitory effect of heme-regulated protein kinase. *Proc Natl Acad Sci U S A* *76*, 1079-1083.

Ray, B.K., Lawson, T.G., Kramer, J.C., Cladaras, M.H., Grifo, J.A., Abramson, R.D., Merrick, W.C., and Thach, R.E. (1985). ATP-dependent unwinding of messenger RNA structure by eukaryotic initiation factors. *J Biol Chem* *260*, 7651-7658.

Reichert, V.L., Le Hir, H., Jurica, M.S., and Moore, M.J. (2002). 5' exon interactions within the human spliceosome establish a framework for exon junction complex structure and assembly. *Genes Dev* *16*, 2778-2791.

Robberson, B.L., Cote, G.J., and Berget, S.M. (1990). Exon definition may facilitate splice site selection in RNAs with multiple exons. *Mol Cell Biol* *10*, 84-94.

Roman, R., Brooker, J.D., Seal, S.N., and Marcus, A. (1976). Inhibition of the transition of a 40 S ribosome-Met-tRNA-i-Met complex to an 80 S ribosome-Met-tRNA-i-Met-complex by 7-Methylguanosine-5'-phosphate. *Nature* *260*, 359-360.

Rozen, F., and Sonenberg, N. (1987). Identification of nuclear cap specific proteins in HeLa cells. *Nucleic Acids Res* *15*, 6489-6500.

Ruby, S.W., and Abelson, J. (1988). An early hierarchic role of U1 small nuclear ribonucleoprotein in spliceosome assembly. *Science* 242, 1028-1035.

Ruskin, B., Zamore, P.D., and Green, M.R. (1988). A factor, U2AF, is required for U2 snRNP binding and splicing complex assembly. *Cell* 52, 207-219.

Salehi, Z., Geffers, L., Vilela, C., Birkenhager, R., Ptushkina, M., Berthelot, K., Ferro, M., Gaskell, S., Hagan, I., Stapley, B., *et al.* (2002). A nuclear protein in *Schizosaccharomyces pombe* with homology to the human tumour suppressor Fhit has decapping activity. *Mol Microbiol* 46, 49-62.

Sasavage, N.L., Friderici, K., and Rottman, F.M. (1979). Specific inhibition of capped mRNA translation in vitro by m7G5'pppp5'G and m7G5'pppp5'm7G. *Nucleic Acids Res* 6, 3613-3624.

Satomi, D., and Kishimoto, Y. (1981). UDP-galactose hydrolysis in brain and its effect on cerebroside synthesis. *J Neurochem* 36, 476-482.

Scarsdale, J.N., Peculis, B.A., and Wright, H.T. (2006). Crystal Structures of U8 snoRNA Decapping Nudix Hydrolase, X29, and Its Metal and Cap Complexes. *Structure* 14, 331-343.

Schneider, C., Leung, E., Brown, J., and Tollervey, D. (2009). The N-terminal PIN domain of the exosome subunit Rrp44 harbors endonuclease activity and tethers Rrp44 to the yeast core exosome. *Nucleic Acids Res* 37, 1127-1140.

Schrank, B., Gotz, R., Gunnarsen, J.M., Ure, J.M., Toyka, K.V., Smith, A.G., and Sendtner, M. (1997). Inactivation of the survival motor neuron gene, a candidate gene for human spinal muscular atrophy, leads to massive cell death in early mouse embryos. *Proc Natl Acad Sci U S A* 94, 9920-9925.

Schwartz, D., Decker, C.J., and Parker, R. (2003). The enhancer of decapping proteins, Edc1p and Edc2p, bind RNA and stimulate the activity of the decapping enzyme. *Rna* 9, 239-251.

Seidle, H.F., Bieganowski, P., and Brenner, C. (2005). Disease-associated mutations inactivate AMP-lysine hydrolase activity of Aprataxin. *J Biol Chem* 280, 20927-20931.

Serizawa, H. (1998). Cyclin-dependent kinase inhibitor p16INK4A inhibits phosphorylation of RNA polymerase II by general transcription factor TFIIH. *J Biol Chem* 273, 5427-5430.

Shatkin, A.J. (1976). Capping of eucaryotic mRNAs. *Cell* 9, 645-653.

She, M., Decker, C.J., Svergun, D.I., Round, A., Chen, N., Muhrlad, D., Parker, R., and Song, H. (2008). Structural basis of dcp2 recognition and activation by dcp1. *Mol Cell* 29, 337-349.

Shen, V., and Kiledjian, M. (2006). A view to a kill: structure of the RNA exosome. *Cell* *127*, 1093-1095.

Shen, V., Liu, H., Liu, S.W., Jiao, X., and Kiledjian, M. (2008). DcpS scavenger decapping enzyme can modulate pre-mRNA splicing. *RNA* *14*, 1132-1142.

Shimba, S., Buckley, B., Reddy, R., Kiss, T., and Filipowicz, W. (1992). Cap structure of U3 small nucleolar RNA in animal and plant cells is different. gamma-Monomethyl phosphate cap structure in plant RNA. *J Biol Chem* *267*, 13772-13777.

Singh, J., Salcius, M., Liu, S.W., Staker, B.L., Mishra, R., Thurmond, J., Michaud, G., Mattoon, D.R., Printen, J., Christensen, J., *et al.* (2008). DcpS as a therapeutic target for spinal muscular atrophy. *ACS Chem Biol* *3*, 711-722.

Siomi, H., and Dreyfuss, G. (1995). A nuclear localization domain in the hnRNP A1 protein. *J Cell Biol* *129*, 551-560.

Skogerson, L., and Wakatama, E. (1976). A ribosome-dependent GTPase from yeast distinct from elongation factor 2. *Proc Natl Acad Sci U S A* *73*, 73-76.

Sonenberg, N., Morgan, M.A., Merrick, W.C., and Shatkin, A.J. (1978). A polypeptide in eukaryotic initiation factors that crosslinks specifically to the 5'-terminal cap in mRNA. *Proc Natl Acad Sci U S A* *75*, 4843-4847.

Song, H., Mugnier, P., Das, A.K., Webb, H.M., Evans, D.R., Tuite, M.F., Hemmings, B.A., and Barford, D. (2000). The crystal structure of human eukaryotic release factor eRF1--mechanism of stop codon recognition and peptidyl-tRNA hydrolysis. *Cell* *100*, 311-321.

Southgate, C., and Busslinger, M. (1989). In vivo and in vitro expression of U7 snRNA genes: cis- and trans-acting elements required for RNA polymerase II-directed transcription. *EMBO J* *8*, 539-549.

Strasser, K., Masuda, S., Mason, P., Pfannstiel, J., Oppizzi, M., Rodriguez-Navarro, S., Rondon, A.G., Aguilera, A., Struhl, K., Reed, R., *et al.* (2002). TREX is a conserved complex coupling transcription with messenger RNA export. *Nature* *417*, 304-308.

Su, T., Suzui, M., Wang, L., Lin, C.S., Xing, W.Q., and Weinstein, I.B. (2003). Deletion of histidine triad nucleotide-binding protein 1/PKC-interacting protein in mice enhances cell growth and carcinogenesis. *Proc Natl Acad Sci U S A* *100*, 7824-7829.

Suzuki, H. (1976). Effect of 7-methylguanosine-5'-phosphate on rabbit globin synthesis. *FEBS Lett* *72*, 309-313.

Tarn, W.Y., and Steitz, J.A. (1996a). Highly diverged U4 and U6 small nuclear RNAs required for splicing rare AT-AC introns. *Science* *273*, 1824-1832.

- Tarn, W.Y., and Steitz, J.A. (1996b). A novel spliceosome containing U11, U12, and U5 snRNPs excises a minor class (AT-AC) intron in vitro. *Cell* 84, 801-811.
- Thach, R.E., Dewey, K.F., Brown, J.C., and Doty, P. (1966). Formylmethionine codon AUG as an initiator of polypeptide synthesis. *Science* 153, 416-418.
- Tsukiyama-Kohara, K., Iizuka, N., Kohara, M., and Nomoto, A. (1992). Internal ribosome entry site within hepatitis C virus RNA. *J Virol* 66, 1476-1483.
- van Dijk, E., Le Hir, H., and Seraphin, B. (2003). DcpS can act in the 5'-3' mRNA decay pathway in addition to the 3'-5' pathway. *Proc Natl Acad Sci U S A* 100, 12081-12086.
- Venkatesan, S., Gershowitz, A., and Moss, B. (1980). Purification and characterization of mRNA guanylyltransferase from HeLa cell nuclei. *J Biol Chem* 255, 2829-2834.
- Wada, T., Takagi, T., Yamaguchi, Y., Watanabe, D., and Handa, H. (1998). Evidence that P-TEFb alleviates the negative effect of DSIF on RNA polymerase II-dependent transcription in vitro. *EMBO J* 17, 7395-7403.
- Wagner, E.J., and Marzluff, W.F. (2006). ZFP100, a component of the active U7 snRNP limiting for histone pre-mRNA processing, is required for entry into S phase. *Mol Cell Biol* 26, 6702-6712.
- Wang, Y., Juranek, S., Li, H., Sheng, G., Wardle, G.S., Tuschl, T., and Patel, D.J. (2009). Nucleation, propagation and cleavage of target RNAs in Ago silencing complexes. *Nature* 461, 754-761.
- Wang, Z., Jiao, X., Carr-Schmid, A., and Kiledjian, M. (2002). The hDcp2 protein is a mammalian mRNA decapping enzyme. *Proc Natl Acad Sci U S A* 99, 12663-12668.
- Wang, Z., and Kiledjian, M. (2001). Functional Link between the Mammalian Exosome and mRNA Decapping. *Cell* 107, 751-762.
- Wen, W., Meinkoth, J.L., Tsien, R.Y., and Taylor, S.S. (1995). Identification of a signal for rapid export of proteins from the nucleus. *Cell* 82, 463-473.
- Winzen, R., Thakur, B.K., Dittrich-Breiholz, O., Shah, M., Redich, N., Dhamija, S., Kracht, M., and Holtmann, H. (2007). Functional analysis of KSRP interaction with the AU-rich element of interleukin-8 and identification of inflammatory mRNA targets. *Mol Cell Biol* 27, 8388-8400.
- Wolff, T., and Bindereif, A. (1993). Conformational changes of U6 RNA during the spliceosome cycle: an intramolecular helix is essential both for initiating the U4-U6 interaction and for the first step of slicing. *Genes Dev* 7, 1377-1389.
- Wu, Q., and Krainer, A.R. (1997). Splicing of a divergent subclass of AT-AC introns requires the major spliceosomal snRNAs. *RNA* 3, 586-601.

- Xu, J., Yang, J.Y., Niu, Q.W., and Chua, N.H. (2006). Arabidopsis DCP2, DCP1, and VARICOSE form a decapping complex required for postembryonic development. *Plant Cell* 18, 3386-3398.
- Yu, J.H., Yang, W.H., Gulick, T., Bloch, K.D., and Bloch, D.B. (2005). Ge-1 is a central component of the mammalian cytoplasmic mRNA processing body. *RNA* 11, 1795-1802.
- Yuo, C.Y., Ares, M., Jr., and Weiner, A.M. (1985). Sequences required for 3' end formation of human U2 small nuclear RNA. *Cell* 42, 193-202.
- Zamore, P.D., Patton, J.G., and Green, M.R. (1992). Cloning and domain structure of the mammalian splicing factor U2AF. *Nature* 355, 609-614.
- Zhang, X., Zou, T., Rao, J.N., Liu, L., Xiao, L., Wang, P.Y., Cui, Y.H., Gorospe, M., and Wang, J.Y. (2009). Stabilization of XIAP mRNA through the RNA binding protein HuR regulated by cellular polyamines. *Nucleic Acids Res* 37, 7623-7637.
- Zhuang, Y.A., Goldstein, A.M., and Weiner, A.M. (1989). UACUAAC is the preferred branch site for mammalian mRNA splicing. *Proc Natl Acad Sci U S A* 86, 2752-2756.

CURRICULUM VITAE
VINCENT SHEN

Education:

- | | |
|--------------|---|
| 2005-present | Ph.D. Biochemistry
Rutgers University/University of Medicine and Dentistry of New Jersey |
| 2002-2005 | Ph.D. Candidate in Biochemistry
Rutgers University/ University of Medicine and Dentistry of New Jersey |
| 1997-2001 | B.A. Biological Sciences
Concentration: Biochemistry
Cornell University |

Research and Teaching Experience:

- | | |
|-----------|---|
| 2008-2010 | Teaching Assistant in General Biology Laboratory
Rutgers University |
| 2001-2002 | Research Technician in Department of Biochemistry
Weill Cornell Medical College |
| 2000-2001 | Research Technician in Department of Chemistry and Chemical Biology
Cornell University |

Peer-Reviewed Publications:

1. **Shen V**, Liu H, Liu SW, Jiao X, Kiledjian M. DcpS scavenger decapping enzyme can modulate pre-mRNA splicing.
RNA 2008;14:1132-1142.
2. Fabrega C, Hausmann S, **Shen V**, Shuman S, Lima CD. Structure and mechanism of mRNA cap (guanine-N7) methyltransferase.
Molecular Cell 2004;13:77-89.
3. Fabrega C, **Shen V**, Shuman S, Lima CD. Structure of an mRNA capping enzyme bound to the phosphorylated carboxy-terminal domain of RNA polymerase II.
Molecular Cell 2003;11:1549-1561.

Review Articles:

1. **Shen V**, Kiledjian M. A view to a kill: Structure of the RNA exosome.
Cell 2006;127:1093-1095.
2. **Shen V**, Kiledjian M. Decapper comes into focus.
Structure 2006;14:171-172.